# Czech Technical University in Prague

## Faculty of Electrical Engineering

### Department of Electrical Power Engineering


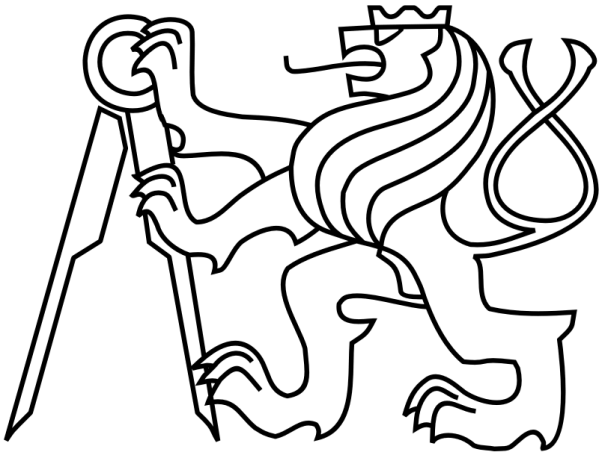

# Diplomová práce

# Diploma Thesis

## Series Arc Fault Detection in the Presence of Household Electrical Loads


**Author:** Amna Farooq Husain

**Supervisor:** doc. Dr. Ing. Jan Kyncl


**2017**

Czech Technical University in Prague
Faculty of Electrical Engineering

Department of Electrical Power Engineering

# DIPLOMA THESIS ASSIGNMENT

Student: **Amna Farooq Husain**

Study programme: Electrical Engineering, Power Engineering and Management
Specialisation: Electrical Power Engineering

Title of Diploma Thesis: **Series Arc Fault Detection in the Presence of Household Electrical Loads**

Guidelines:

1. Outline the current state of art of AFD
2. Analyse the simulated and measured data in a software environment
3. Provide recommendation on the possible future research in the field of series AFD

Bibliography/Sources:

[1] IEC 62606
[2] http://mathworld.wolfram.com
[3] Restrepo, Carlos E. "Arc fault detection and discrimination methods." Electrical contacts-2007, the 53rd ieee holm conference on. IEEE, 2007.

Diploma Thesis Supervisor: doc. Dr. Ing. Jan Kyncl

Valid until the end of the winter semester of academic year 2017/2018

L.S.

doc. Ing. Zdeněk Müller, Ph.D.
Head of Department

prof. Ing. Pavel Ripka, CSc.
Dean

Prague, February 20, 2017

## Prohlášení

Prohlašuji, že jsem předloženou práci vypracoval samostatně a že jsem uvedl veškeré použité informační zdroje v souladu s Metodickým pokynem o dodržování etických principů při přípravě vysokoškolských závěrečných prací.

## Declaration

I hereby declare that I carried out and wrote the assigned thesis by myself only and I used only the referenced source materials.

V Praze dne/Prague ……..

……

Podpis/Signature

## Acknowledgements

First and foremost I would like to thank my manager, Mgr. Oleksiy Chumak Ph.D., at Eaton European Innovation Center (EEIC), without whose support and guidance this thesis would not have been possible. I would like to express my gratitude to EEIC Director, Dr. Engelbert Hetzmannseder, for ensuring this collaboration and offering me this opportunity. I would also like to thank the members of the CRT team at EEIC.

Furthermore, I would like to thank my supervisor doc. Dr. Ing. Jan Kyncl for his support and for always guiding me towards the right direction.

Last but not least I would like to express my deepest gratitude to my family for standing by me, supporting me every step of the way, and encouraging me to pursue my dreams.

## Abstract

An arc fault as a result of a damaged electrical wire may cause an electrical fire. The ability of arc faults to cause electrical fires has necessitated research and development in the field of arc fault detection. This thesis studies and analyzes series arc faults at a low voltage level in the presence of household electrical loads. The thesis will provide a component-based approach to characterizing domestic electrical loads and to observe and process the signals and characteristics of these loads in the presence and absence of a series arc fault. The results will be used to conclude the behavior of different load types and whether loads falling under the same category show similar characteristics. These results are intended to assist in improving the detection of series arc faults in the presence of household electrical loads. The data obtained was analyzed using signal STFT and CWT. For all tested load categories, the characteristic features of the arc were analyzed. The CWT had better characterization capability due to its resolution.

## Keywords

Arc fault, Household loads, Component-based load categorization, Series arcing, AFDD, Arc fault detection devices.

## Abstrakt

Elektrický oblouk způsobený poškozeným elektrickým vedením může způsobit požár. Fakt, že elektrické oblouky způsobují požáry podporuje výzkum a vývoj jejich detekce. Diplomová práce se zabývá studiem a analýzou sériových elektrických výbojů při nízkém napětí v přítomnosti elektrických zátěží běžně používaných v domácnostech. Tato práce poskytuje postupy pro charakterizaci domácích elektrických zátěží. Poskytuje také pozorování spolu se zpracováním dat z těchto zátěží v přítomnosti a při absenci sériového elektrického výboje v závislosti na charakteristice zařízení. Výsledky budou použity pro vyhodnocení chování jednotlivých typů zátěží, a také zjištění, zda jednotlivé zátěže ve stejných kategoriích vykazují podobné charakteristiky. Výsledky budou sloužit jako podklad pro zlepšení detekce sériových elektrických výbojů. Data byla získána pomocí STFT a CWT. Pro všechny testované zátěžové kategorie byly analyzovány charakteristické vlastnosti. CWT má lepší schopnost charakterizace díky svému rozlišení.

## Klíčová slova

Elektrický oblouk, Domácí spotřebiče, Kategorizace zátěží v závislosti na zařízení, Sériový elektrický výboj, Zařízení pro detekci elektrických výbojů.

# Table of Contents

# 1. Introduction

## 1.1. Motivation

According to the Health and Safety Executive (HSE), the main electricity related hazards are; exposure to live parts which may cause shock and burns, faults which may result in fire, and fire or explosion in a flammable or explosive atmosphere due to an electrical source of ignition [1]. The potential risk of fire in households is one of the major concerns related to electricity. There are many devices which aim to protect from the abovementioned hazards. Although Residual Current Devices (RCDs) can successfully reduce the risk of fire by detecting leakage, and arcing to ground current, they are unable to detect series and parallel arc fault between live conductors. The IEC 62606 describes an arc fault as dangerous unintentional parallel or series arc between conductors [2].

An arc fault as a result of a damaged electrical wire may cause an electrical fire. Fires have been initiated at currents as low as 0.9 Arms, which is equivalent to a 100 W bulb [3]. The damaged wiring causes the wire to heat up. There are two main means which may cause the wire and its surrounding insulation to heat up. These are glowing connections and over surface char. The increase in temperature causes the insulation to carbonize and produce ignitable gasses [3]. The copper wire would also melt and result in the formation of a gap between the conductors. The carbon deposits further encourage the arcing process by making it more sustainable. The ability of arc faults to cause electrical fires has necessitated research and development in the field of arc fault detection.

In order to successfully detect series and parallel arc faults, we need an Arc Fault Detection Device (AFDD). An AFDD intends to diminish the effects of arcing faults by disconnecting the circuit when an arc fault is detected [2]. The AFDD is able to recognize and distinguish the unique characteristics of arcs.

The absence of a leakage to the ground during a series arc fault event prevents the RCD from detecting such a fault. Furthermore, as the load current is lowered due to the impedance of the series arc fault itself, the current is below the tripping threshold of the circuit breaker and the fuse [2].

It becomes even more important to be able to detect arc faults at the Low Voltage (LV) level, especially in households. The ability of some electrical appliances, used in households, to interfere with or mask arc faults is a major concern to those dealing with arc fault detection. The possibility of an arc fault causing a fire in a home when the owner is not present or asleep has motivated much research in the field of arc fault detection.

Therefore, in order to prevent fire hazards, it is vital to investigate and analyze the characteristics of arc faults and to study household electrical loads that may interact or interfere with the functioning of this device.

## 1.2. Aim of the Thesis

The aim of this thesis is to study and analyze series arc faults at a low voltage level in the presence of household electrical loads. The thesis will provide a component-based approach to characterizing domestic electrical loads and to observe and process the signals and characteristics of these loads in

the presence and absence of a series arc fault. The results will be used to conclude the behavior of different load types and whether loads falling under the same category show similar characteristics. These results are intended to assist in improving the detection of series arc faults in the presence of household electrical loads.

### 1.3. Thesis Overview

The thesis is divided into six chapters. The first chapter is an introduction to the thesis and discusses the motivation behind this work.

The second chapter describes AC arcing faults and major characteristics of arcs which assist in the detection of arc faults.

The third chapter describes the component-based approach to load categorization used in this thesis to categorize household electrical loads in an attempt to analyze their behavior when a series arc is present.

The fourth chapter summarizes the tests required by the IEC62606 standard and explains the test procedure for data collection.

The fifth section gives a brief introduction to continuous wavelet transform (CWT) and explains the characteristics of the arc. It also presents and analyzes the data collected from the tests of the various loads. The data is presented in the time domain, and in time-frequency domain using short-time Fourier transform (STFT) and CWT. Finally, the sixth chapter provides a conclusion of the work.

## 2. AC Arc Fault Detection

### 2.1. AC Arcing Faults

The IEC 62606 is an International Standard which provides the necessary requirements and the testing procedures for Arc Fault Detection Devices (AFDD). In the IEC 62606, an arc is defined as a luminous discharge of electricity across an insulating medium, which usually results in the partial volatilization of the electrodes. The definition of an arc fault is given as a hazardous unintentional arc between two conductors [2]. Evidently, the type of arcing defined as an arc fault is different than the nonhazardous arcs which occur under normal operation of household equipment like dimmers, air compressors, electric drills, etc.

An AFDD is described as a device able to detect and mitigate the effects of arc faults by disconnecting the circuit when such a fault is detected [2].

These arcs may occur due to damaged electrical wiring or misuse of electrical equipment. Electrical wiring may be damaged as a result of drilling into walls with wires behind them, furniture or doors pinching cords, exposure to heat, environmental factors causing aging of wires, etc.

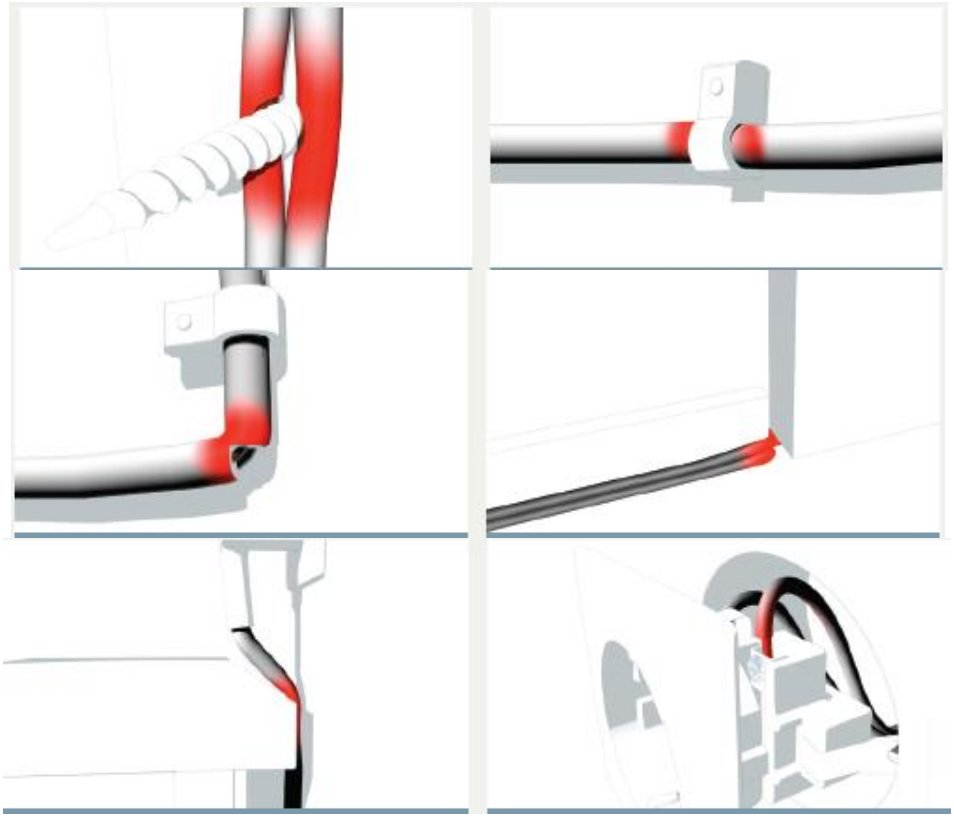

*Figure 2.1. Fault situations frequently discovered in electrical installation systems [4].*

### 2.1.1. Types of Arcing Faults and the Corresponding Protection Devices

There are three types of arc faults which an AFDD must be able to detect. IEC 62606 defines these faults as an earth arc fault, parallel arc fault, and series arc fault. The standard defines the earth arc fault as one which occurs when the current flows from the active conductor to the earth. The parallel arc fault is defined as one where the current is flowing between the active conductors which are parallel to the load of the circuit. Finally, a series arc fault is a result of current flowing through the load of the circuit [2].

#### 2.*1.1.1. Earth arc faults:*

This type of arc fault occurs between a live conductor and the earth conductor. The flow if the current is through the arc from the line conductor to the earth conductor. An RCD with a maximum rated residual current of 300 mA may be used for such a fault [4]. However, if the impedance of the faulty circuit is too high, these devices fail to protect the circuit from such faults. The shutdown conditions necessary for the device to trip are not met and the value of the energy at the fault location cannot be limited in the time necessary to prevent fire.

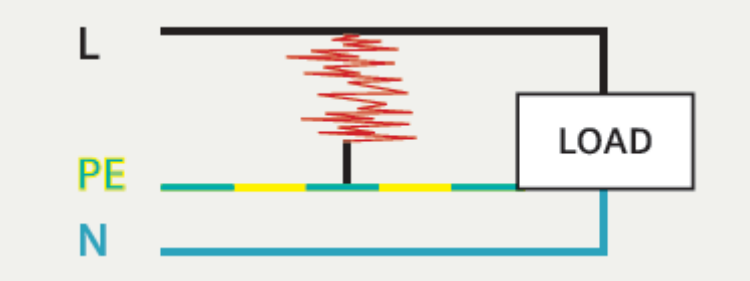


*Figure 2.2. Earth arc fault [4]*

### *2.1.1.2. Parallel arc fault*

These faults occur between two live conductors or a live conductor and a neutral conductor. Since no current flows through the earth conductor, RCDs fail to protect during such faults. MCBs may be able to protect from parallel arc faults depending on factors like the impedances in the faulty circuit, the magnitude of the arc voltage, and whether the conditions for shutdown are met for values like current/time. The limited current level in the case that the impedance is high, prevents the device from tripping in the required time [4].

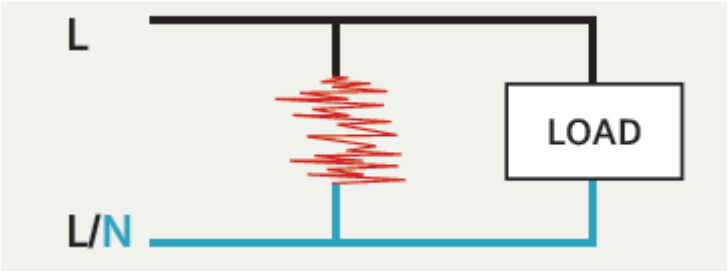


*Figure 2.3. Parallel arc fault* [4]

### *2.1.1.3. Series arc fault*

A series arcing fault occurs in a live conductor in series with the load. There is no current flowing through the earth or the neutral conductor. The current is further reduced as a result of the arc voltage in the series with the load. Hence, RCDs and MCBs are of no use in during the occurrence of such a fault.

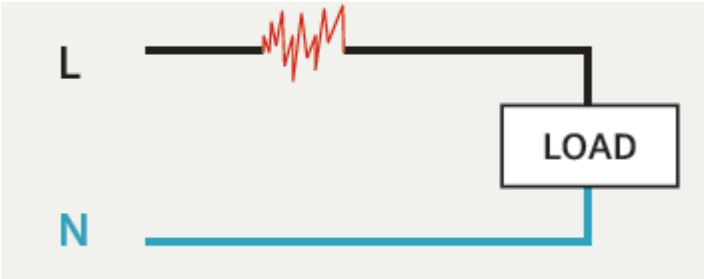


*Figure 2.4. Series arc fault* [4]

In light of this knowledge, it can be concluded that there is a lack of a protection device for series arc faults and an improvement in the protection for parallel arc faults is required.

### 2.1.2. Contact Arcing

There are two hazardous types of arcing which one might expect to see in a low voltage residential circuit. They are:

#### *2.1.2.1. High-energy arc:*

These types of arcs are a result of faults with high levels of current. These high-energy arcs occur when there is either an earth arc fault or a parallel arc fault in the circuit. These faults are high current faults and draw current equal to or greater than the rated capacity of the circuit. These high current faults either arc explosively when the contacts are made and broken physically, dim lights and other loads showing the presence of an excessive load, and/or trip the protective device. These faults are characterized as short-lived and therefore the increase in temperature in the feed conductors is always below a certain level. Hence, the fire danger in these faults is primarily due to the explosive expulsion of tiny glowing globules of copper from the area of contact which may ignite flammable materials close by. Even in the case of an outbreak of a fire, the fact that the fault is highly visible and the likelihood of the presence of someone, who physically brought the conductors together, severely diminishes the probability of an uncontrolled fire [5].

#### *2.1.2.2. Contact Arc:*

These types of arcs are a result of persistent, low-current faults. Contact arcing takes place at connections in series with a load. This means that the maximum current in this arc is limited to the load current. The fact that the load controls the arc current means that it may be low enough to be below the trip rating and hence go unnoticed by the protection device.

Contact arcing is a complex physical phenomenon and, it may be caused by loose connections, oxidized contacts, foreign non-conducting material interfering with the conduction path, differences in contact materials, contact shapes, etc. Under the right conditions, this type of arcing may persist and become a significant fire hazard [5].

At fault locations, contact arcs are caused by direct or indirect physical connection between metal parts which are either moving or have low conductivity. Arcing is a result of the movement of metal parts which were initially physically connected. This movement may be a result of vibration or thermal expansion. This arcing further causes heating and finally results in a fused link. The repetition of this process of heating and breaking of the fused link further contribute to the formation of unstable arcs. Consequently, the electrodes (metal parts) experience high temperatures. The air in the surrounding is ionized and the arc reignites after the zero crossing point of the current. Any combustible materials in the area surrounding the arc are carbonized [4].

Figure 2.5 in [4] describes how a series arcing fault in a constricted cable may result in the outbreak of a fire. Current flowing in a damaged cable tends to increase the temperature of that cable at the point of the constriction. The increase in temperature results in the oxidation of copper into copper oxide. This results in increased resistance which further increases the temperature. This process may even lead to the melting of the copper. At the point when the current is at its peak, gas is formed

resulting in an air gap with arcing. The insulation at the location of the fault is carbonized. Hence a stable arc may burn and result in the outbreak of a fire.

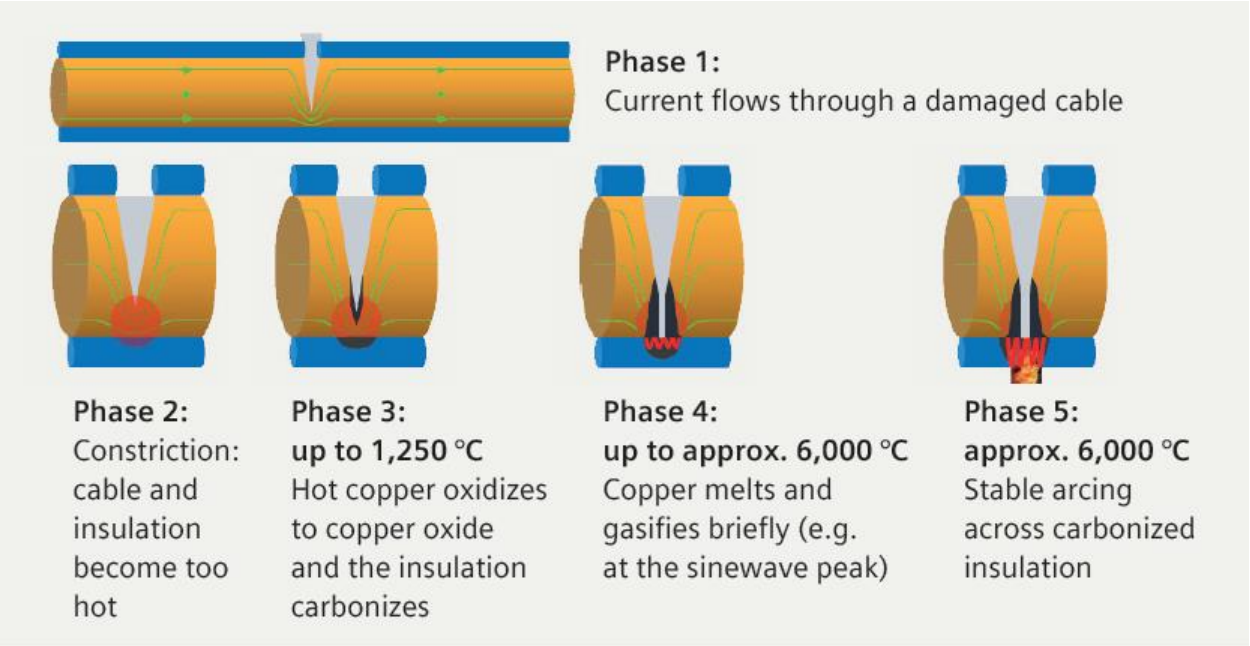


*Figure 2.5.Outbreak of fire due to series arc* [4]

In homes contact arcing may occur in many different locations. Following are a few other examples of conditions which may result in contact arcing, as described in [5].

A wall outlet which applies inadequate pressure to the contacts of the inserted plug. This inadequate pressure fails to guarantee a low resistance connection. The reduction in spring pressure is mostly as result of age and use.

Extension cords with low current carrying capacity are another cause of contact arcing. The elastomeric insulating material surrounding the contacts slowly decomposes due to the heating of the plug. The resistive heating may then result in the insulating material melting and flowing into the contact area. The lack of a proper contact due to this melted insulating material would promote arcing. The process may become repetitive, carbonizing the insulating material, and then forming a thin film of insulation on the surface of the contact.

Oxidation of the contacts in aluminum wiring is also another cause of contacts arcing. Although contact material, which is likely to oxidize, is made to be gas tight, oxidation occurs as contacts become loose over time. Oxidation results in the accumulation of semi-conductive or non-conductive layer around the contacts resulting in arcing.

The wear down of springs, which allow the switches to turn on and off, results in an increase in the time to close and a reduction in the force holding the contacts together.

Another example of contact arcing which is generally found in households is at a light bulb's central contact. The repetitive exposure of the center contact to high temperatures causes it to loosen and oxidize, thereby greatly increasing the probability of contact arcs. The low melting point solder at

the lamp contact melts and reforms during arcing. This process either results in the breaking of the contact or the creation of a new one.

### 2.1. Characteristics of an Arc

According to [6] arcing results in the generation of broadband noise, which could propagate from tens of hertz to 1GHz. Furthermore, the energy pattern of the broadband noise is more likely to fit that of pink noise. Frequency is inversely proportional to energy, hence as frequency increases the energy of the noise decreases.

There tend to be gaps in the frequency spectrum as a result of the extinguishing of arc near the zero crossings regions. The arc gets extinguished when the voltage approaches the zero-crossing and re-ignites when the voltage is sufficient to reestablish the arc across the cable [7].

The AC current waveform of the arc shows that there is a correlation between the zero-crossings region and the absence of broadband energy across the spectrum. In a residential circuit, at the zero-crossing of the AC source, the arc extinguishes itself. An interruption, which matches the periodicity of the AC source, occurs periodically as the arc extinguishes and the flow of current is disrupted [7].

A very important feature of arc faults is that they generate broadband noise. This noise spectrum can range up to 1 GHz. If the behavior of the arc is very consistent, this noise tends to appear only during the conduction of the current as the arc is sustained. As soon as the arc is extinguished the broadband noise disappears. Experimentation has shown that the energy levels of the broadband noise are affected by the branch circuit as well as the magnitude of the current flowing through the arc fault. There is approximately a 60 dB per 50 feet loss due to the branch circuit itself. The amount of current, on the other hand, tends to have a more indirect attenuation. Due to the more violent nature, higher currents make it more difficult to support self-sustained arcs. Furthermore, with higher currents, the amount of broadband noise is reduced as a result of an increase in ionization in the air gap [7].

Another important discriminator of the arc fault is its interruption and periodicity. As the AC source approaches the zero-crossings, the broadband noise disappears. The arc re-establishes and re-extinguishes based on the periodicity of the of the AC source [7]. This means that we are able to distinguish noise which is uncorrelated to the 50Hz.

Moreover, the higher the current the more aggressive the arc fault condition. Arc faults are likely to be more violent at higher magnitudes of current. This also causes a distortion in the time period the fault can last. The time a fault lasts when the current is high is less than that when the current is lower.

## 3. Household Electrical Loads

### 3.1. Characterization of Household Electrical Loads

A systematic approach to categorizing household loads was established to be able to successfully

assess the effect of these loads on arc fault detection. Market research on products available in the market concluded that there are more than 200 different appliances which may be used in residents. Furthermore, each appliance has multiple manufacturers and models, leading to hundreds of thousands of different electrical appliances. In light of this knowledge, it is of crucial importance that a systematic approach, with valid technical specification, be employed in order to study the effect of loads on series arc faults.

The Google product category list [8], which Google provides to ensure that advertisements of products are shown with the right search results, was used to narrow down about 300 loads from a list of more than 5427 end products, and it is important to note that this number does not include models or manufacturers. Other lists were also consulted, like Amazon, Walmart, Alibaba, etc [9, 10]. Finally, a database of all the possible household loads was created.

The task further requires the classification of household loads in order to simplify analysis. The component-based categorization method was utilized. Figure 3.1 shows the load categorization used, which was adapted and adequately modified from [11].

The loads tested in this thesis are categorized according to this method. Unfortunately, it was not possible to test loads from all the categories. Nonetheless, the aim was to obtain as many loads categories as possible. The EEL category was not tested in this work, as well as the SASD subcategory of the SPIM, and the no-PFC subcategory of SMPS.

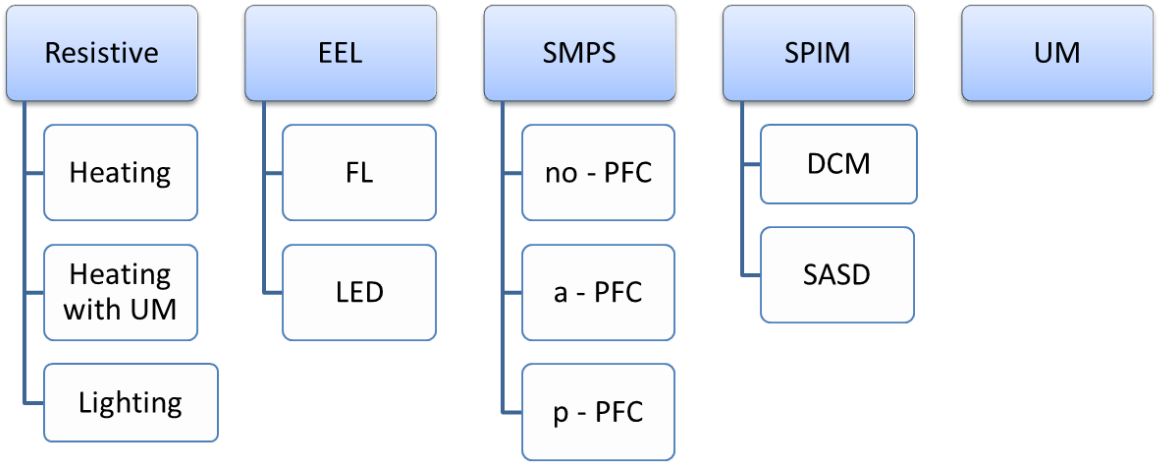


| | |
|---|---|
| UM | Universal Motor |
| SPIM | Single Phase Induction Motor |
| DCM | Directly Connected Motor |
| SASD | Single Phase Adjustable Speed Drive |
| SMPS | Switched Mode Power Supply |
| No-PFC | No Power Factor Correction |
| A-PFC | Active Power Factor Correction |
| P-PFC | Passive Power Factor Correction |
| EEL | Energy Efficient Lighting |
| FL | Fluorescent Lamp |
| LED | Light Emitting Diode |

*Figure 3.1. Component-based approach to load categorization.*

## 3.2. Resistive Loads

In residential settings, resistive loads are typically used to convert energy into heat. Most electrical heaters and general incandescent lamps fall under this category of household loads.

Resistive loads do not generate a magnetic field. Their main characteristic is that the current and voltage are in phase. However, due to the instantaneous rise of the current from zero to the steady state value, and not a value higher than that, they are said to have a small inrush current.

The following are the three categories which resistive loads were further divided into.

- **Heating**

Common examples of resistive, heating loads are; soldering irons, hair straighteners, irons, cooktops, electric kettles, and space heaters. These are the loads which will also be observed in this thesis under this category.

- **Heating with UM**

Common examples of resistive, heating with UM loads are; hair dryers, dishwashers, space heaters (with a fan). These are the loads which will also be observed in this thesis under this category.

- **Lighting**

Common examples of resistive, lighting loads are incandescent light bulbs. These are the loads which will also be observed in this thesis under this category.

## 3.3. Energy Efficient Lighting

The survey held in 2006 by the International Energy Agency [12] concluded that lighting makes up approximately 19% of the total global electricity consumption. The residential sector makes up around 31% of the electricity consumed by lighting. Furthermore, 18% of the total residential sector demand is estimated to be due to lighting.

Energy efficient lighting (EEL) has gained popularity worldwide and are highly likely to replace GILs. In light of this information, it is important to include this category while characterizing household load.

The two main types of energy efficient light bulbs are Compact Fluorescent Lamps (CFLs), and Light Emitting Diodes (LEDs).

- **Fluorescent Lamps**

The main type of fluorescent lamps used in residential settings is Compact Fluorescent Lamps (CFLs). They get their name from their compact design, which is obtained by bending a traditional fluorescent tube. They are designed to fit into most present light fixtures. They are characterized as a smaller version of the fluorescent tube. The main mechanism involves glowing phosphor gas using electric current. The electromagnetic ballast, which caused flickering, is now being replaced with an

electronic ballast. CFLs are approximately four times more energy efficient than GILs. Furthermore, CFLs tend to have a longer lifetime.

Figure 3.2 shows the components of a CFL bulb. Light is produced when an electric current passes through the tube which contains argon and a small amount of mercury vapor. CFLs require a higher level of energy when they are first turned on. However, they are more efficient than incandescent bulbs after the first turn on. The ballast assists in starting the bulb and regulates the current during the first 30 second to 3 minutes. This results in a delay in the time it takes the bulb to light up fully.

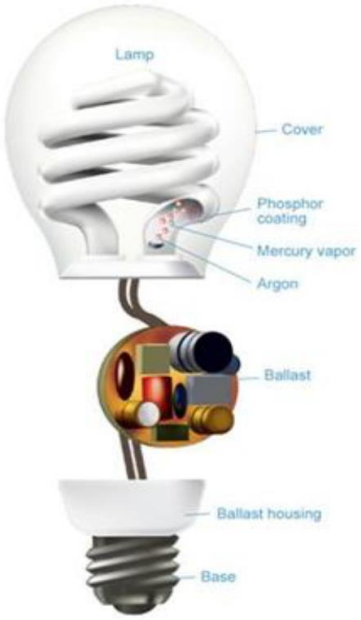


*Figure 3.2. Components of a CFL [13].*

The electronic ballast first converts the AC to DC at a low frequency, then performs a DC-to-AC conversion on a high frequency at the output. Once the bulb is ignited the current is controlled in order to achieve the required power and brightness level [13].

- **Light Emitting Diodes**

Although LEDs were being used in household appliances and computers, their potential as an energy-efficient alternative to GILs has recently been acknowledged. The lack of a burning gas or filament in LEDs reduces the amount of heat produced and increases their durability.

LEDs are solid state semiconductor devices. They operate like a semiconductor diode and emit light when current passes through the PN junction, from the anode to the cathode. LEDs operate on direct current and hence the supplied voltage needs to be rectified and applied across the diode semiconductor crystal. The rectified voltage provides the required forward voltage, across the junction, to turn on the diode. The excess energy released during the recombination of holes and electrons at the PN junction is converted to light [13].

## 3.4. Switched Mode Power Supply

Switched mode power supplies (SMPSs) are among the most common loads found in domestic applications. Common Loads falling under this category are PCs, monitors, televisions, DVD players, recorders, etc.

The higher efficiency and smaller size of SMPS make it more popular than a linear power supply. SMPSs draw a non-sinusoidal waveform, which gives rise to a phase angle between the input current and the voltage. When the current and voltage are not in phase, we get a power factor which is less than 1. A power factor of less than 1 causes power losses. Furthermore, a power factor of less than 1 introduces harmonics down the neutral line and cause disruption of other devices in the AC mains line. The harmonic content ointroduced to the AC line increases as the power factor decreases.

The IEC61000-3-2 requires that switched mode power supplies must comply with the regulatory requirements. In order to reduce their harmonic content, devices with input power greater than 75W must use some sort of power factor correction [14].

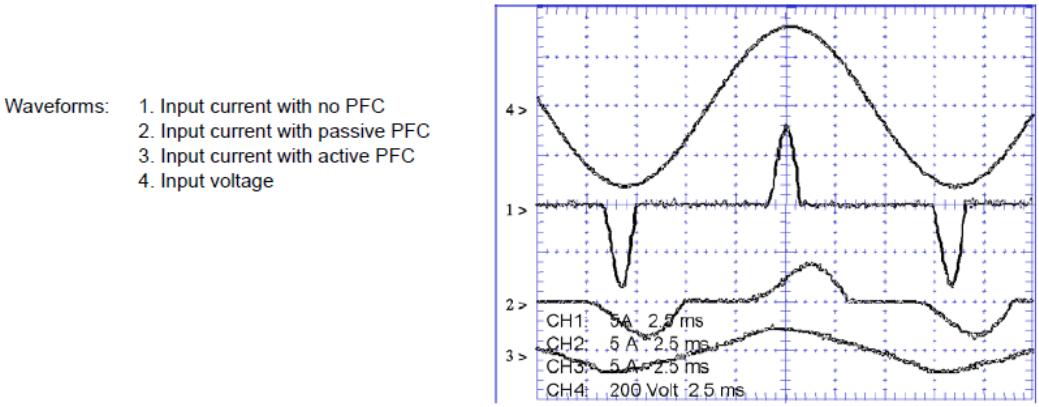


*Figure 3.3. Input characteristics of PC power supply with different PFC types [14].*

The harmonic limits discussed above mean that the dc power supply load type should be subdivided into three following sub-types:

- **No Power Factor Correction**

If the rated power of the SMPS is below 75W, it does not include an inductor in the rectifier circuit.

- **Active Power Factor Correction**

If the rated power of the SMPS is above 75W, it has an additional dc-dc converter stage to control the input current, making it sinusoidal and in-phase with the supply system voltage

- **Passive Power Factor Correction**

If the rated power of the SMPS is above 75W, it has an inductor in the rectifier circuit.

## 3.5. Single Phase Induction Motors

Single-phase induction motors (SPIM) make up a major fraction of the household loads. They are one of the most widely used AC motors. In residential settings, they are part of loads like refrigerators, freezers, household air conditioners, fans, and pumps.

SPIM are used in situations where a fixed speed is required. It is reliable and has a simple design. The construction includes a magnetic core and a pair of stationary coils called the stator. The rotating part is called the rotor.

Evidently, they are called single phase because they run on a single-phase AC supply. However, these motors are not self-starting and may require capacitors or inductor for starting and in some cases even running.

Speed control in SPIM tends to be more difficult compared to universal motors. Continuous speed control is usually not provided, but dual speed control may be possible by selecting the wiring of the stator winding. In order to rectify this situation, there has been an increase in the popularity of the more sophisticated single-phase adjustable speed drives (SASD).

There are two main sub-categories which the SPIM may be divided into. These are:

- **Directly Connected Motors**
- **Single Phase Adjustable Speed Drive**

In order to improve efficiency, there is an interest in replacing directly connect motor (DCM) with SASD. SASD deliver better speed and performance control and offer improved efficiency. According to [15] annual energy savings of approximately 13% may be achieved by using SASD.

## 3.6. Universal Motors

The universal motor is a major component of many household loads. In domestic appliances, they are mainly used for their wide speed range. It is widely found in handheld appliances like routers, jigsaws, sanders, table saws, small jointers, portable drills, hair dryers, grinders, polishers, blowers, and kitchen appliances etc. Universal motors are also employed in cases where high speed or speed control is required. They tend to be significantly smaller in size when compared to AC motors operating at the same frequency.

The universal motor gets its name from the fact that it can operate on both AC and DC power. It is a commutated series-wound motor. The stator's field winding is connected in series with the rotor windings through a commutator. The universal motor differs from a DC series motor only slightly, and in such a way that it allows it to work properly in AC. The fact that the current in both the armature and the field coils alternates synchronously with the supply allows this motor to work well on AC. Therefore, the resulting mechanical force occurs in a consistent rotational direction, which is not dependent on the direction of the supply voltage but is controlled by the commutator and the polarity of the field windings.

Universal motors are able to run at high speeds, have high starting torque, and are lightweight and compact. They can be easily controlled electromechanically with the use of tap coils or electronically. A drawback of the universal motor is that the commutator brushes tend to wear out, which makes them less common in appliances which are used for long periods without breaks. Another drawback is that they are acoustically and electromagnetically noisy [16].

# 4. Tests and Measurements

## 4.1. European Standard Test Procedure

This section includes a description of the test procedure and the list of the equipment used during the testing. The test procedure is outlined in the European Standard IEC 62606. The standard provides the testing procedure for series arc fault and also describes the procedure for preparing the cable specimen to be used to generate an arc fault.

In order to test for a series arc fault, a cable specimen, prepared according to the instructions given in the succeeding section, will be used.
Nonetheless, the required specifications of an arc generator have also been included. However, as mentioned in [2], the arc energy during arcing generated with a carbonized path (prepared cable specimen) is approximately 2.5 times the arc energy provided when using the arc generator. This further concludes that when an arc generator is used, the AFDD should clear a series arc fault in less than 2.5 times the break time given in Table 4.1.

### 4.1.1. Cable Specimen

In the IEC 62606 standard, the cable type could be made up of two separate conductors, with a cross-sectional area of 1.5 $mm^2$, which may be joined together using adhesive tape or an equivalent medium. The cable with parallel conductors may also be used. The standard specifies that the cable H05VV-F, which has two conductors, is particularly appropriate, and is the one used in the tests conducted for this thesis.

The chosen cable will be prepared in the following way, as specified in the European Standard. Figure 4.1 shows a diagram of the preparation of the cable specimen.

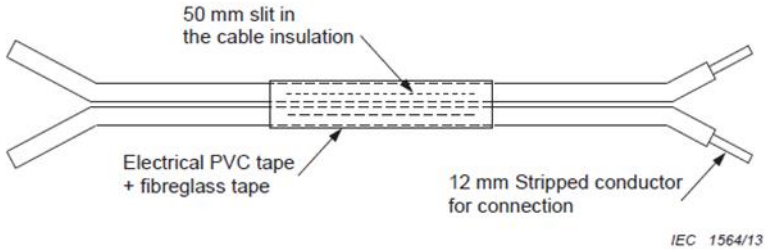


*Figure 4.1. Preparation of the cable specimens [2].*

1. A cable with a suitable material and geometry must be chosen, in order to perform a satisfactory carbonization between the conductors and initiate arcing when rated voltage is applied.
2. The length of the cable specimen must not be less than 200 mm and the individual wires at each end of the cable are to be separated for a length of 25 mm.
3. The conductors are to be exposed by slitting both wires (without damaging any strands). This slit is to be made at a length of 50 mm from one end.
4. The slit in the insulation must then be covered with a double layer of electrical grade black PVC tape and further wrapped with a double layer of fiberglass tape.

5. The test circuit will be connected at the end of the conductor which is furthest from the slit. The insulation at this end will be stripped to a length of 12 mm approximately.

In order to create a carbonized conductive path through the insulation between the two conductors of the cable, the cable specimen will be conditioned in the following way;

6. Connect the cable specimen to a circuit with a short circuit current of 30 mA and an open circuit voltage of minimum 7 kV. This connection is to be maintained for approximately 10 s or until the smoking stops.
7. Next, connect the cable specimen to a circuit with short circuit current of 300 mA at a voltage of minimum 2 kV or appropriate to cause the current to flow. The connection is to be maintained approximately one minute or until smoking stops.

The carbonized path is complete when a 100 W/230 V incandescent lamp turns on at 230 V or a resistance with an equivalent resistance value.

### 4.1.2. Arc Generator

As shown in figure 4.2, the arc generator consists of a stationary and a moving electrode.

One of the electrodes is a carbon-graphite rod with a diameter of 6 mm ± 0,5 mm. The other electrode is a copper rod. The end of the rod/s at which arcing will occur may be pointed.

In order to have repeatable arc conditions, cleaning and sharpening the rods may be required.

Connecting the arc generator to the test circuit will result in the generation of a consistent arc between the two electrodes given that they are separated at a convenient distance.

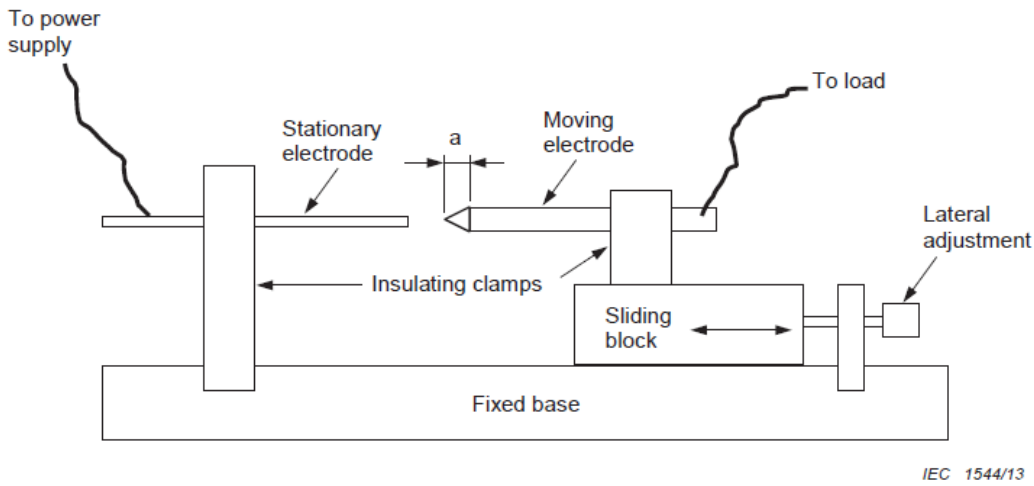


*Figure 4.2. Arc generator* [2].

### 4.1.3. Series Arc Fault Tests

An AFDD with rated voltage of 230 V must clear an arc fault in the break time given in Table 4.1.

5.3.7.1 **Limit values of operating criteria for AFDDs at low arc currents up to 63 A**

**Table 1 – Limit values of break time for $U_n$ = 230 V AFDDs**

| **Test arc current** (r.m.s. values) | 2,5 A | 5 A | 10 A | 16 A | 32 A | 63 A |
|---|---|---|---|---|---|---|
| **Maximum break time** | 1 s | 0,5 s | 0,25 s | 0,15 s | 0,12s | 0,12 s |

*Table 4.1. Limit values of break time for AFDDs with 230V nominal voltage [2].*

The following test procedures must be conducted using the cable specimen prepared according to the procedure explained in Section 4.1.1, and according to the circuit given in Figure 4.3.

The test is to be conducted at the rated voltage of the AFDD, in this case at 230 V. The general procedure for series arc fault tests as described in the European Standard IEC 62606 requires that the device be tested at each arc current level and the measured value must not, at any time, exceed the times given in Table 4.1 [2].

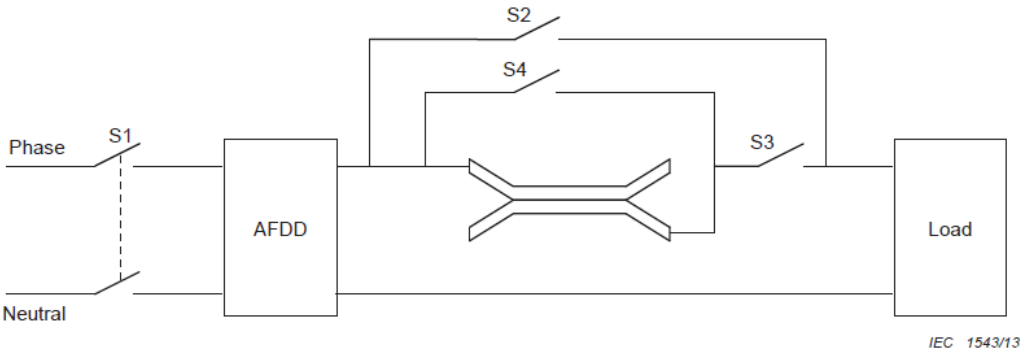


*Figure 4.3. Test circuit for series arc fault tests* [2].

The tests for series arc fault tests, as described in [2] are to test for arc faults occurring at different operating cycles. The following section provides a description of the tests as explained in [2].

*4.1.3.2. Sudden appearance of series arc in the circuit:*

This test verifies the correct operation of the AFDD in the case of a sudden appearance of a series arc.

The procedure of the test requires that the switches S1, S3, S4, and the AFDD, shown in figure 4.3, are closed (conducting) and the test current is stable. The resistive load is used to adjust the test arc current from lowest arc current till the rated current of the AFDD. Then, the test switch S2 is opened (not-conducting).

In order to insert the cable specimen in series with the load, the switch S4 is suddenly opened. Three measurements of the break time are taken and all should be within the limit provided in Table 4.1.

The switches S2 and S4 when closed, bypass the prepared cable specimen. In order to introduce an arc fault into the circuit, they should both be closed.

#### *4.1.3.3. Inserting a load with a series arc fault:*

This test verifies the correct operation of the AFDD in the case of a load is inserted with a series arc fault.

The procedure of the test requires that switches S3 and S4 are open, and switch S1 and the AFDD are closed. The resistive load is used to adjust the test arc current to the lowest current value provided in Table 4.1. The switch S2 is then opened. While the AFDD and the switch S1 are closed and the switches S4 and S3 are open, the switch S3 is closed abruptly to supply the load with a series arc fault.

Three measurements of the break time are taken and all should be within the limit provided in Table 4.1. The test is repeated for the rated current value of the AFDD.

#### *4.1.4.4. Closing on series arc fault:*

This test verifies the correct operation of the AFDD in the case of closing on a series arc fault.

The procedure of the test requires that switches S1, S3, and the AFDD are closed. The resistive load is used to adjust the test arc current to the lowest current value provided in Table 4.1. First, the switch S1 is opened, then the switch S2 is opened. While the switches S1 and S4 are open, the switch S1 is abruptly closed to supply the load and the AFDD with a series arc fault.

Three measurements of the break time are taken and all should be within the limit provided in Table 4.1. The test is repeated for the rated current value of the AFDD.

## 4.2. Test Procedure

The test circuit of figure 4.4 shows the setup of the experiment. The voltage V1 refers to the mains voltage, V2 to the arc voltage, and I is the current passing through the test circuit.

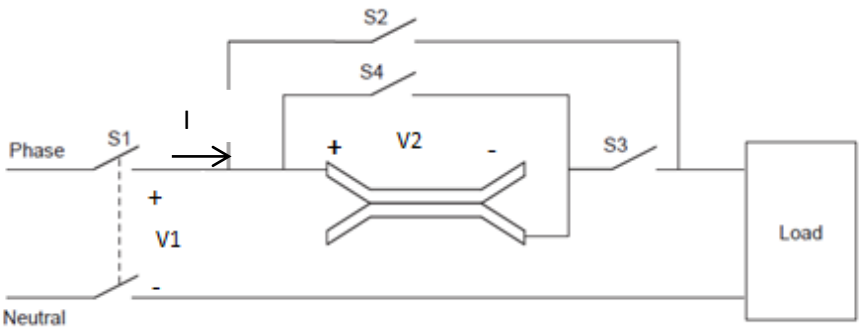


*Figure 4.4. Test circuit*

The cable was prepared using the high voltage power source and the high voltage test cage shown in figure 4.5. The prepared cable was placed inside a casing with a transparent lid to contain the smoke and ensure the safety of the testers. Furthermore, a fume extractor was also used for safety purposes.

The carbonized path was prepared in accordance with the IEC 62606 standards. Please refer to the relevant section for more information regarding the preparation of the cable.

Table 4.2 gives a list of the equipment used in this experiment.

| Test Equipment | Specification |
|---|---|
| Oscilloscope | Teledyne Lecroy - HDO4054-MS 500MHz High Definition Mixed Signal Oscilloscope 2.5GS/s |
| Spectrum Analyzer | Keysight MXA Signal Analyzer N9020B, 10Hz – 8.4GHz |
| Current Probe | Teledyne Lecroy - 30A 100MHz |
| Current Probe | Solar Electronics - R.F. Current Probe, Type 99123-1N, 10kHz to 500MHz |
| Voltage Probe | Teledyne Lecroy – High Voltage Differential Probe |
| Voltage Probe | Teledyne Lecroy – High Voltage Differential Probe |
| Fume Extractor | Weller - WFE2ESKIT1 |
| High Voltage Power Source | Technix - 10 kV, 300 mA |
| High Voltage Test Cage | Sefelec (Eaton) |

*Table 4.2. List of Equipment used in the test.*

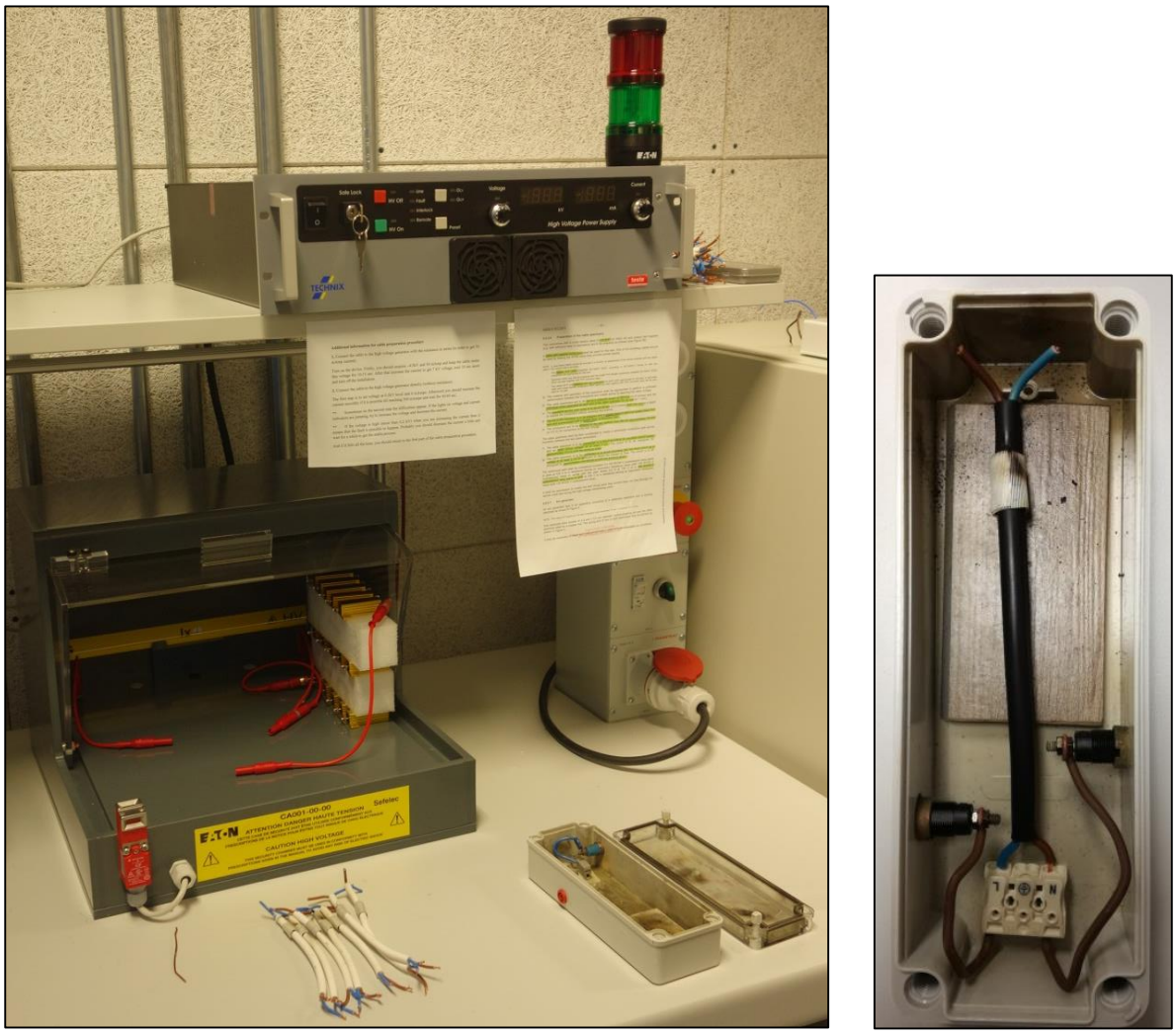

*Figure 4.5. The high voltage power source and test cage (left) and prepared cable (right).*

Table 4.3 gives the loads that were tested.

| Household Load Tested | Load Type |
|---|---|
| **Space Heater** | Resistive – Heating |
| **Iron** | Resistive – Heating |
| **Hair Straightener** | Resistive – Heating |
| **GIL** | Resistive – Lighting |
| **Hair Dryer** | Resistive + UM - Heating |
| **Vacuum Cleaner** | UM |
| **Cultivator** | UM |
| **Humidifier** | SPIM + Resistive – DCM +Heating |
| **Desk Fan** | SPIM – DCM |
| **Power Drill** | SMPS – p-pfc |
| **Power Supply with p-pfc** | SMPS – p-pfc |
| **Power Supply with a-pfc** | SMPS – a-pfc |

*Table 4.3. Loads used.*

The test setup is given in figure 4.6. The oscilloscope was used to measure V1, V2, and I. The probes used to measure the voltages are the Teledyne Lecroy high-voltage differential probes and the current was measured using the Teledyne Lecroy current probe. The high-frequency component of the same current was measured with the spectrum analyzer using the RF current probe by Solar Electronics. Both the current probes are placed inside the casing shown on the right in figure 4.6. The high-voltage differential probes are also visible. The casing was prepared according to the test circuit given in the IEC62606 standard and is identical to the test circuit provided in figure 4.4.

The sampling rate of the oscilloscope was 100MS/s. In the case of the spectrum analyzer the sample rate chosen was 50MHz and the measurement time was 60ms.

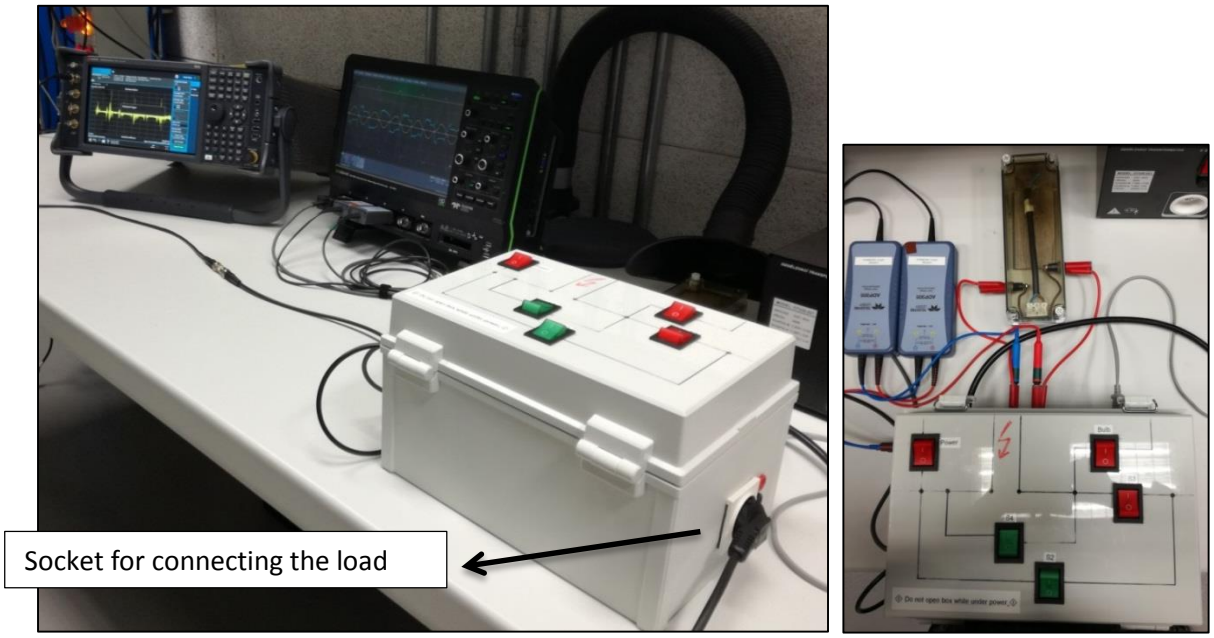


*Figure 4.6. Test setup(left) and the casing (right).*

The test was conducted in a systemized manner to make the most efficient use of resources at hand. Each load was tested twice, the first time to record the load characteristic waveforms, and the second time to record the load characteristics in the presence of a series arc.

The switch S4 shown in figure 4.4 bypasses the carbonized path when it is closed (conducting). Hence it is kept in the position for the first part of the test. In order to add the series arcing the S4 is opened (not-conducting) and the waveform is recorded.

After the collection of the data, MATLAB was used for processing the data. The Wavelet Toolbox and the Signal Processing Toolbox were utilized for obtaining the STFTs and CWTs. In order to be able to read the data from the Oscilloscope, a special function was required.

# 5. Test Results and Data Analysis

## 5.1. A Brief Introduction to Continuous Wavelet Transform

The Continuous Wavelet Transform (CWT), much like the Fourier transform, measures the similarities between a signal and an analyzing function by making use of inner products.

The Fourier transform employs complex exponentials, $e^{j\omega t}$, as the analyzing function. This results in a transform which is a function of a single variable, ω. The short-time Fourier transform (STFT), on the other hand, employs windowed complex exponentials, $w(t)e^{j\omega t}$, as the analyzing function. The result of the STFT is a function of two variables. The STFT coefficients, $F(\omega,\tau)$, signify the match between a signal and a sinusoid. Where ω denotes the angular frequency of the sinusoid and τ denotes the center of an interval of a specified length [17].

The analyzing function used in the CWT is called a mother wavelet and is denoted by ψ. The wavelet is shifted and compressed or stretched and compared to the signal. Scaling is the term used to define the compression or the stretching of a signal, and the scale refers to the factor by which the scaling is achieved. The signal is compared to the wavelet at numerous scales and positions, and a function of two variables is obtained. The CWT for a scale parameter, a>0, and position, b, is:

$$C(a,b;f(t),\psi(t)) = \int_{-\infty}^{\infty} f(t)\,\frac{1}{a}\,\overline{\psi}\left(\frac{(t-b)}{a}\right)dt$$

*Equation 5.1. Continuous wavelet transform* [17]

Where Ψ(t) represents the mother wavelet and the over-line denotes the operation of complex conjugate. The values of coefficients are highly dependent on not only the values of the scale and position but also on the chosen wavelet.

The CWT coefficients, C(a,b), are obtained by continuously changing the values of a and b, the scale parameter and the position parameter respectively.

In order to obtain the wavelets of the original signal, one only has to multiply each coefficient by the suitably scaled and shifted wavelet.

One of the greatest strengths of the wavelet transform is that it allows you to choose any mother wavelet which simplifies your detection of a particular signal feature.

The time-scale representation is a different way to view data. The scale is inversely proportional to the frequency. The more stretched the wavelet, the higher it's scale. This means that when we stretch a wavelet, the portion of the signal with which it is compared is longer, which makes the signal features of the wavelet coefficients coarser.

This feature has been summarized in [17] in the following way:

- Low scale *a* ⇒ Compressed Wavelet ⇒ Rapidly changing details ⇒ High-frequency ω.
- High scale *a* ⇒ Stretched Wavelet ⇒ Slowly changing, coarse features ⇒ Low-frequency ω.

The STFT creates a local frequency analysis by windowing the signal. A limitation of this approach is the constant window size. If a longer time window is selected, the frequency resolution is improved, but the time resolution is compromised. This compromise in the time resolution results in the loss of all time resolution over the duration of the window. On the other hand, if a shorter time window is selected, time localization improves but frequency resolution diminishes [17].

Wavelet analysis solves this problem by introducing a windowing technique with variable-sized regions. Wavelet analysis permits the utilization of long time intervals when more detailed low-frequency information is required, and shorter regions when high-frequency information is required [17].


*Figure 5.1. Wavelet Transform with variable-sized windows* [17].

Figure 5.2 compares and contrasts time, frequency, time-frequency, and time-scale representations of a signal.

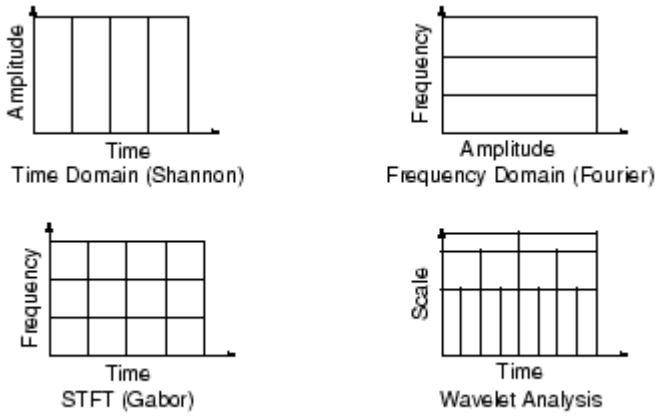


*Figure 5.2. Time, frequency, time-frequency, and time-scale representations of a signal* [17]

The mother wavelet used to obtain the CWT of the data is analytic Morse wavelet with symmetry parameter of 3 and a time-bandwidth product of 6. The comparison with bump and Morlet wavelets is was conducted and Morse wavelet was chosen as the most suitable mother wavelet.

## 5.2. Arc Characteristics

The following figures show the characteristics of arcing. The load connected was a 1200W Space Heater, which assisted in capturing the arc current and voltage.

Figure 5.3 shows the time domain representation of the arc. The property of the arc to extinguish itself before the voltage reaches the zero crossing, and then to re-ignite once the voltage has reached a certain value, is clearly visible in the second waveform in figure 5.3. The arc current clearly has a shoulder-like feature at these zero crossing points.

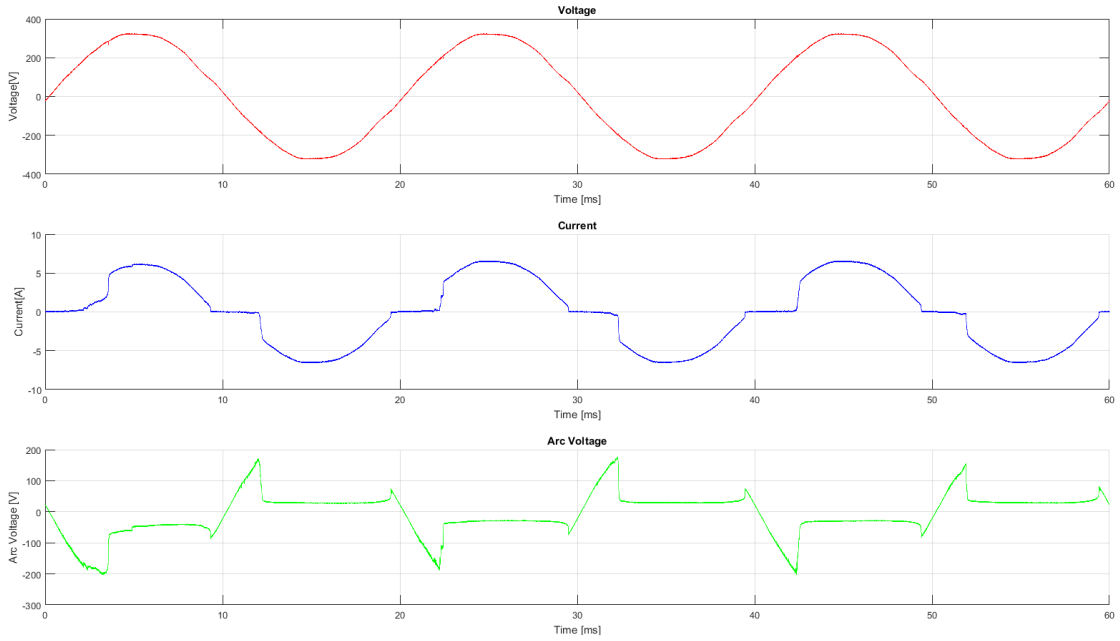


*Figure 5.3. Time domain representation of the arc.*

In figure 5.4 we see the broadband noise that is generated during arcing. The second waveform in this figure shows the high-frequency component of the arc current in the time domain. We observe that there are clusters before and after the zero crossing points. The third waveform shows the spectrogram obtained using the high-frequency component of the arc current. The yellow bursts, shortly after the zero crossing points, are clearly visible along with the lower magnitudes of noise level showing silence time at the zero crossings. The yellow bursts correspond to a sudden increase in the magnitude of the current as a firm conducting channel of arcing is established. This is the reason why the maximum lies in the lower frequency region. The “bands” of higher magnitude parallel to the zero crossings, however, seem to be more significant in the lower frequencies in the spectrogram. The interruption and periodicity of the arc are clearly visible.

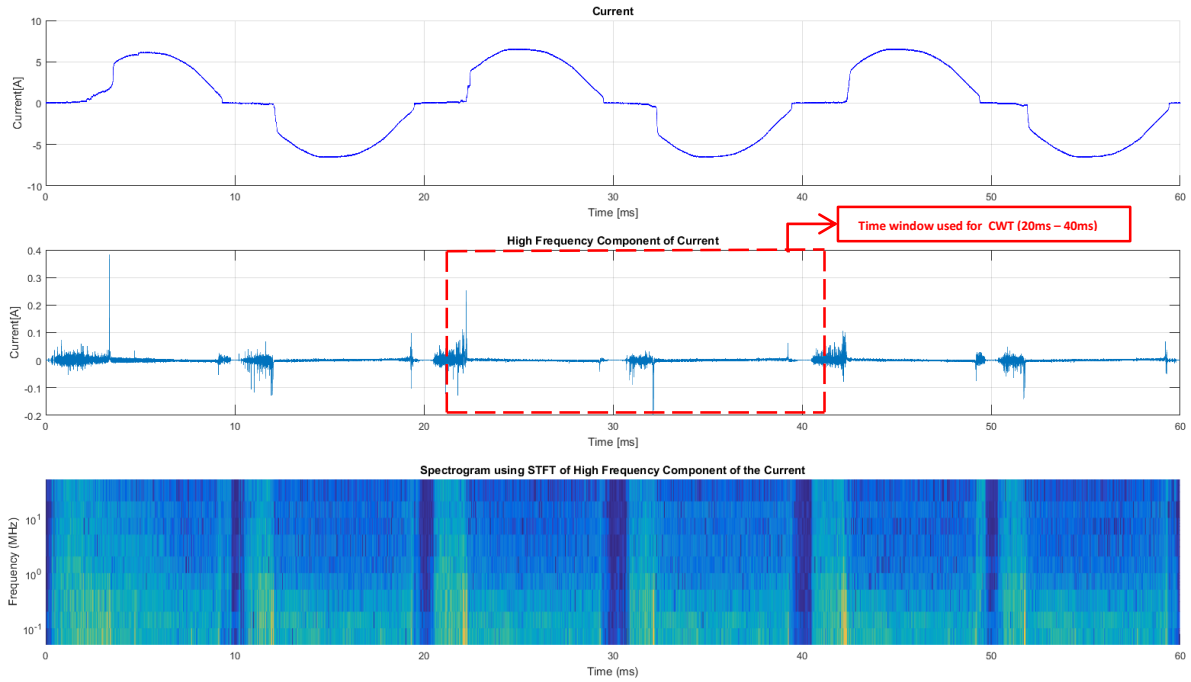


*Figure 5.4. High-frequency component and STFT of the arc.*

The CWT was applied to the high-frequency component of the arc current from the period starting from 20ms to 40ms.

In figure 5.5 a scalogram shows the time-frequency domain representation of the high-frequency component of the arc current. The scalogram was obtained using the CWT. Here we have got a much better visualization of the broadband noise, due to arcing, which propagates from around 31 kHz all the way to 16 Mhz. Furthermore, the zero crossing, having components with lower magnitudes, are clearly visible. Finally, we also observe the higher frequency components of the arc around zero crossings and throughout the whole period that the arc is present. The disappearance of the broadband noise as soon as the arc extinguishes is evident. The periodicity of the arc is also highlighted.

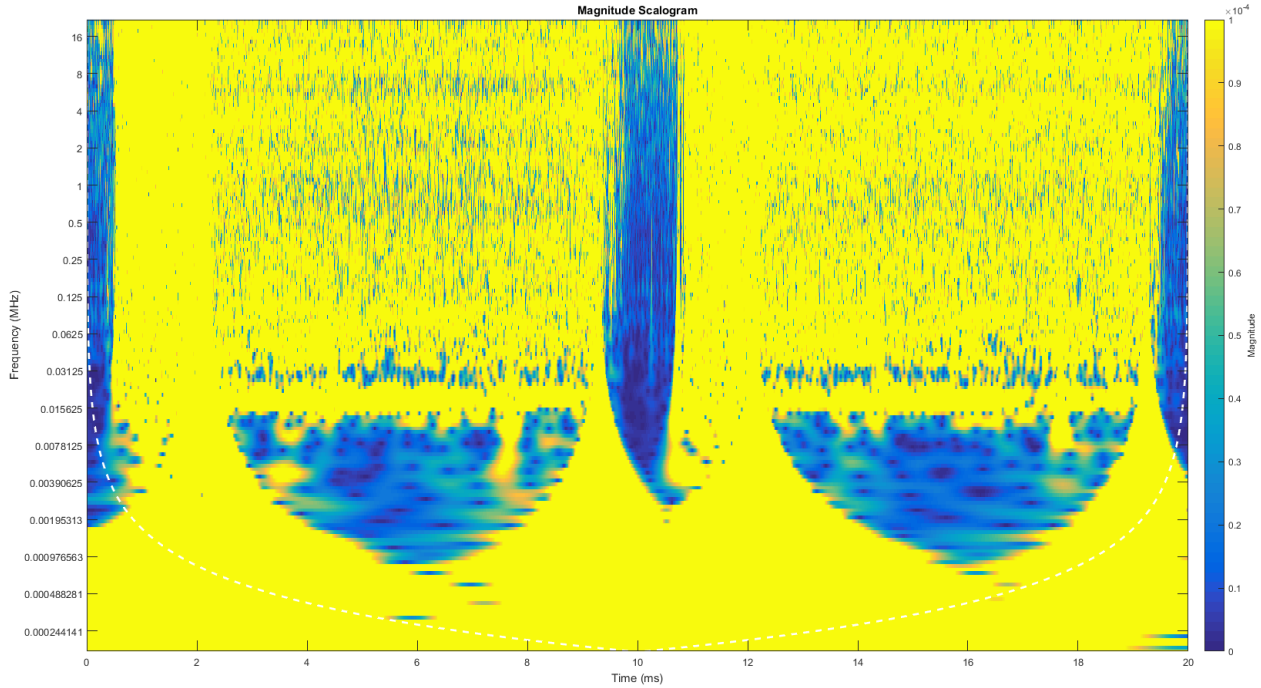


*Figure 5.5. Scalogram of arc obtained using CWT.*

## 5.3. Resistive:

A resistive load is the simplest of the loads and does not contribute to nuisance tripping. The following resistive loads were and will be studied.

### 5.3.1. Space Heater

A 2000W space heater was used in the test. Two tests were conducted with this load, the first one was to capture the load signal. The second test captures the load in series with the arc. The two cases (with and without arcing) were compared in the time domain and in the time-frequency domain, using STFT and CWT.

#### *5.3.1.1. Time Domain*

The arc current and voltage, when a resistive load is connected in series with an arc, show typical arcing behavior.

Figure 5.6 shows the waveforms of the resistive load without arcing (a) and with arcing (b). The second waveform in both figures is that of current. In the case with the arc, the shoulders at and next to the zero crossings are clearly visible. The arc voltage is also very typical. The resistive load does not cause any distortion in the arc current or voltage. The arc voltage waveform in the figure 5.6a shows the noise level.

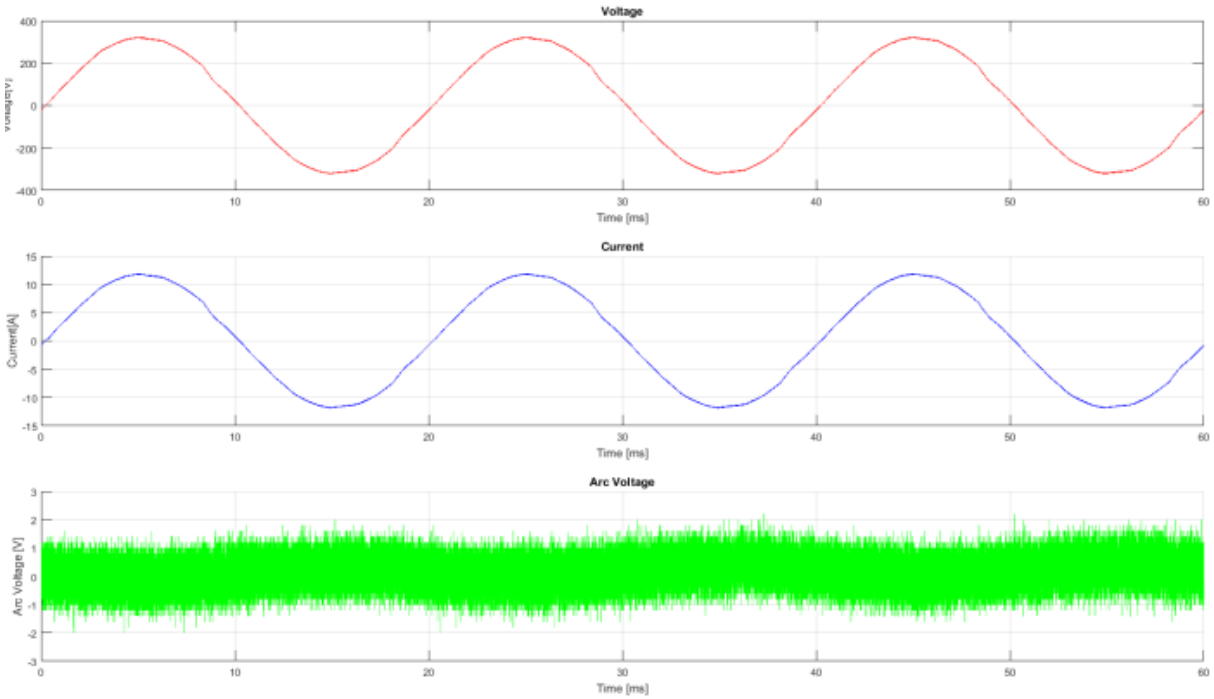


*Figure 5.6a. Time domain representation of the space heater.*

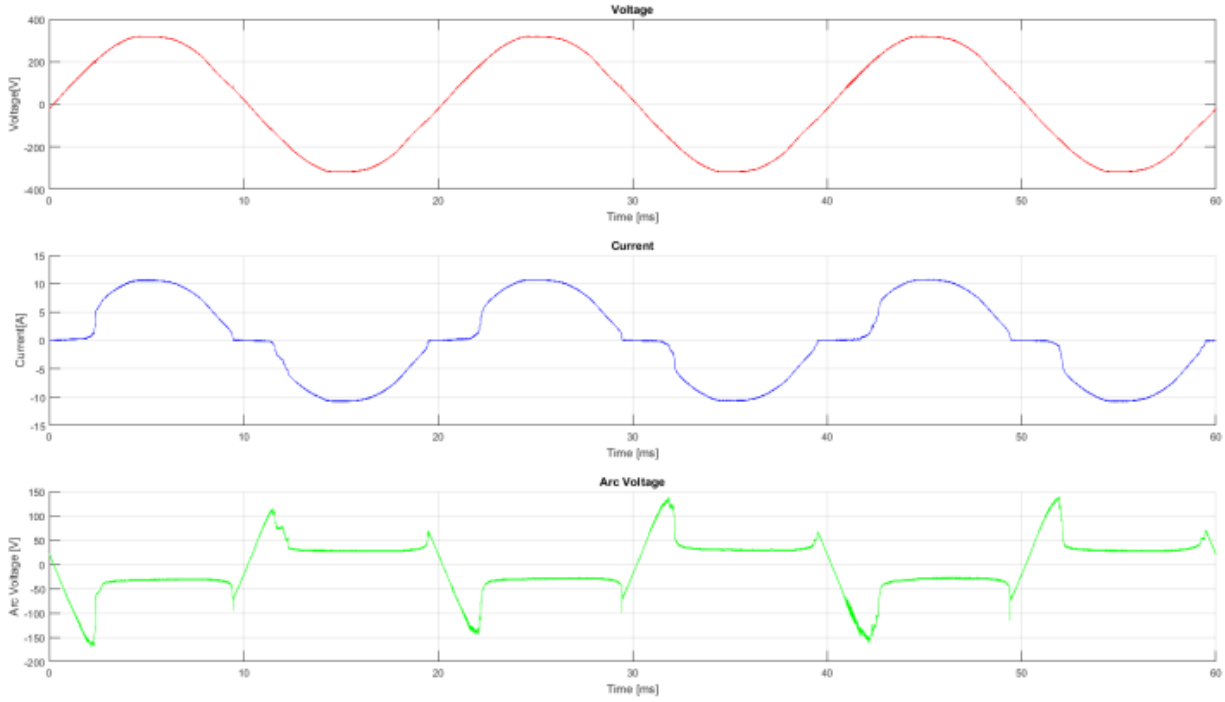


*Figure 5.6b. Time domain representation of the space heater with series arc.*

### *5.3.1.2. Short Time Fourier Transform*

Figure 5.7b shows the high-frequency component of the arc and its STFT. The high-frequency component of the current is periodic and shows clusters before and after the zero crossings. The STFT of the high-frequency component of the current shows that there are components of the signals with higher frequencies present around the zero crossings. However, we cannot observe the broadband noise during the time when the arc is stable.

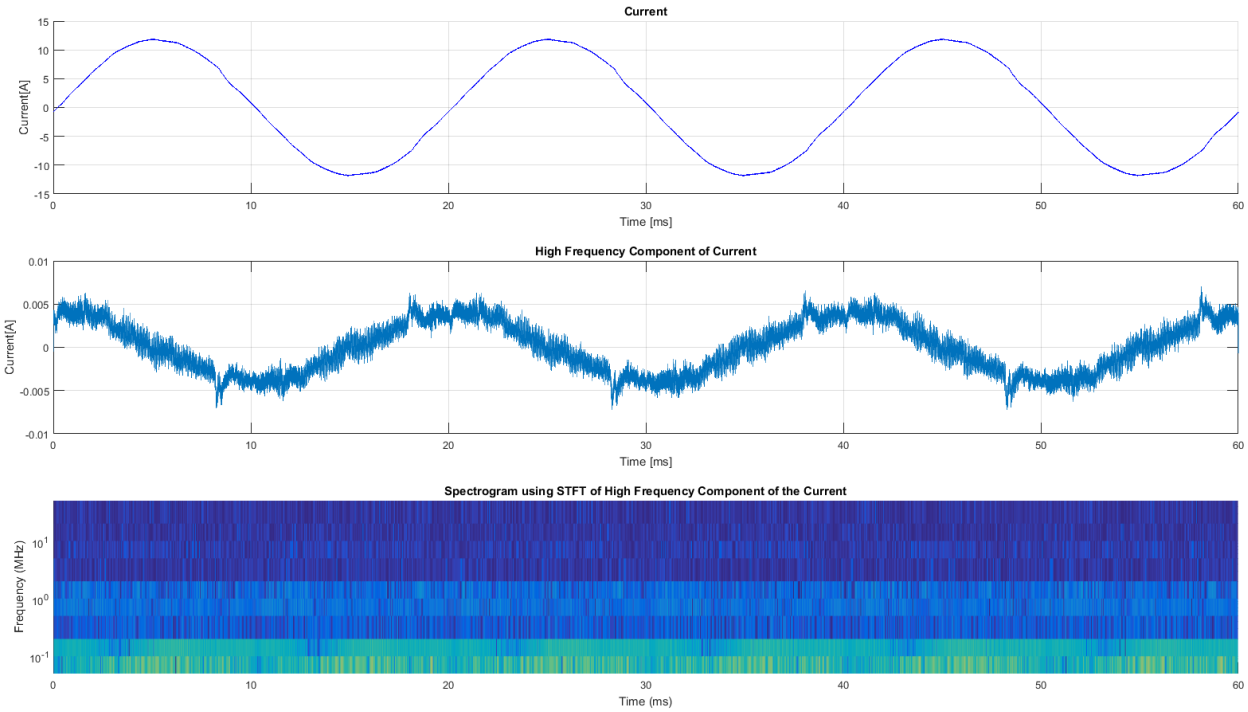


*Figure 5.7a. High-frequency component and STFT of space heater.*

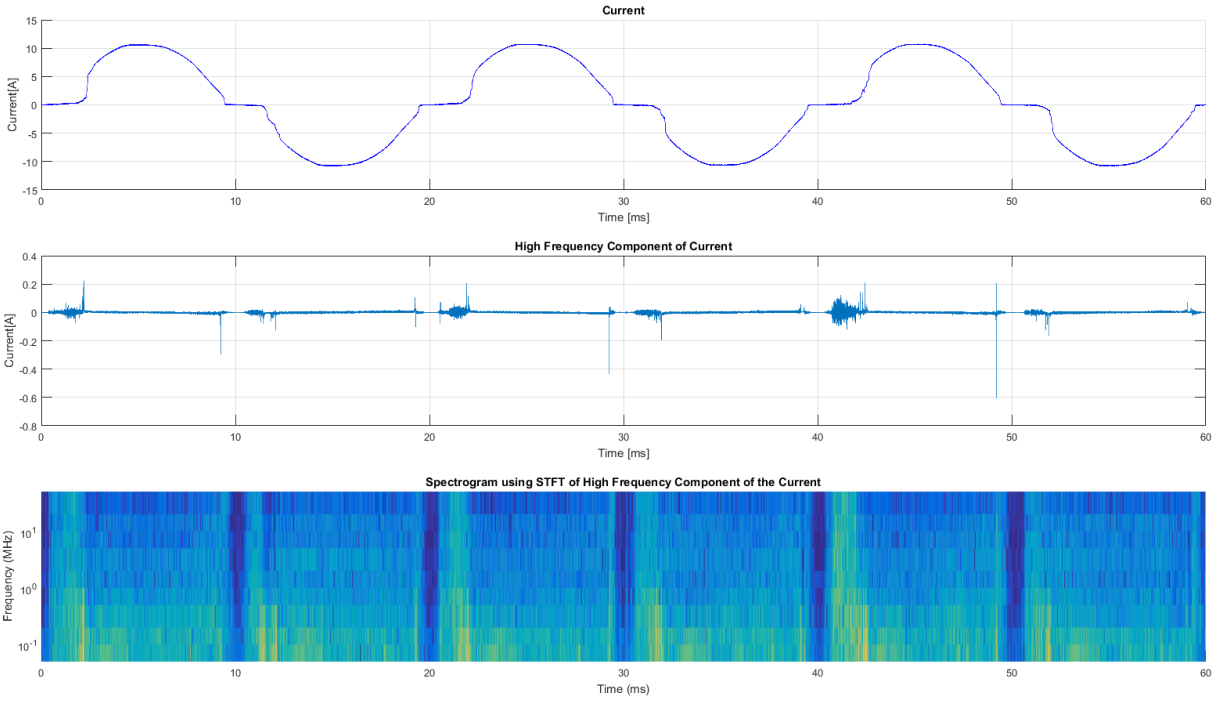


*Figure 5.7b. High-frequency component and STFT of a space heater with the series arc.*

### *5.3.1.3. Continuous Wavelet Transform*

The scalograms in figure 5.8a and 5.8b are the CWT of the high-frequency component of the current of a space heater without a series arc and with series arc respectively. It is clear that there is a

frequency band which propagates from around 31 kHz all the way to 16 Mhz. Furthermore, the zero crossing, having components with lower magnitudes, are clearly visible.

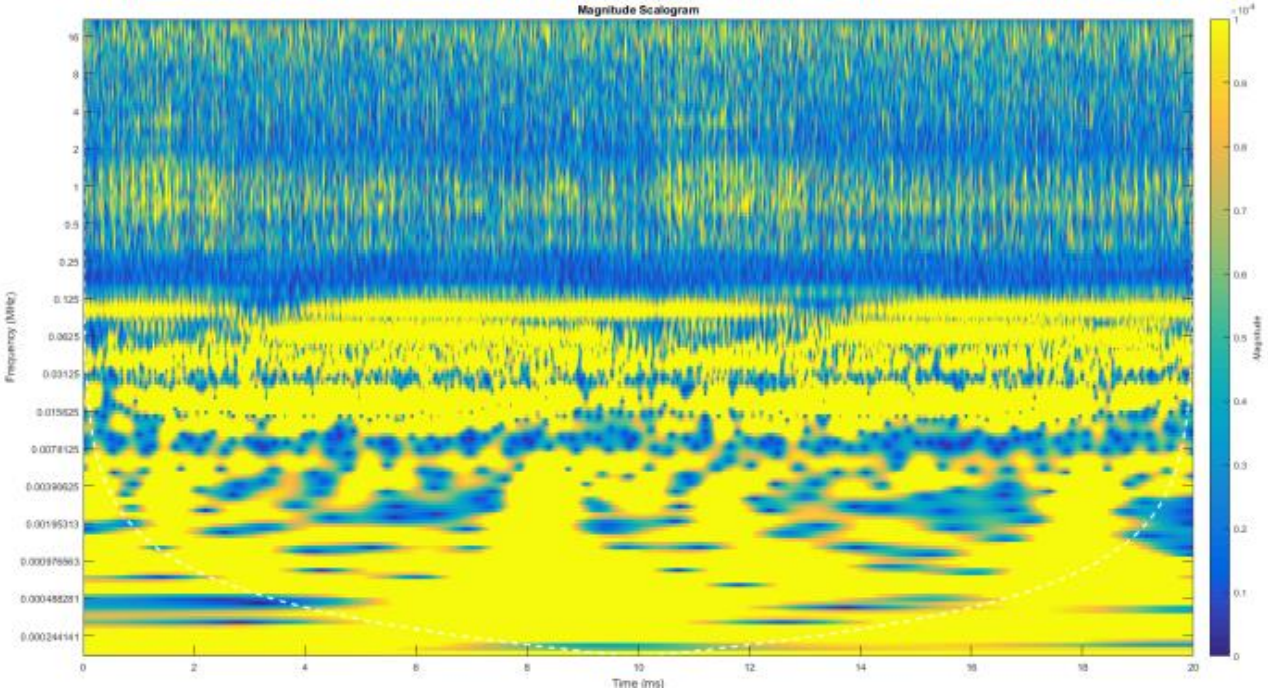


*Figure 5.8a. Scalogram of space heater obtained using CWT.*

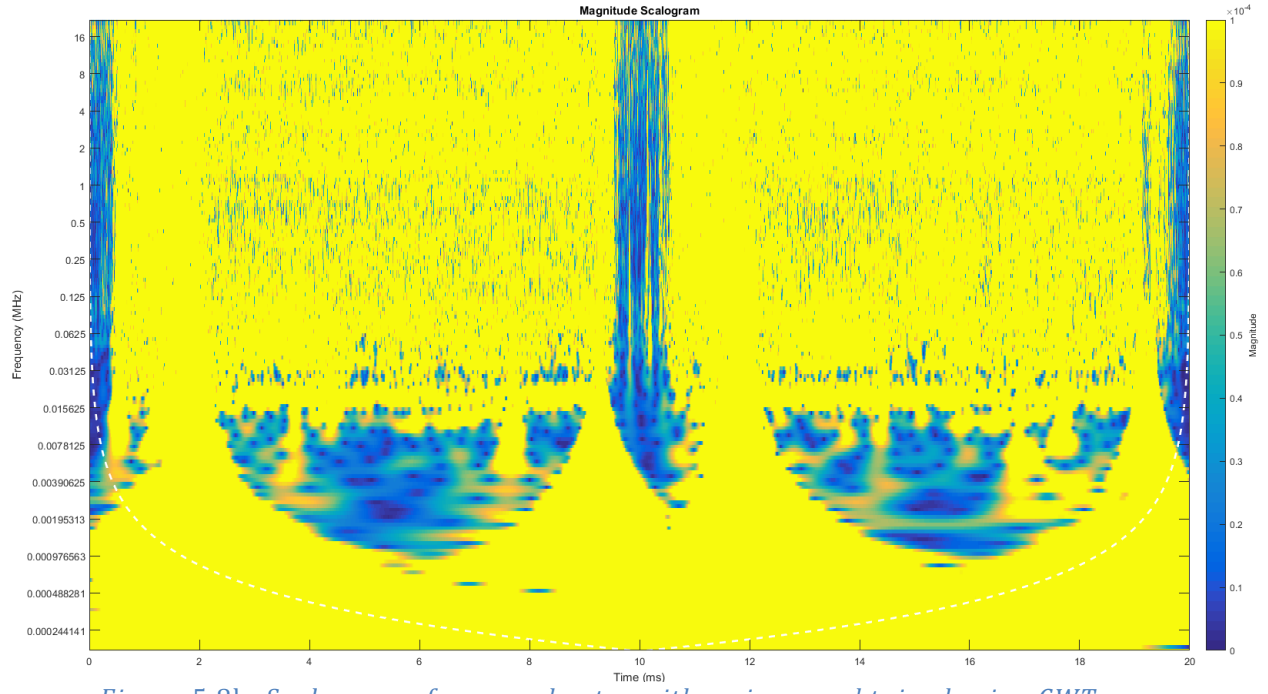


*Figure 5.8b. Scalogram of a space heater with series arc obtained using CWT.*

### 5.3.2. Iron

A 1000W iron was used in the test. Two tests were conducted with this load, the first one was to capture the load signal. The second test captures the load in series with the arc. The two cases (with

and without arcing) were compared in the time domain and in the time-frequency domain, using STFT and CWT. As waveform without arcing does not exhibit any specific features or distortions other than those typical of a resistive load, only the waveforms with serial arcing are provided.

### *5.3.2.1. Time Domain*

Figure 5.9 shows the waveforms of the resistive load, iron with arcing. The result is similar to that explained for the previous load, as both are purely resistive. The load signature has not been provided to prevent repetition as it is identical to the case of all resistive loads.

In the case with the arc, the shoulders at and next to the zero crossings are clearly visible. The arc voltage is also very typical. The resistive load does not cause any distortion in the arc current or voltage.

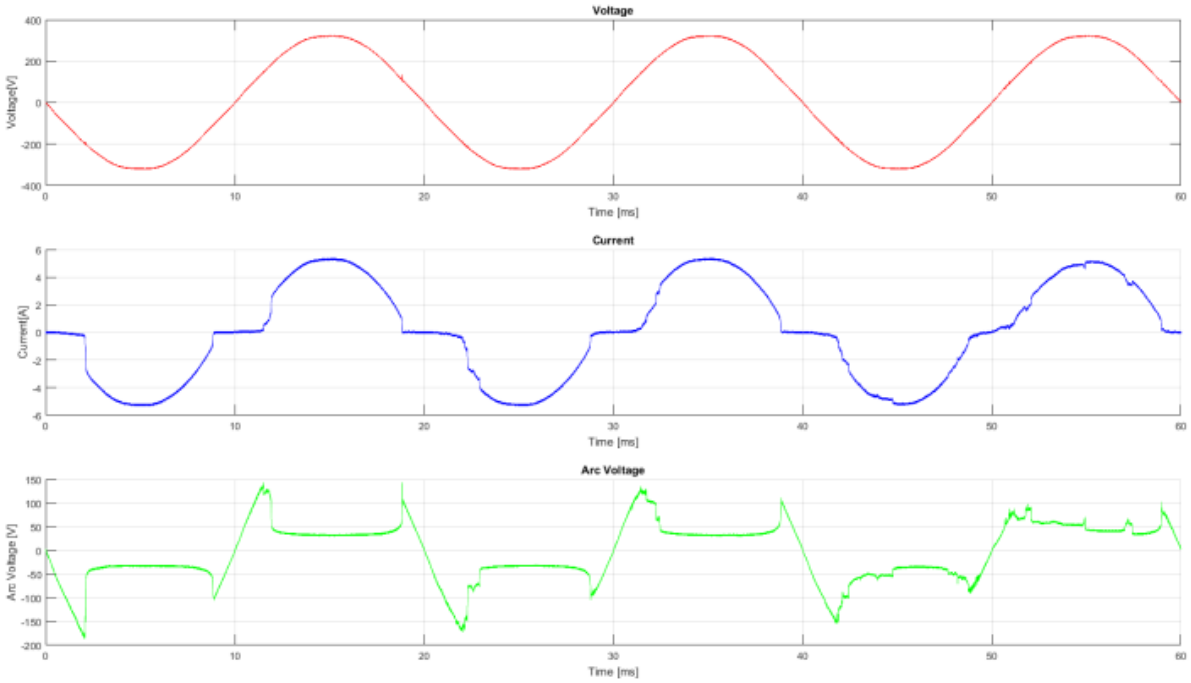


*Figure 5.9. Time domain representation of an iron with the series arc.*

### *5.3.2.2. Short Time Fourier Transform*

Similarly, figure 5.10 shows the high-frequency component of the arc and its STFT. The high-frequency component of the current is periodic and shows clusters before and after the zero crossings. The STFT of the high-frequency component of the current shows that there are components of the signals with higher frequencies present around the zero crossings. However, we cannot observe the broadband noise during the time when the arc is stable.

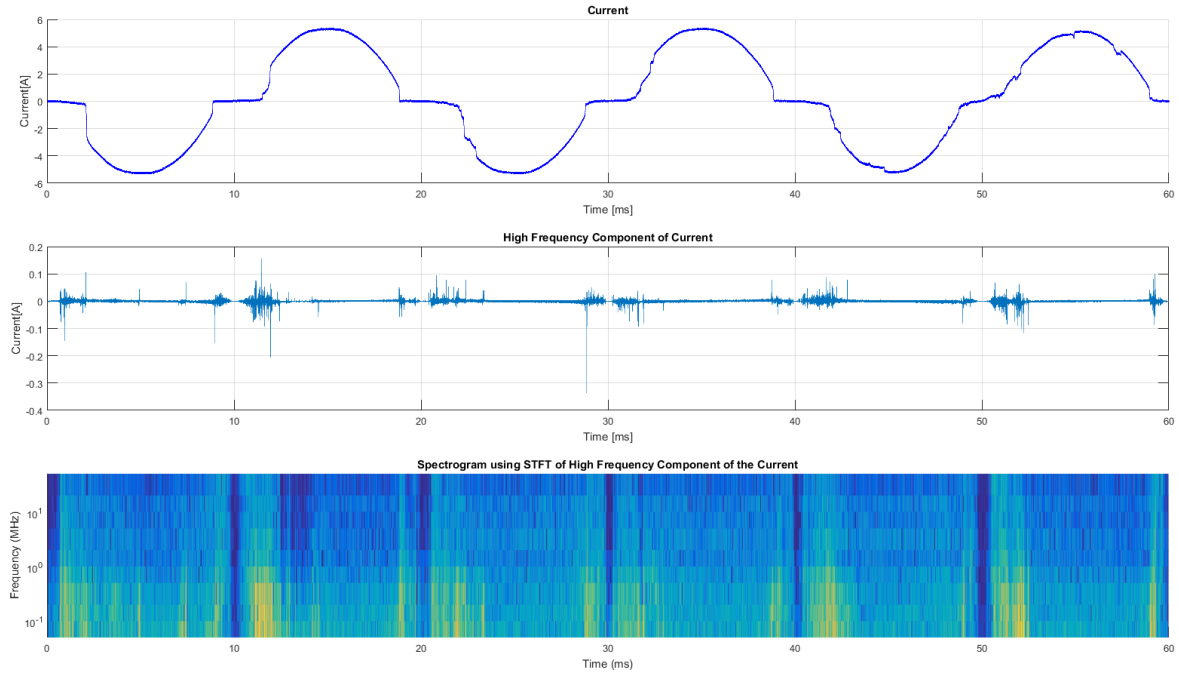


*Figure 5.10. High-frequency component and STFT of an iron with series arc*

### *5.3.2.3. Continuous Wavelet Transform*

The scalograms in figure 5.11 are the CWT of the high-frequency component of the current. It is clear that there is a frequency band which propagates from around 31 kHz all the way to 16 Mhz. Furthermore, the zero crossing, are clearly visible.

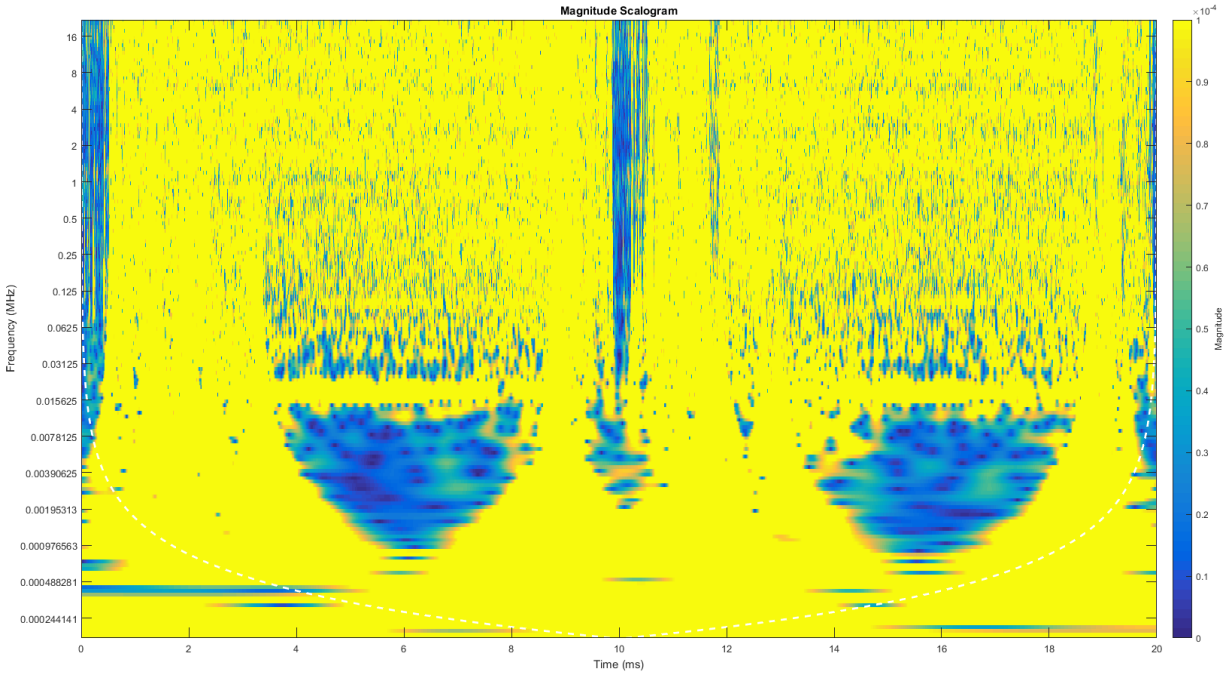


*Figure 5.11. Scalogram of an iron with series arc obtained using CWT.*

### 5.3.3. Hair Straightener

A 45W hair straightener was used in the test. Two tests were conducted with this load, the first one was to capture the load signal. The second test captures the load in series with the arc. The two cases (with and without arcing) were compared in the time domain and in the time-frequency domain, using STFT and CWT. However, the waveforms provided are ones with series arcing, as the load signature is identical in the case of all resistive loads.

#### *5.3.3.1. Time Domain*

Figure 5.12 shows the time domain signal of hair straightener, which is another resistive load and the arcing current shoulders and the arc voltage is clearly visible.

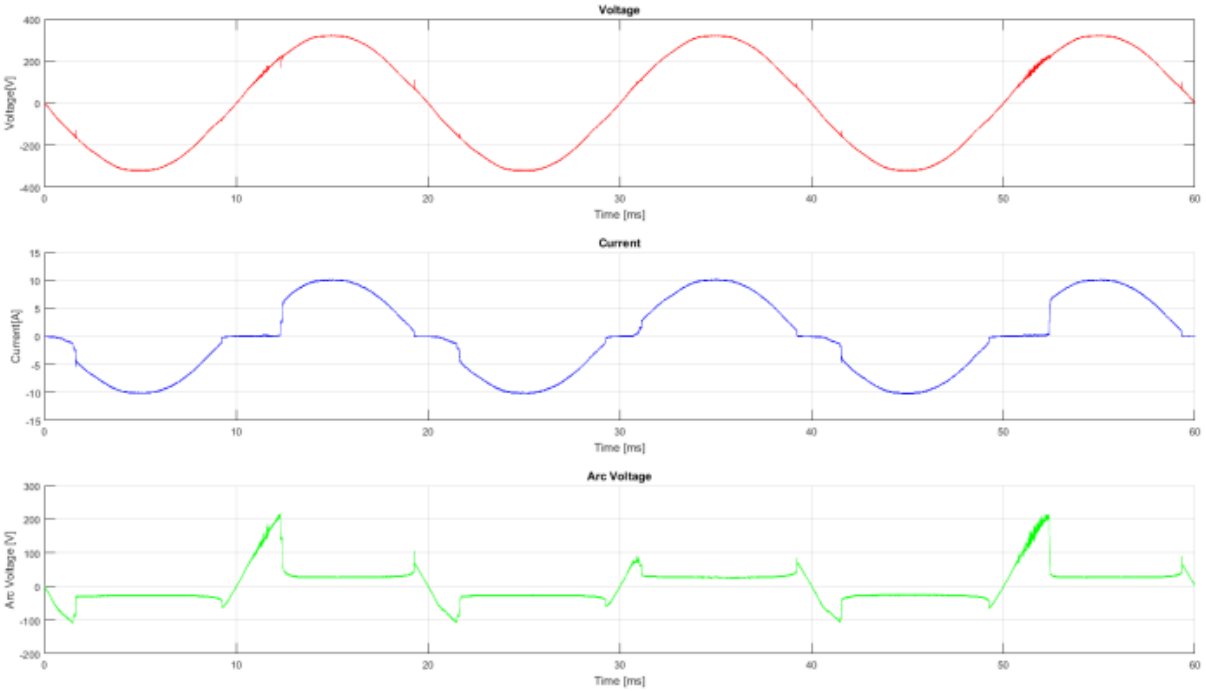


*Figure 5.12. Time domain representation of hair straightener with the series arc.*

#### *5.3.3.2. Short Time Fourier Transform*

Figure 5.13 shows the high-frequency component of the current through a hair straightener with arc and its STFT. The results are similar to those described previously.

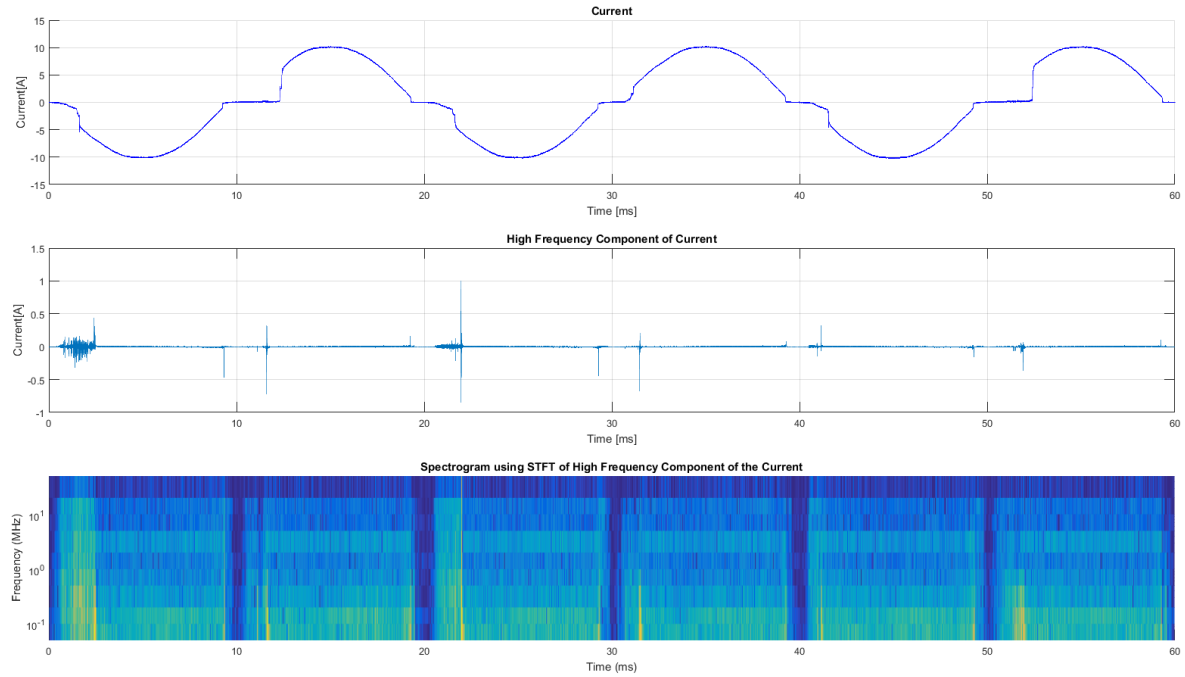


*Figure 5.13. High-frequency component and STFT of hair straightener with the series arc.*

### *5.3.3.3. Continuous Wavelet Transform*

Figure 5.14 shows the CWT of the high-frequency component of the current through a hair straightener with the series arc. The results are similar to those described previously.

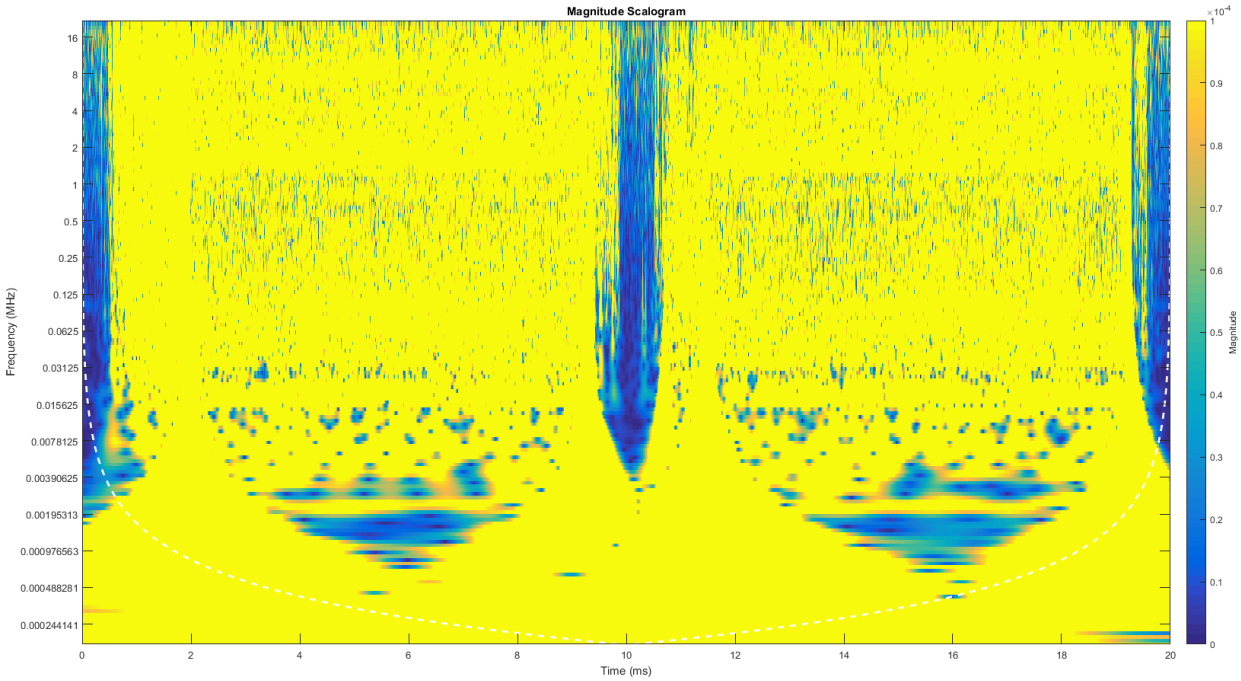


*Figure 5.14. Scalogram of hair straightener with series arc obtained using CWT.*

### 5.3.4. General Incandescent Lamp

Four GILs with a total power of 600W were used in the test. Two tests were conducted with this load, the first one was to capture the load signal. The second test captures the load in series with the

arc. The two cases (with and without arcing) were compared in the time domain and in the time-frequency domain, using STFT and CWT. The load signature has not been provided to prevent repetition as it is identical to the case of all resistive loads

### *5.3.4.1. Time Domain*

Figure 5.15 shows the time domain signal of GILs with arcing, which is another resistive load and the arcing current shoulders and the arc voltage is clearly visible.

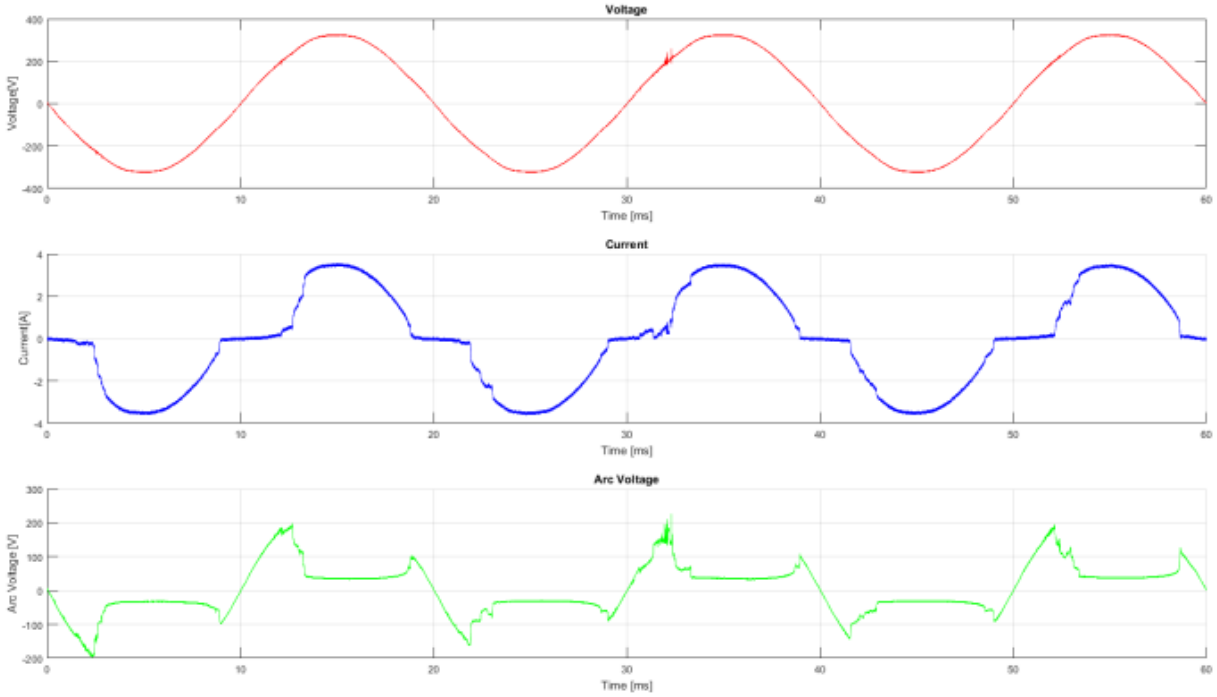


*Figure 5.15. Time domain representation of the GIL with series arc*

### *5.3.4.2. Short Time Fourier Transform*

Figure 5.16 shows the high-frequency component of the current through the GILs with arc and its STFT. The results are similar to those described previously.

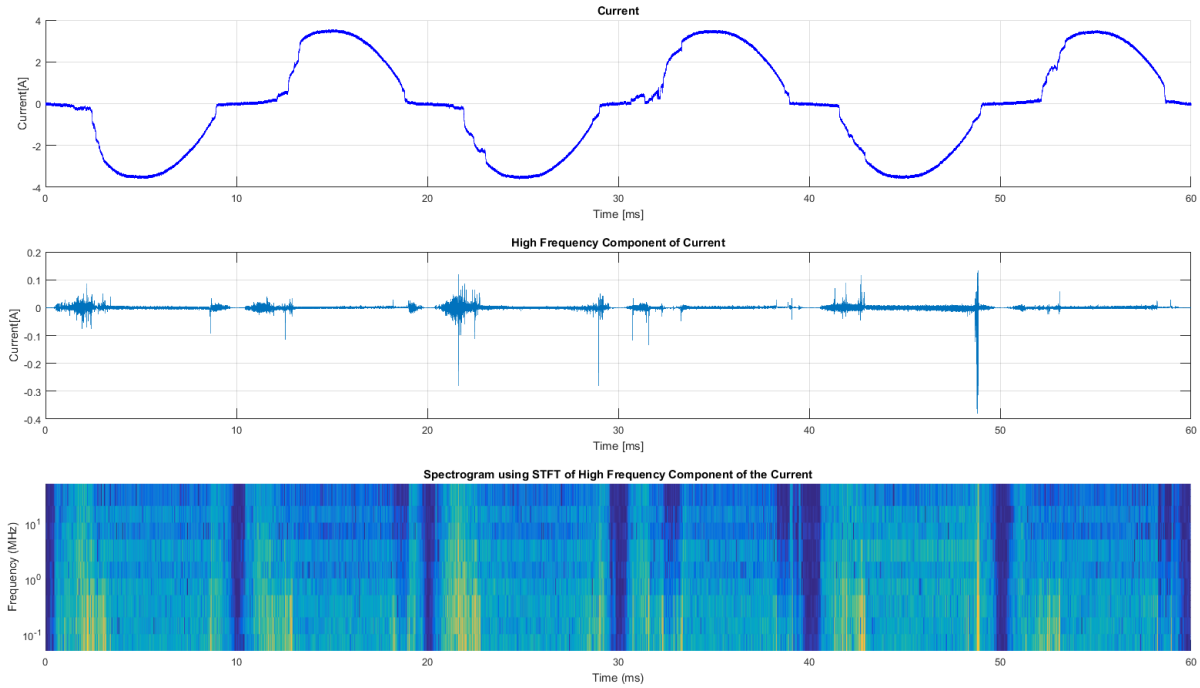


*Figure 5.16. High-frequency component and STFT of GIL with the series arc.*

### *5.3.4.3. Continuous Wavelet Transform*

Figure 5.17 shows the CWT of the high-frequency component of the current through GILs with the series arc. The results are similar to those described previously.

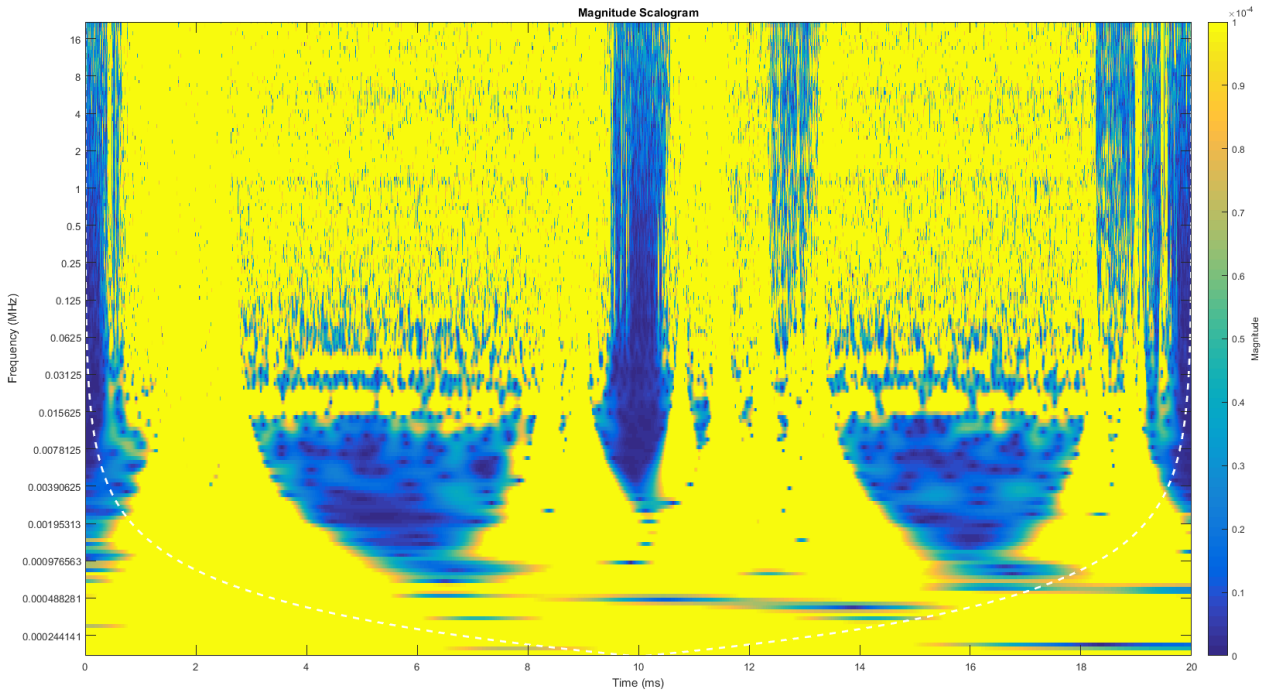


*Figure 5.17. Scalogram of GIL with series arc obtained using CWT.*

### 5.3.5. Hair Dryer

A 2100W hair dryer was used in the test. Two tests were conducted with this load, the first one was to capture the load signal. The second test captures the load in series with the arc. The two cases, with and without arcing, were compared in the time domain and in the time-frequency domain, using STFT and CWT.

#### *5.4.1.1. Time Domain*

The arc current and voltage, when a hairdryer is connected in series with an arc is similar to that of other resistive loads in the time domain.

Figure 5.18 shows the waveforms of the hair dryer load with arcing. The second waveform in the figure is that of the current. The shoulders at and near to the zero crossings are visible. As is evident from the current waveforms, in the time domain there is barely any noticeable variation in the current when a resistive load is connected to a universal motor.

Moreover, the arc voltage waveform is also very similar to the characteristic arc voltage.

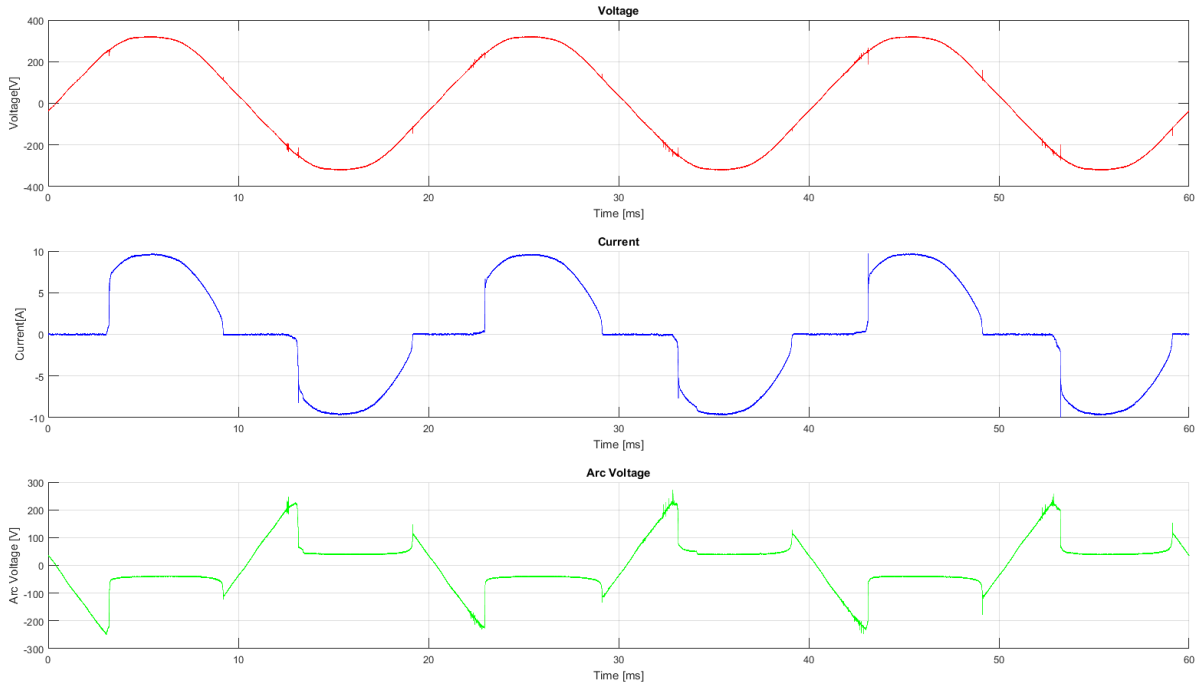


*Figure 5.18. Time domain representation of the hair dryer with the series arc.*

#### *5.3.5.2. Short Time Fourier Transform*

The second waveform in figure 5.19 shows the high-frequency component of the current passing through a hair dryer in series with an arc (b). The STFT of these signals is also given.

In the time domain, the appearance of the current waveform of a hair dryer does not show much difference. However, when the high-frequency components of the current with and without arcing is compared, we notice a significant difference. In the case where arcing is present, there appear to be

frequency components of higher magnitudes during the time where arcing is present. That is we see high-frequency components appear after the zero crossing region had been passed.

The STFT also shows the broadband noise that is characteristic of arcing. The STFT for a hair dryer with series arcing clearly shows the presence of higher frequencies. However, it seems like the broadband noise does not propagate all the way to the top. It also marks the points near and at the zero crossings very significantly.

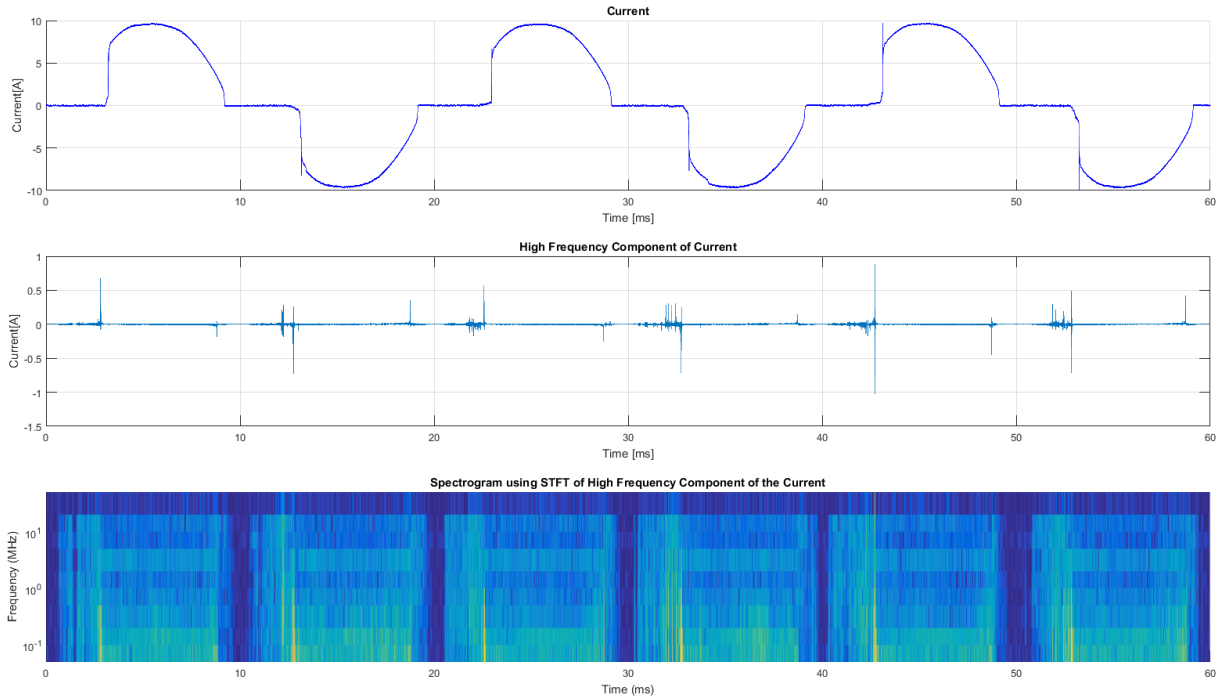


*Figure 5.19. High-frequency component and STFT of a hair dryer with the series arc.*

### *5.3.5.3. Continuous Wavelet Transform*

The scalograms in figure 5.20 are the CWT of the high-frequency component of the current passing through a hair dryer with series arcing. The scalogram was obtained by applying CWT to the time period from 20ms to 40ms of the high-frequency component of the current.

The broadband noise is clearly visible as frequency band which propagates from around 31 kHz all the way to up to 16 Mhz. The intensity of the signal at these higher frequencies during the arcing event is highlighted. Furthermore, the zero crossings are clearly visible. The periodicity and interruption, as well as the broadband noise, is much better visible in the scalogram.

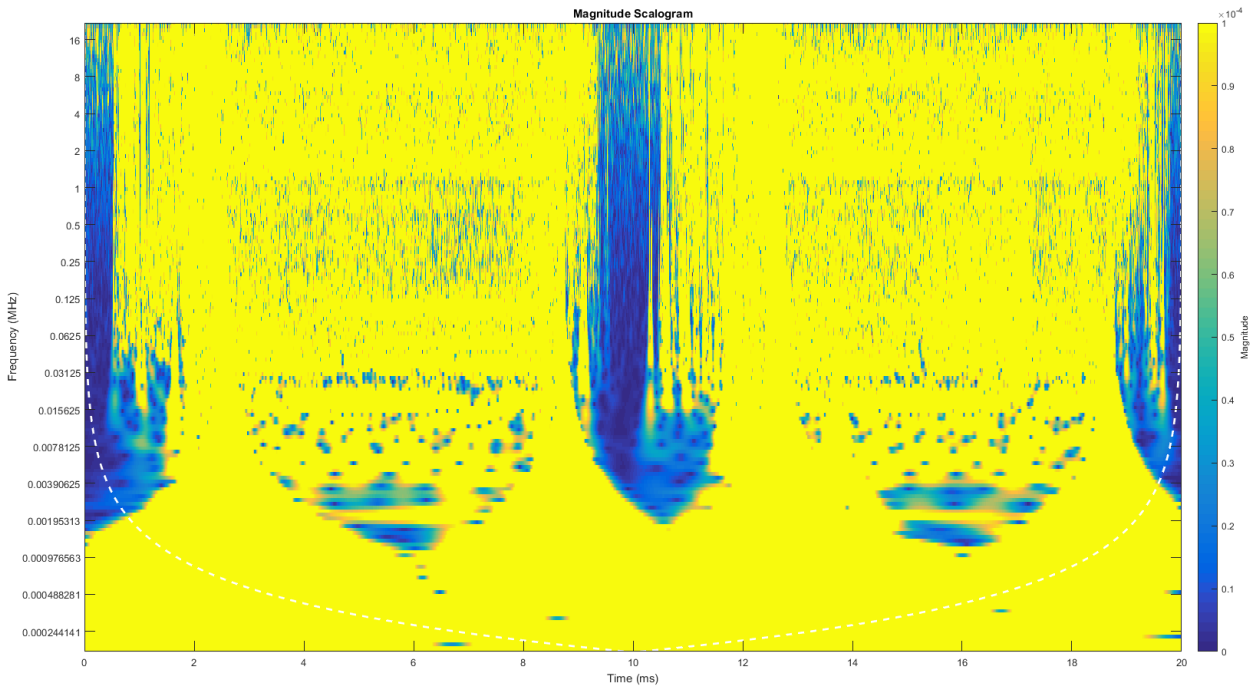


*Figure 5.20. Scalogram of a hair dryer with series arc obtained using CWT.*

## 5.4. Universal Motor:

### 5.4.1. Vacuum Cleaner

A 1200W vacuum cleaner was used in the test. Two tests were conducted with this load, the first one was to capture the load signal. The second test captures the load in series with the arc. The two cases, with and without arcing, were compared in the time domain and in the time-frequency domain, using STFT and CWT.

#### *5.4.2.1. Time Domain*

The arc current and voltage, when a universal motor is connected in series with an arc, is difficult to interpret in the time domain, as the current waveforms look very similar.

Figure 5.21 shows the waveforms of the universal motor load without arcing (a) and with arcing (b). The second waveform in both the figure is that of the current. In the case with the arc, the shoulders at and near to the zero crossings are not visible. This very crucial characteristic of the arc is suppressed by the UM. As is evident from the current waveforms, in the time domain there is barely any noticeable variation in the current with series arcing and without.

In figure 5.21b there are visible spikes in the current around zero crossings, where there is a sudden increase or decrease in the arc voltage. If one observes the arc voltage, one can see that the spikes in the arc current occur exactly at the time when the arc voltage jumps.

The arc voltage waveform is very similar to the characteristic arc voltage. The arc voltage waveform in figure 5.21a shows the noise level.

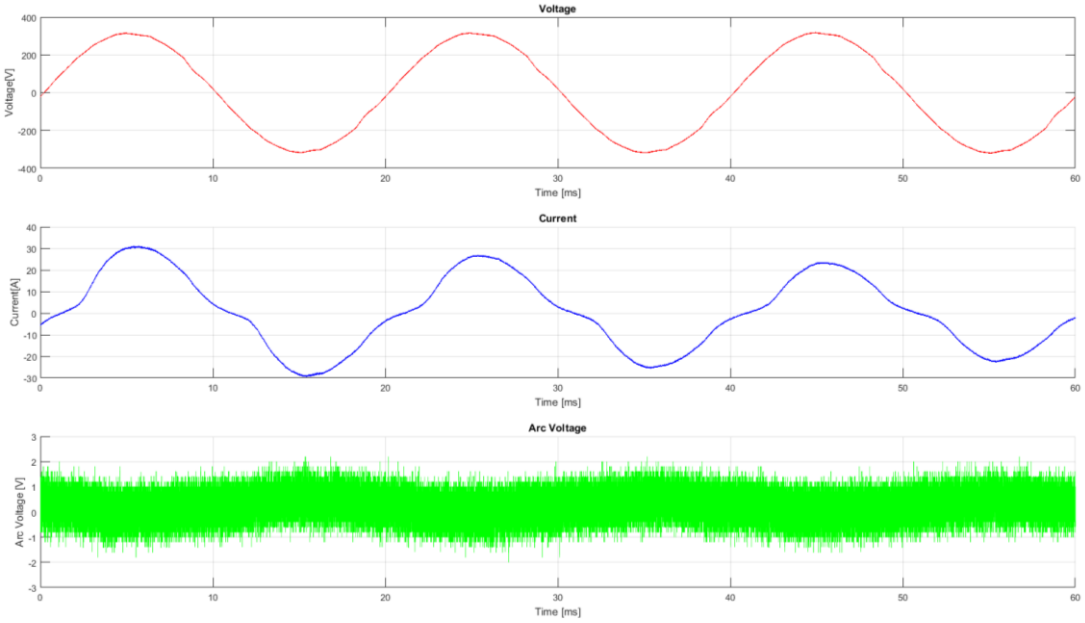


*Figure 5.21a. Time domain representation of a vacuum cleaner.*

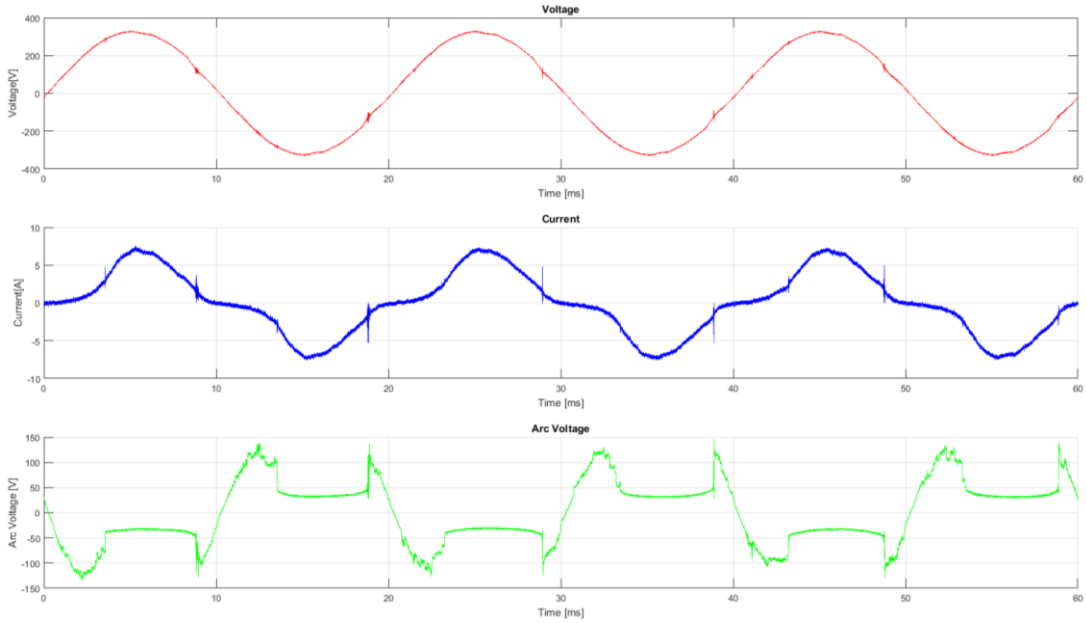


*Figure 5.21b. Time domain representation of a vacuum cleaner with the series arc.*

### *5.4.1.2. Short Time Fourier Transform*

The second waveforms in figure 5.22a and 5.22b show the high-frequency component of the current passing through a vacuum cleaner, and through a vacuum cleaner in series with an arc respectively. The STFTs of these signals are also given.

In the time domain, the appearance of the current waveform of a vacuum cleaner does not show much difference, except for the visible spikes near the zero crossing points where the arc voltage jumps suddenly.

However, when the high-frequency components of the current with and without arcing is compared, we notice a significant difference. In the case where arcing is present, there appear to be frequency

components of higher magnitudes during the time where arcing is present. That is, we see high-frequency components appear after the zero crossing region had been passed. In other words, the high-frequency components are not present in the regions with lower voltage where the arc is not able to sustain itself and extinguishes.

The STFT also show the broadband noise that is characteristic of arcing. The STFT for a vacuum cleaner without arcing shows the absence of very high frequencies. The high frequencies visible are below 1MHz. Whereas the STFT for a vacuum cleaner with series arcing clearly shows the presence of higher frequencies, above 1 MHz. It also marks the points near and at the zero crossings very significantly.

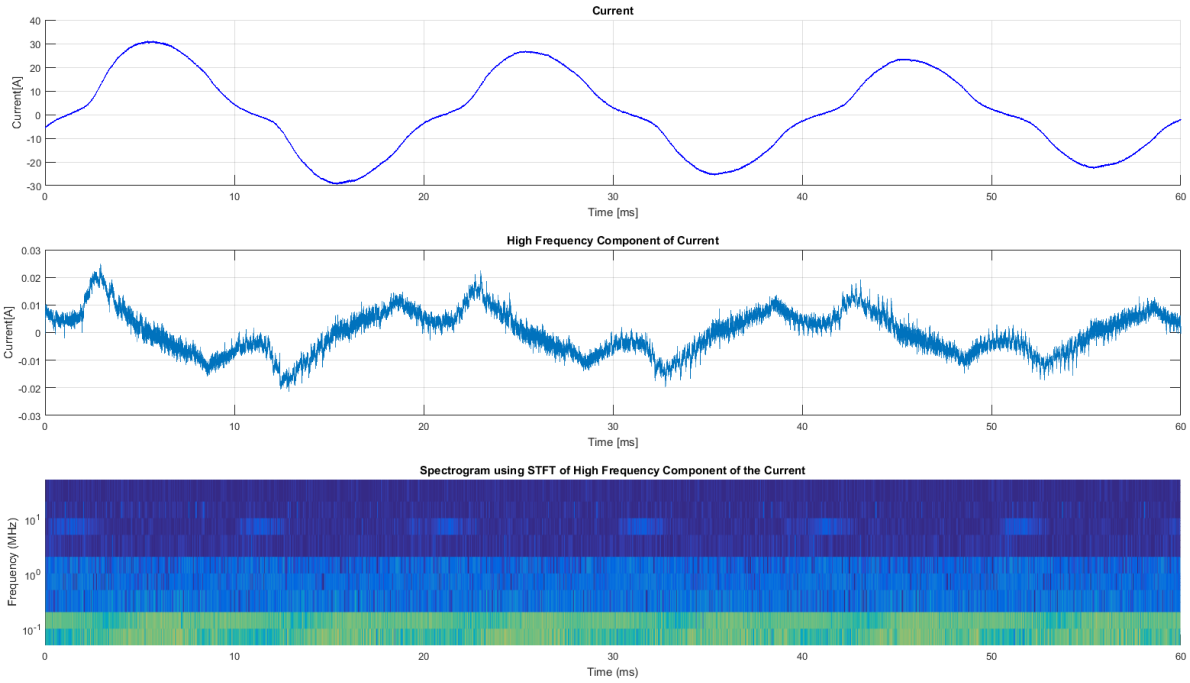


*Figure 5.22a. High-frequency component and STFT of a vacuum cleaner.*

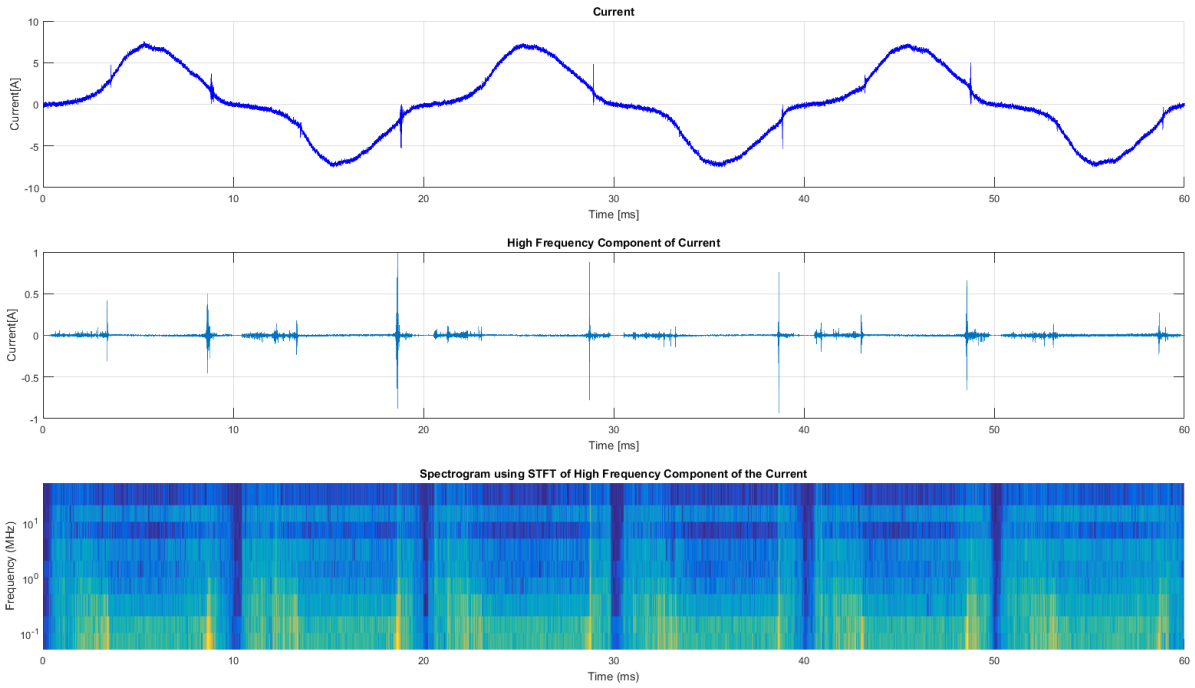


*Figure 5.22b. High-frequency component and STFT of a vacuum cleaner with the series arc.*

### *5.4.1.3. Continuous Wavelet Transform*

The scalograms in figure 5.23 are the CWT of the high-frequency component of the current passing through a vacuum cleaner (a) and a vacuum cleaner with series arcing (b). The scalogram was obtained by applying CWT to the time period from 20ms to 40ms of the high-frequency component of the current.

The broadband noise is clearly visible as frequency band which propagates from around 31 kHz all the way to up to 16 Mhz. The intensity of the signal at these higher frequencies during the arcing event is highlighted. Furthermore, the zero crossings are clearly visible. Vacuum cleaner generates a significant amount of noise at lower frequencies up to 150kHz, hence the band starting from 150 kHz is more efficient for arc detection.

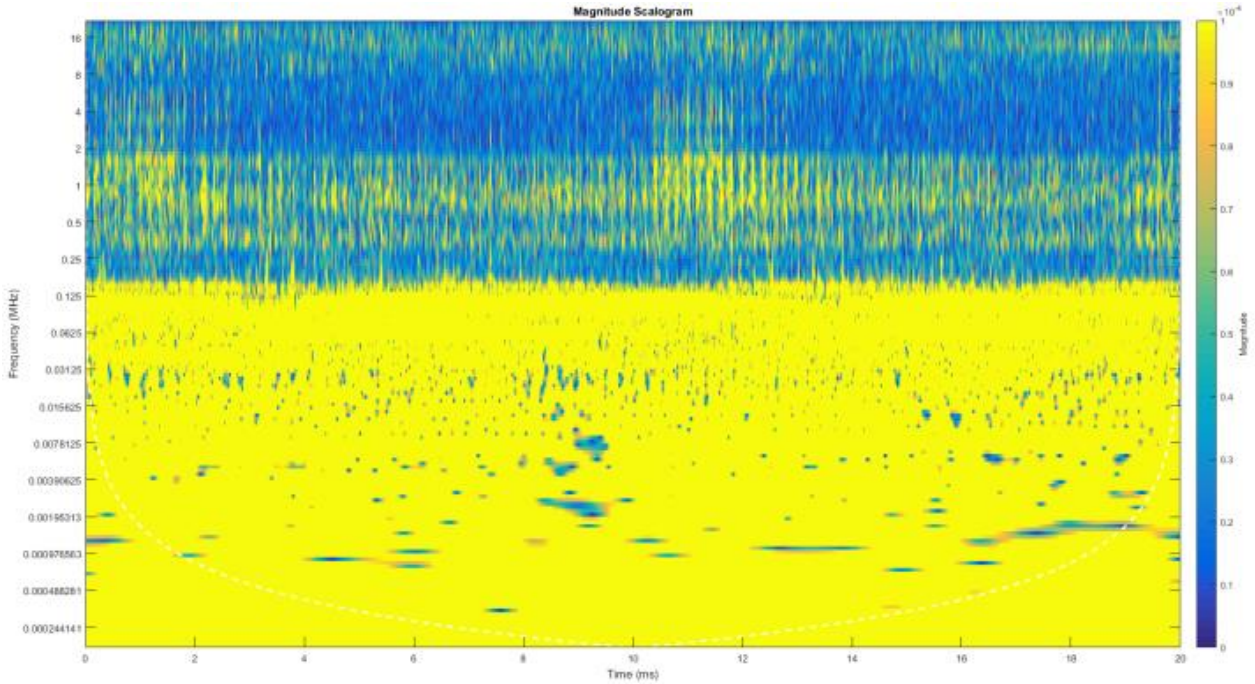


*Figure 5.23a. Scalogram of vacuum cleaner obtained using CWT*

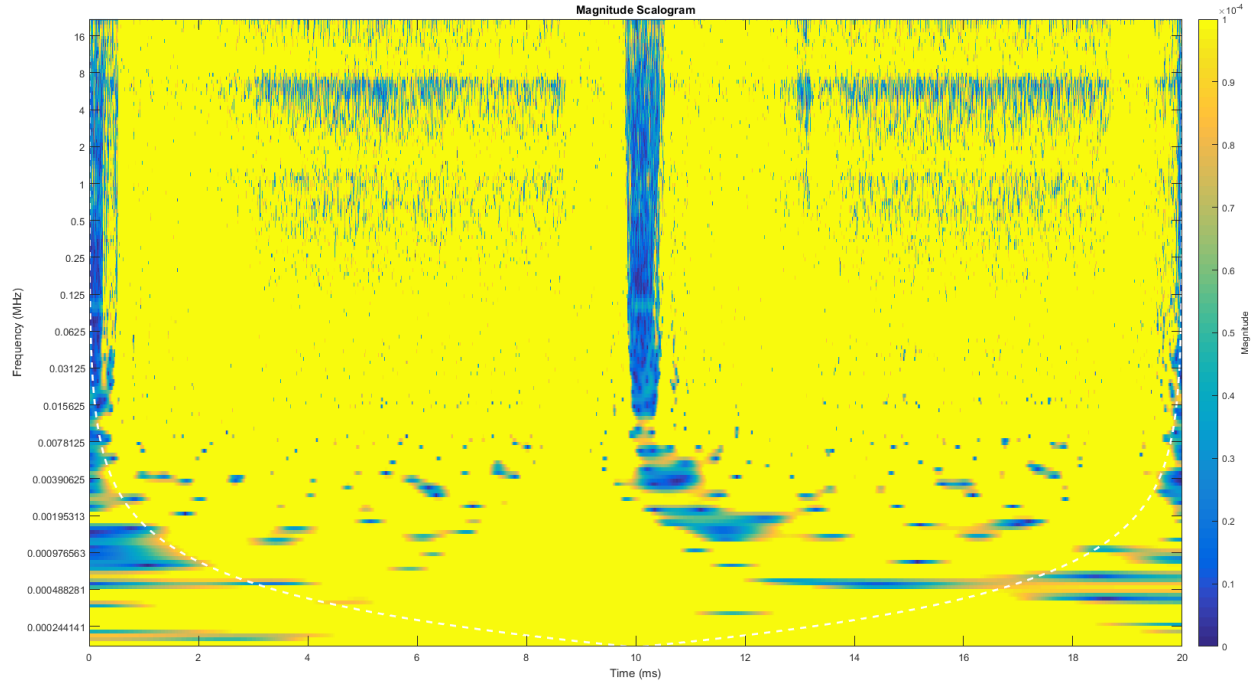


*Figure 5.23b. Scalogram of a vacuum cleaner with series arc obtained using CWT.*

### 5.4.2. Cultivator

A 1400W cultivator was used in the test. Two tests were conducted with this load, the first one was to capture the load signal. The second test captures the load in series with the arc. The two cases, with and without arcing, were compared in the time domain and in the time-frequency domain, using STFT and CWT.

*5.4.4.1. Time Domain*

The arc current and voltage, when a cultivator is connected in series with an arc, is difficult to interpret in the time domain, as the current waveforms look very similar. However, we notice that in the case of the cultivator the current when a series arc is present has well-defined shoulders at the zero crossings.

Figure 5.24 shows the waveforms of the universal motor load without arcing (a) and with arcing (b). The second waveform in both the figure is that of the current. In the case with the arc, the shoulders at and near to the zero crossings are moe visible than other UM loads tested.

The arc voltage waveform is very similar to the characteristic arc voltage. The arc voltage waveform in figure 5.24a shows the noise level.

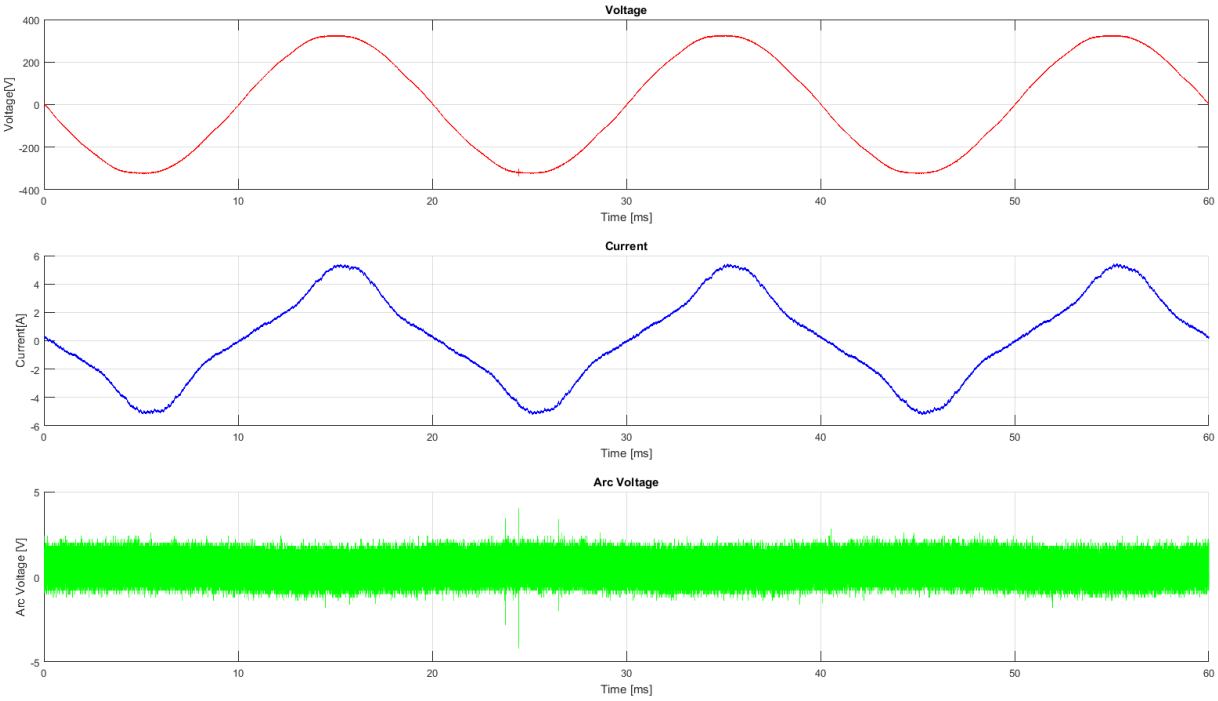


*Figure 5.24a. Time domain representation of the cultivator.*

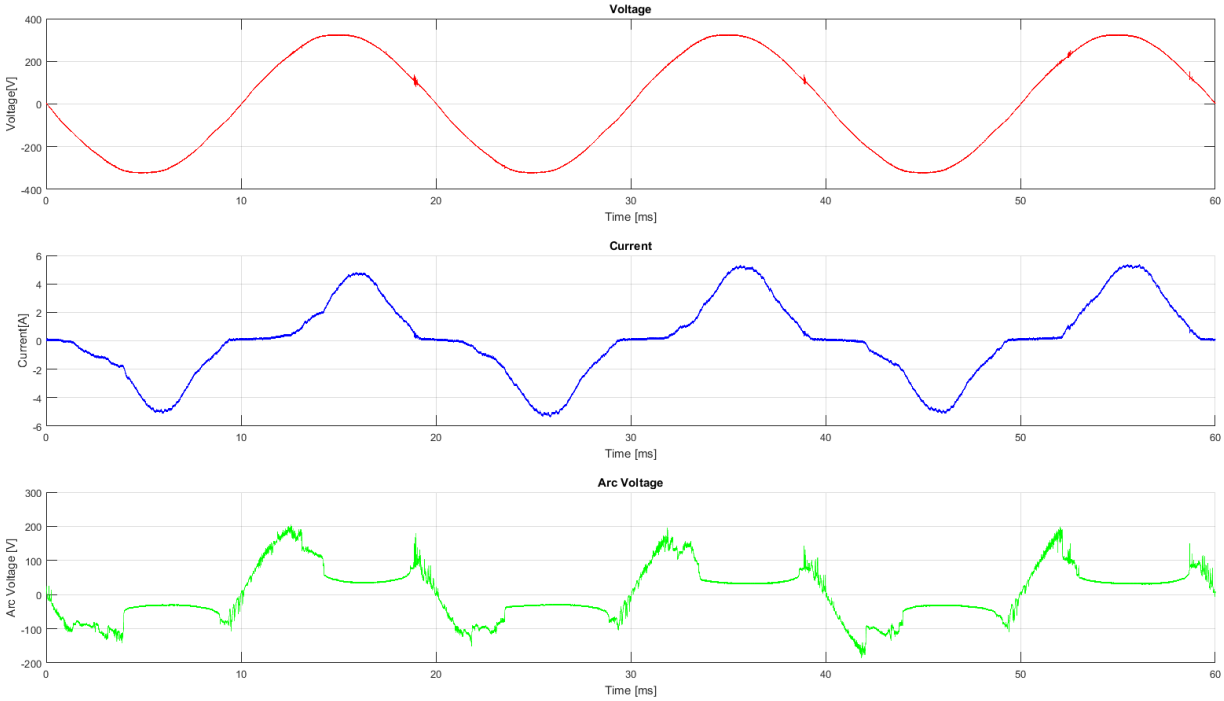


*Figure 5.24b. Time domain representation of the cultivator with the series arc.*

### *5.4.4.2. Short Time Fourier Transform*

The second waveforms in figure 5.25a and 5.25b show the high-frequency component of the current passing through a cultivator, and through a cultivator in series with an arc respectively. The STFTs of these signals are also given.

When the high-frequency components of the current with and without arcing is compared, we notice a significant difference. In the case where arcing is present, there appear to be frequency components of higher magnitudes during the time where arcing is present. That is, we see high-frequency components appear after the zero crossing region had been passed. In other words, the high-frequency components are not present in the regions with lower voltage where the arc is not able to sustain itself and extinguishes.

The current fluctuation emitted by a cultivator itself is of the same amplitude as arcing. However, it seems that the resulting high-frequency pattern is typical of arcing with silence periods near zero crossings. The detection of high-frequency on its own would prove to be a poor practice for arc fault detection. The time development of the high-frequency component should be taken into account to successfully distinguish normal operation from an arc fault.

The STFT in figure5.25b also shows the broadband noise that is characteristic of arcing. The STFT for a cultivator with series arcing clearly shows the presence of higher frequencies. In the case of a cultivator, the high frequencies are present in the case without arcing. Hence we can see that the cultivator as a load itself has high-frequency components. The most significant characteristic of the arcing that is visible in the STFT for a cultivator with series arcing is the zero crossings. The zero crossings are clearly marked.

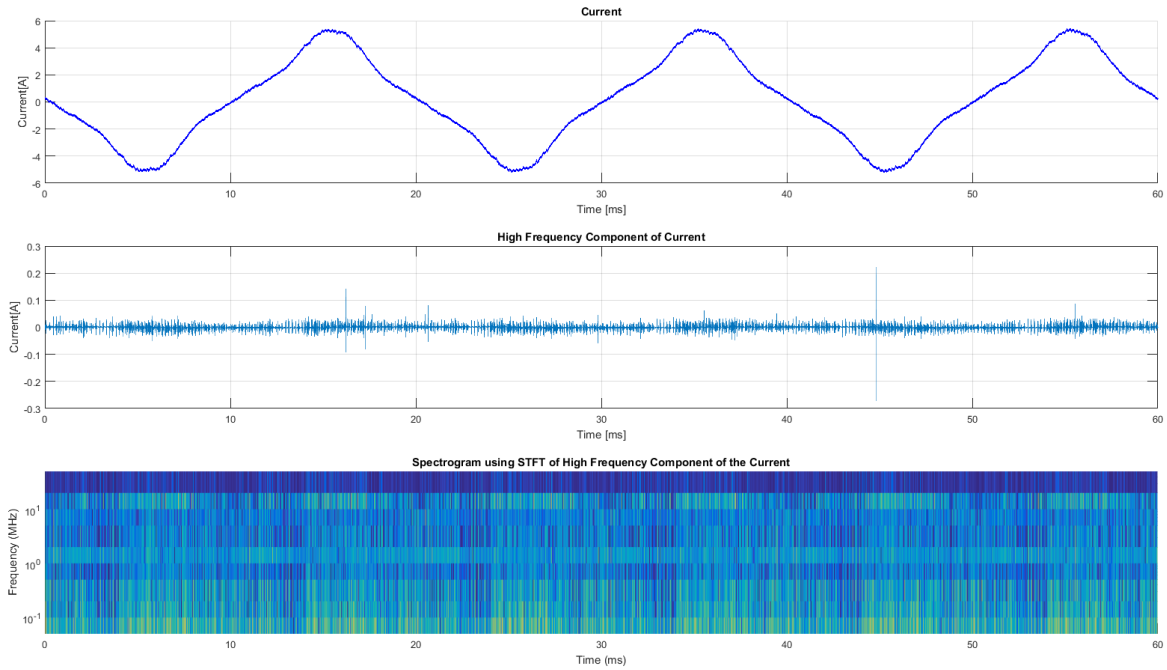


*Figure 5.25a. High-frequency component and STFT of the cultivator.*

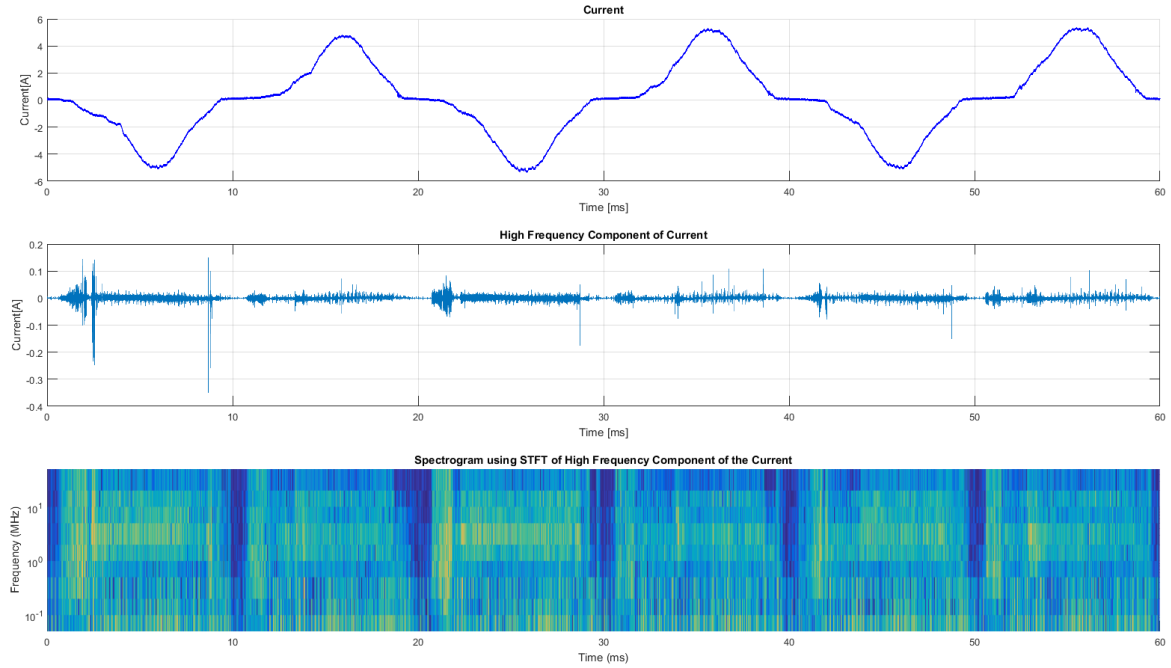


*Figure 5.25b. High-frequency component and STFT of the cultivator with the series arc.*

### *5.4.4.3. Continuous Wavelet Transform*

The scalograms in figure 5.26 are the CWT of the high-frequency component of the current passing through a cultivator (a) and a cultivator with series arcing (b). The scalogram was obtained by applying CWT to the time period from 20ms to 40ms of the high-frequency component of the current.

The broadband noise is clearly visible as frequency band which propagates from around 0.5MHz all the way to up to 16 Mhz. The intensity of the signal at these higher frequencies during the arcing event is highlighted. Furthermore, the zero crossings are clearly visible.

The conclusion is similar to that obtained using STFT. However, when a series arc is present, the CWT is better at revealing the more stable and intensive high-frequency component in the band higher than 1MHz.

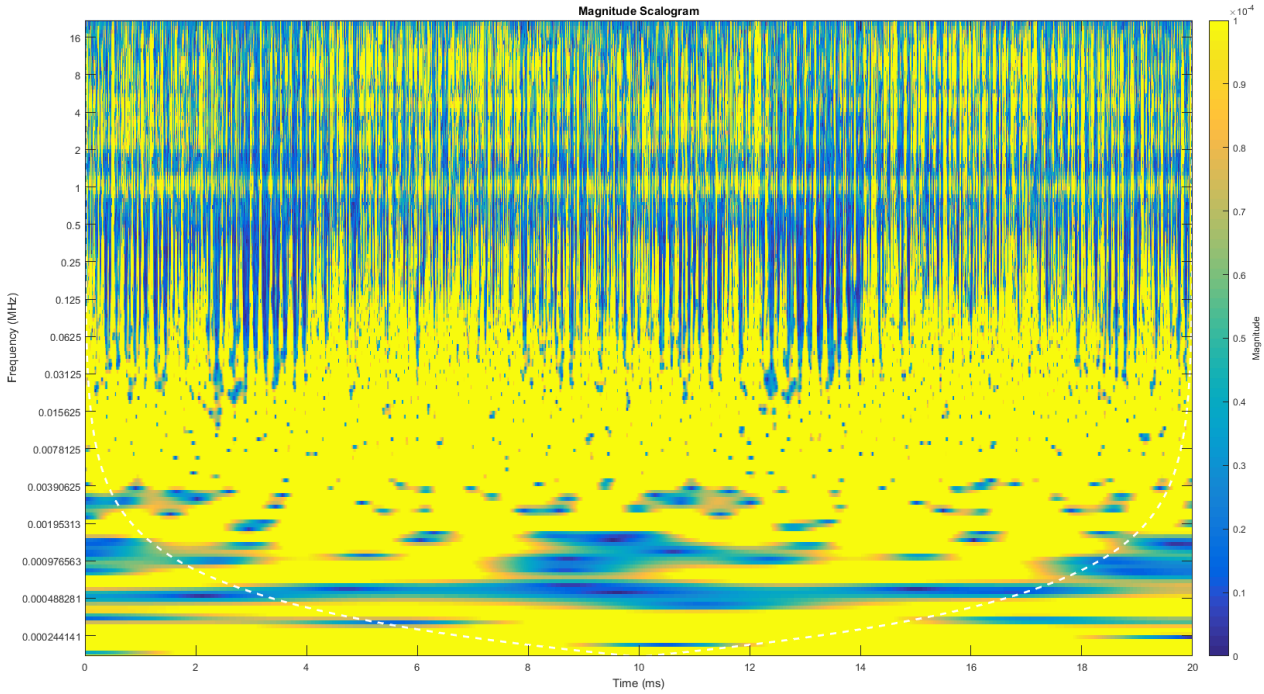


*Figure 5.26a. Scalogram of cultivator obtained using CWT.*

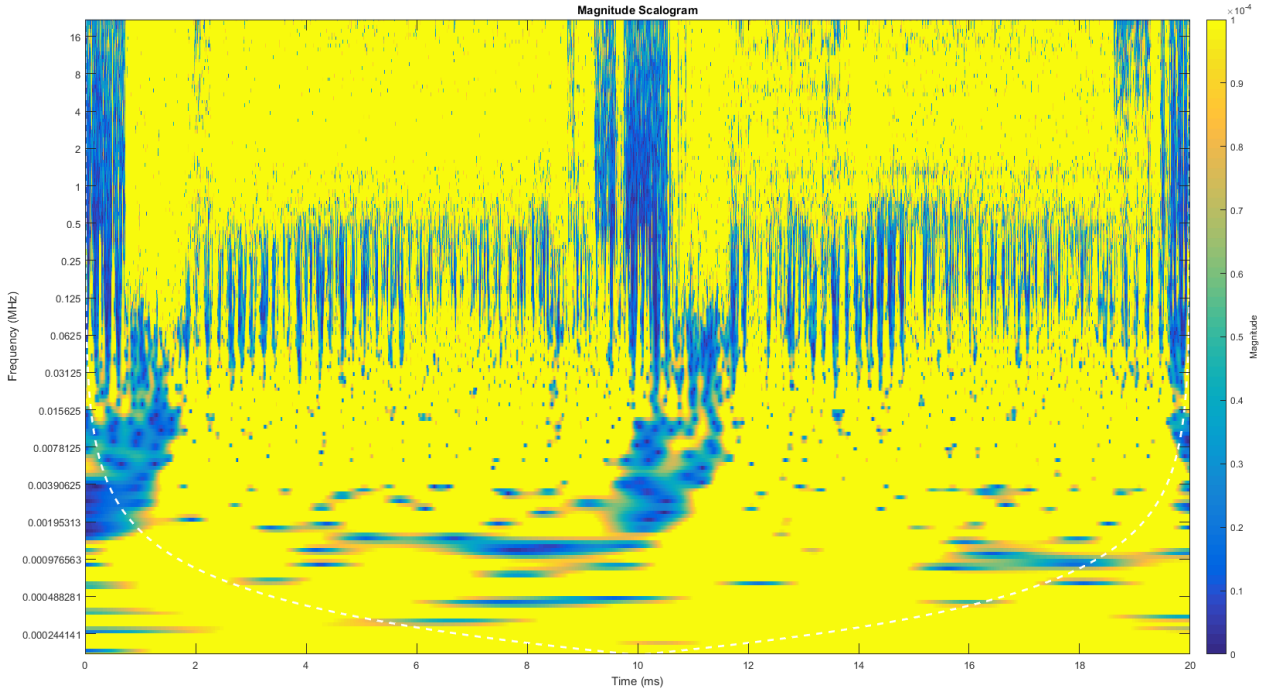


*Figure 5.26b. Scalogram of cultivator with series arc obtained using CWT.*

## 5.5. Single Phase Induction Motor

### 5.5.1. Desk Fan

A 30W desk fan was used in this test. Two tests were conducted with this load, the first one was to capture the load signal. The second test captures the load in series with the arc. The two cases, with and without arcing, were compared in the time domain and in the time-frequency domain, using STFT and CWT.

#### *5.5.1.1. Time Domain*

The arc current and voltage, when a desk fan is connected in series with an arc, is significantly different to that when there is no series arcing.

Figure 5.27 shows the waveforms of the SPIM load without arcing (a) and with arcing (b).

The second waveform in both the figures is that of the current. In the case with the arc in series with the desk fan, the current waveform changes drastically. It seems to have shoulders at the zero crossings which are correlated to the frequency of the mains, 50Hz. However, it is evident that although the changes in the current in the time domain are drastic, they do not assist greatly in defining the case with the arc.

The arc voltage waveform is represented similarities to the characteristic arc voltage. However, it seems to be very sporadic. This erratic behavior was confirmed to be due to the load, as the carbonized path was checked twice to confirm that the arcing is stable. The arc voltage waveform in the figure 5.27a shows the noise level.

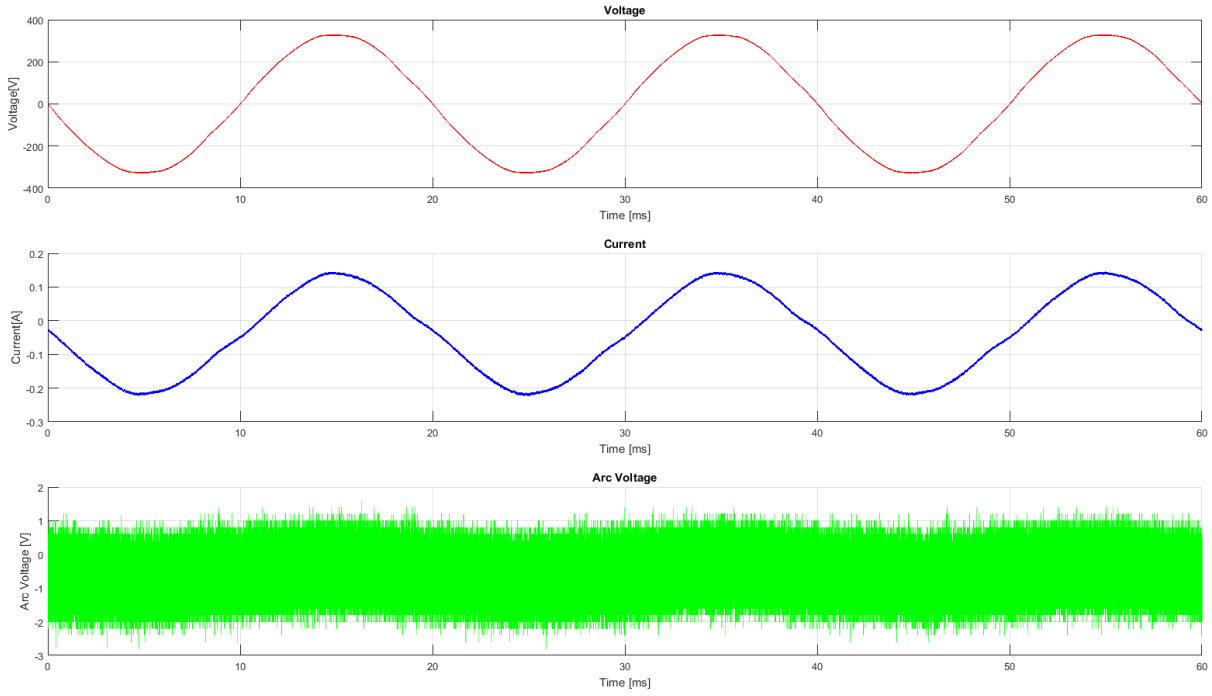


*Figure 5.27a. Time domain representation of desk fan.*

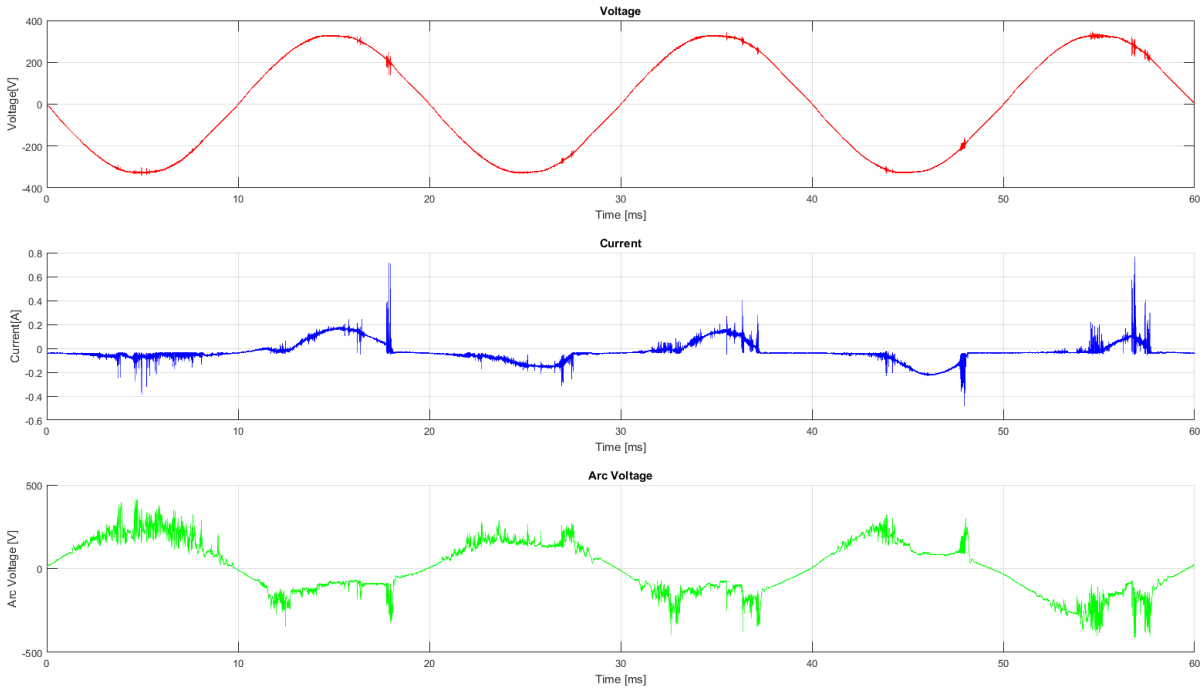


*Figure 5.27b. Time domain representation of the desk fan with the series arc.*

### *5.5.1.2. Short Time Fourier Transform*

The second waveforms in figure 5.28a and 5.28b show the high-frequency component of the current passing through a desk fan, and through the desk fan in series with an arc respectively. The STFTs of these signals are also given.

When the high-frequency components of the current with and without arcing is compared, we notice a significant difference. In the case where arcing is present, there appear to be frequency components of higher magnitudes during the time where the arc is present. That is, we see high-frequency components appear after the zero crossing region has been passed. In other words, the high-frequency components are not present in the regions with lower voltage where the arc is not able to sustain itself and extinguishes.

In the case of the desk fan without a series arc, the high-frequency component shows a periodicity at what seem to be the maximas and minimas of the current.

The STFT in figure 5.28b also shows the broadband noise that is characteristic of arcing. The STFT for a desk fan with series arcing clearly shows the presence of broadband noise. In the case of a desk fan, the high frequencies are present without arcing. Hence we can see that the desk as a load itself has high-frequency components. However, these high-frequency components are most visible at 1MHz. We observe that the interruption of the arc, periodically, at the zero crossings is highly visible in the spectrogram given in figure 5.28b. Furthermore, the broadband noise due to arcing is present.

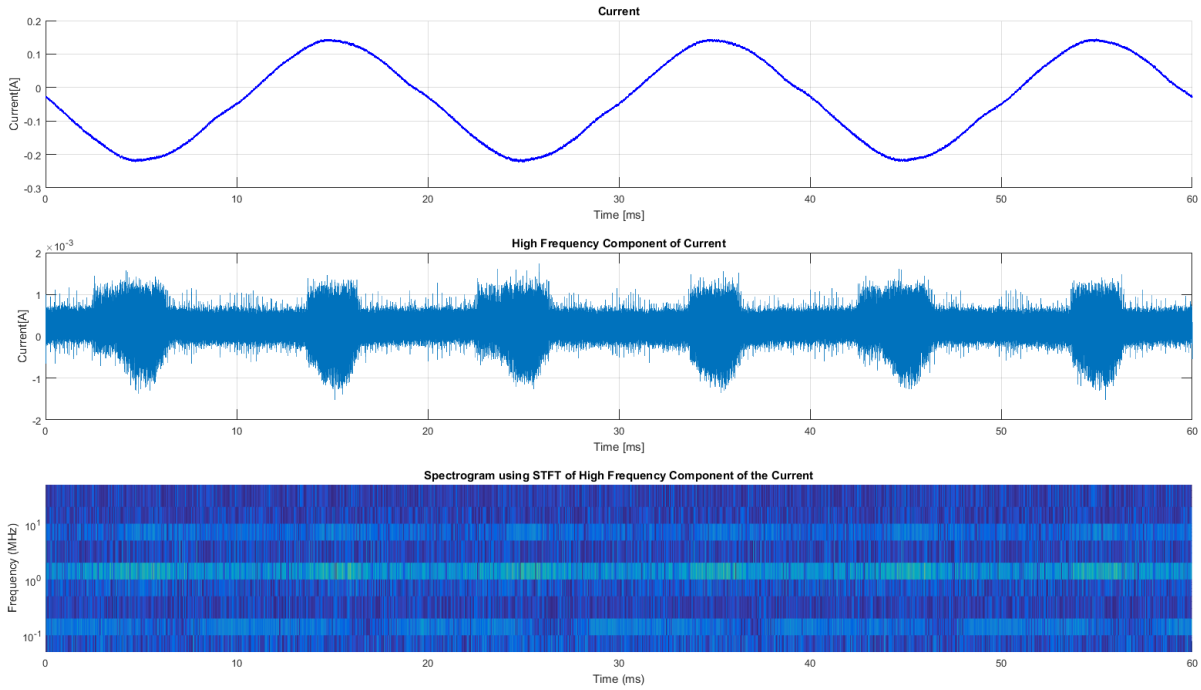


*Figure 5.28a. High-frequency component and STFT of a desk fan.*

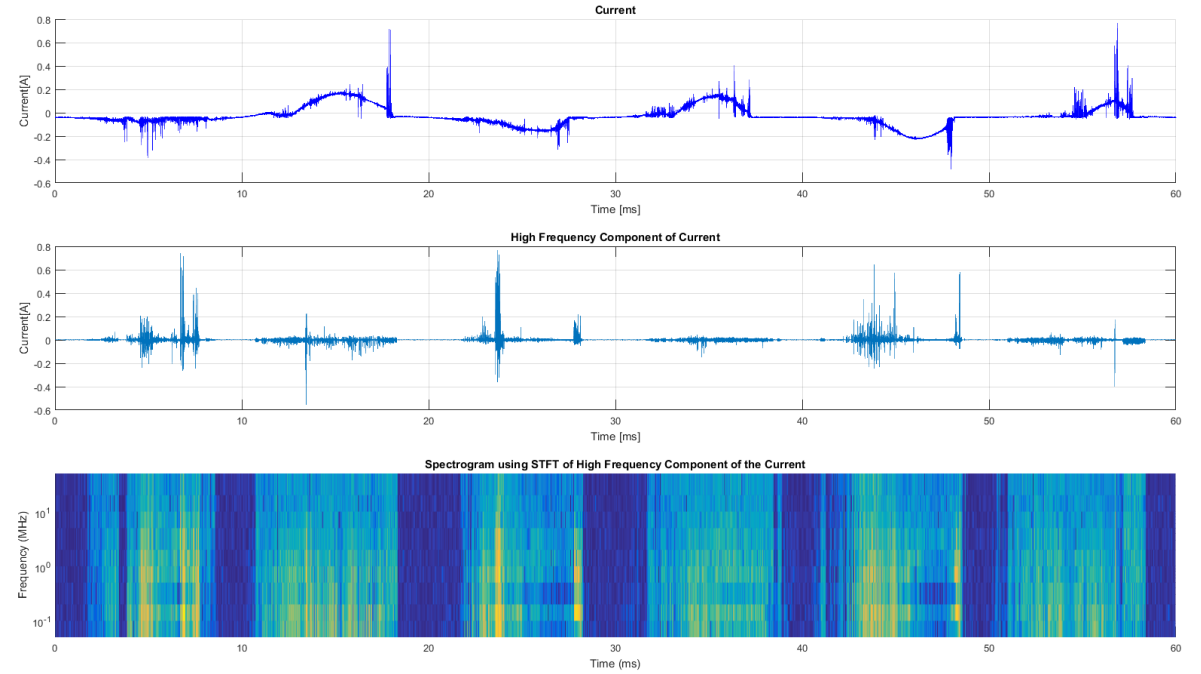


*Figure 5.28b. High-frequency component and STFT of desk fan with the series arc.*

### *5.5.1.3. Continuous Wavelet Transform*

The scalograms in figure 5.29 are obtained using the CWT and applying it to the high-frequency component of the current passing through a desk fan (a) and a desk fan with series arcing (b). The scalogram was obtained by applying CWT to the time period from 20ms to 40ms of the high-frequency component of the current.

The broadband noise is clearly visible as the frequency band which propagates from around 31 kHz all the way to up to 16 Mhz. The intensity of the signal at these higher frequencies during the arcing event is highlighted. Furthermore, the zero crossings are clearly visible. Hence, periodicity and interruption are clearly marked. Furthermore, CWT highlights the broadband noise much better than STFT.

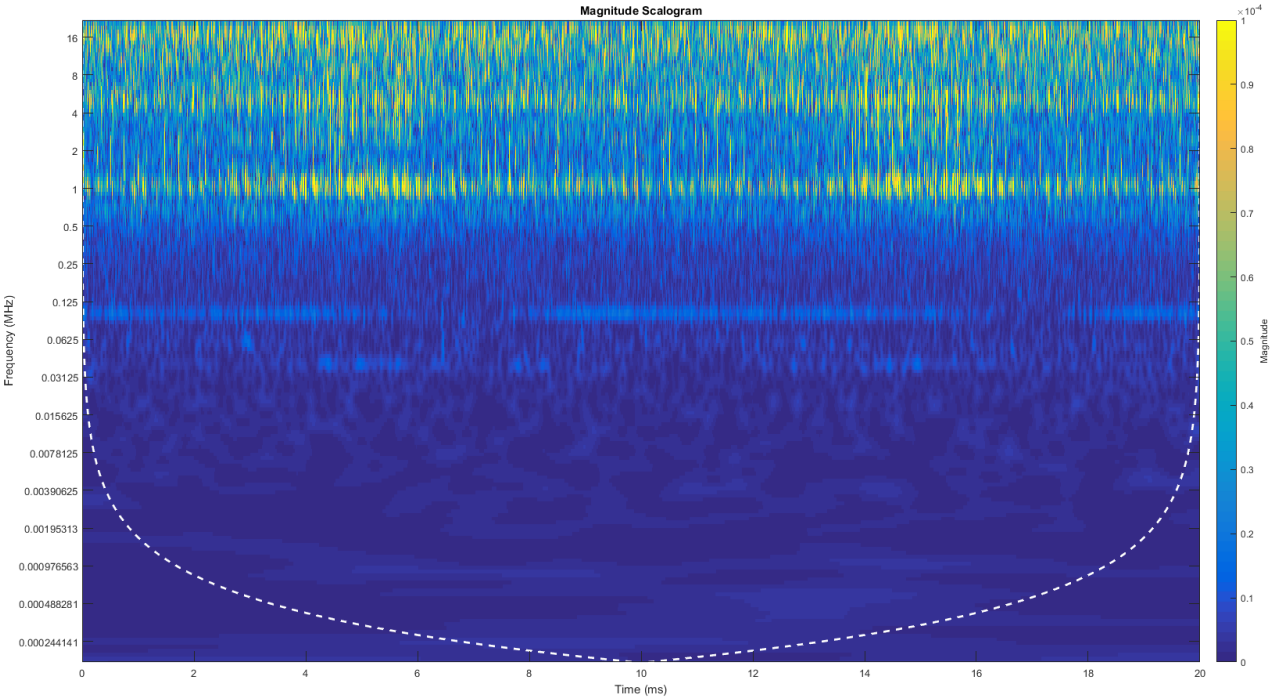


*Figure 5.29a. Scalogram of desk fan obtained using CWT.*

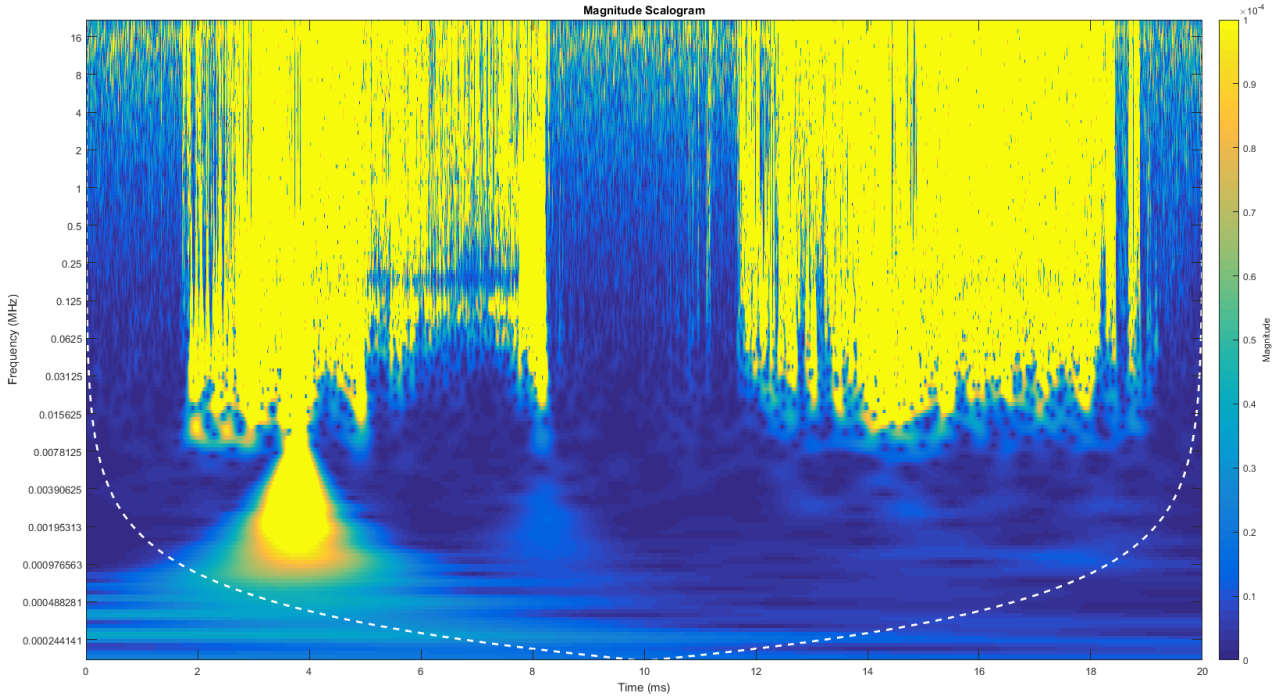


*Figure 5.29b. Scalogram of desk fan with series arc obtained using CWT.*

### 5.5.2. Humidifier

A 140W humidifier was used in the test. Two tests were conducted with this load, the first one was to capture the load signal. The second test captures the load in series with the arc. The two cases, with and without arcing, were compared in the time domain and in the time-frequency domain, using STFT and CWT.

#### *5.5.2.1. Time Domain*

Figure 5.30 shows the waveforms of the SPIM load without arcing (a) and with arcing (b). The humidifier shuts itself off during arcing and hence we notice that there is not current in figure 5.30b. This behavior is observed in certain loads with power supplies.

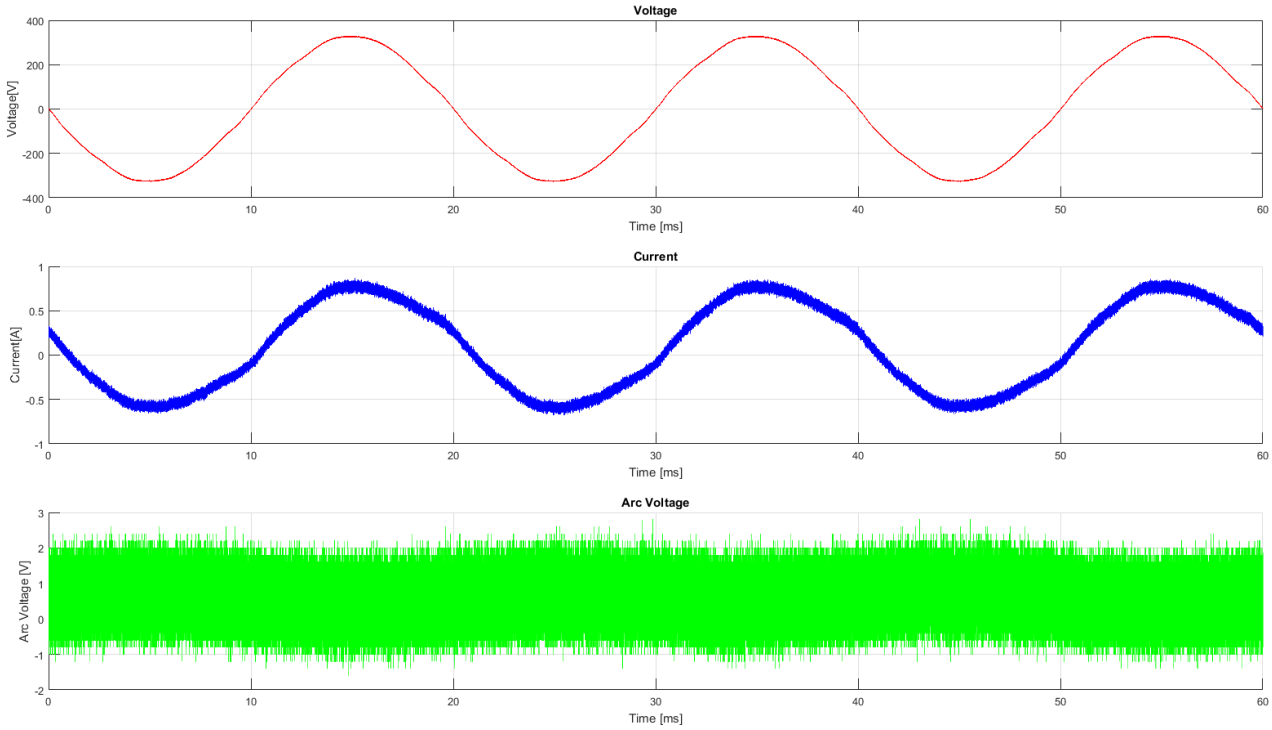


*Figure 5.30a. Time domain representation of the humidifier.*

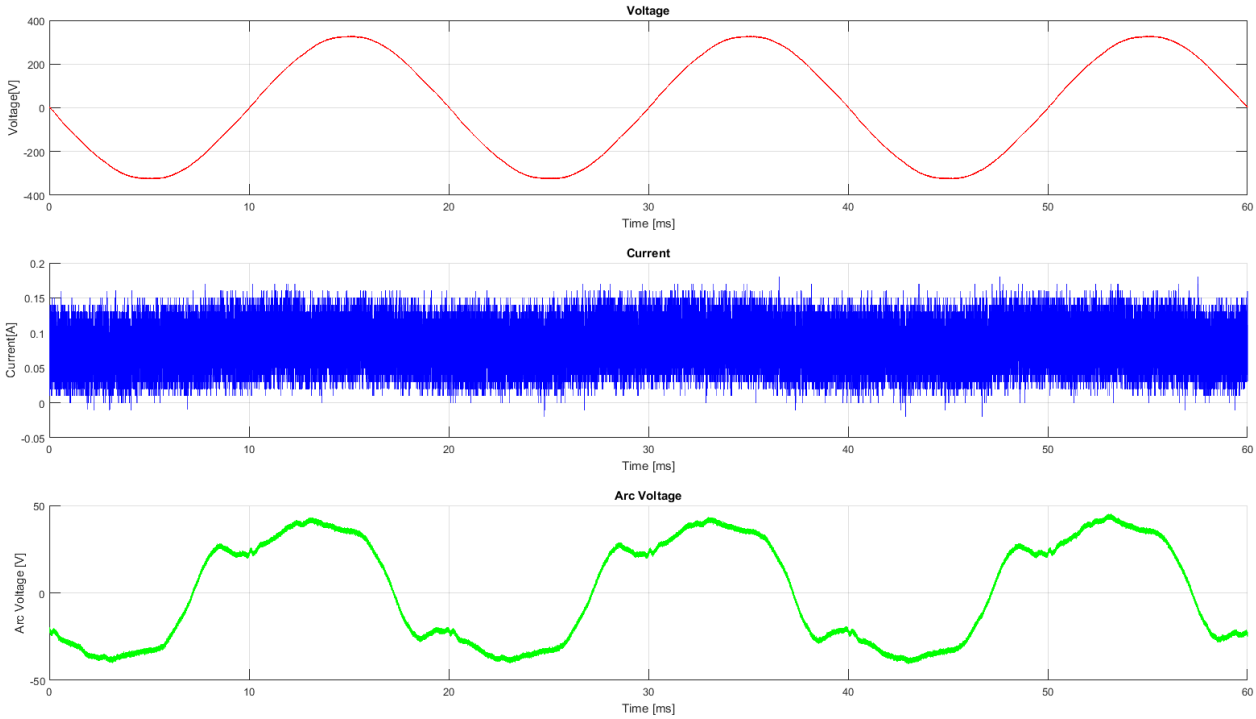


*Figure 5.30b. Time domain representation of the humidifier with the series arc.*

### *5.5.2.2. Short Time Fourier Transform*

The second waveforms in figure 5.31a and 5.31b show the high-frequency component of the current passing through a humidifier, and through the humidifier in series with an arc respectively. The STFTs of these signals are also given.

Since the humidifier turned off, there is nothing to analyze.

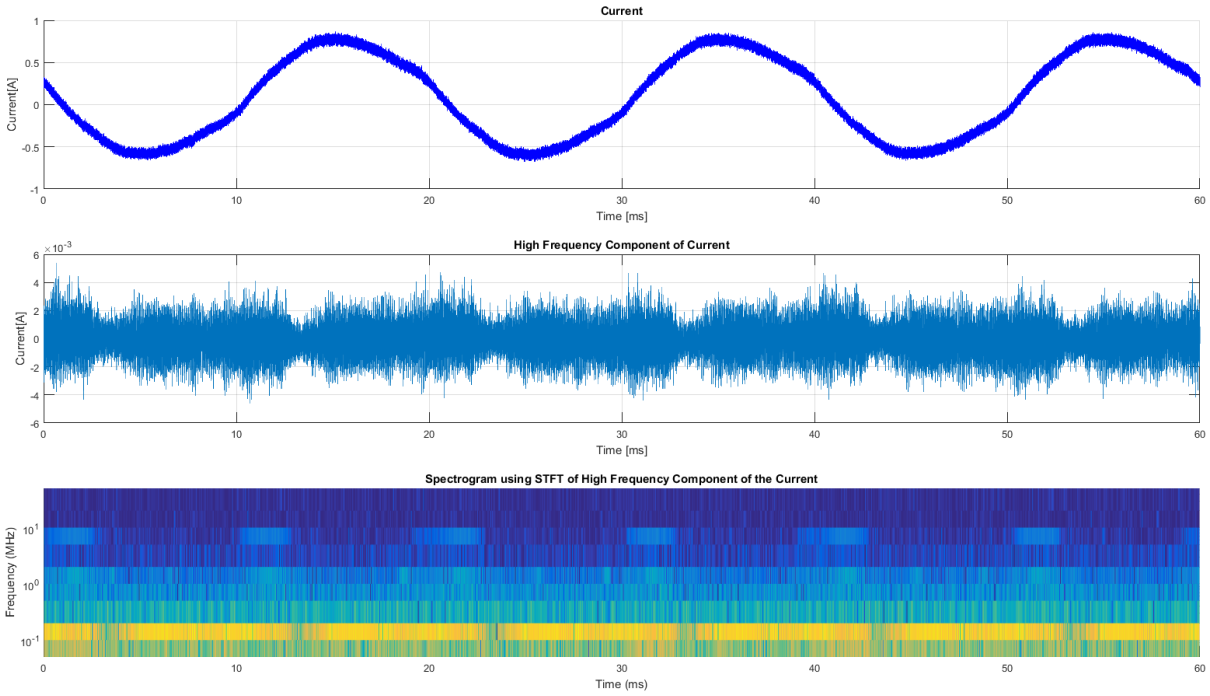


*Figure 5.31a. High-frequency component and STFT of the humidifier.*

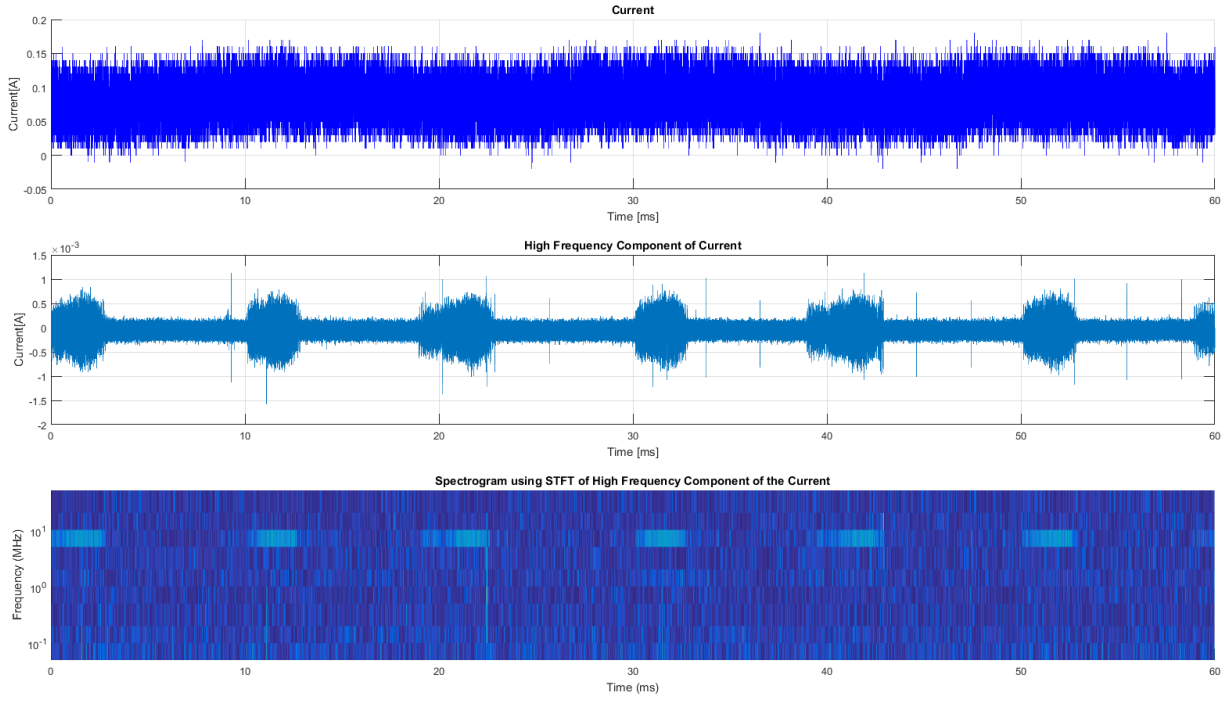


*Figure 5.31b. High-frequency component and STFT of humidifier with the series arc*

.

### *5.5.2.3. Continuous Wavelet Transform*

The scalograms in figure 5.32 are obtained using the CWT and applying it to the high-frequency component of the current passing through a humidifier (a) and humidifier with series arcing (b). The scalogram was obtained by applying CWT to the time period from 20ms to 40ms of the high-

frequency component of the current. However, we observe that the scalogram given in figure 5.32b does not show any data due to the humidifier turning itself off.

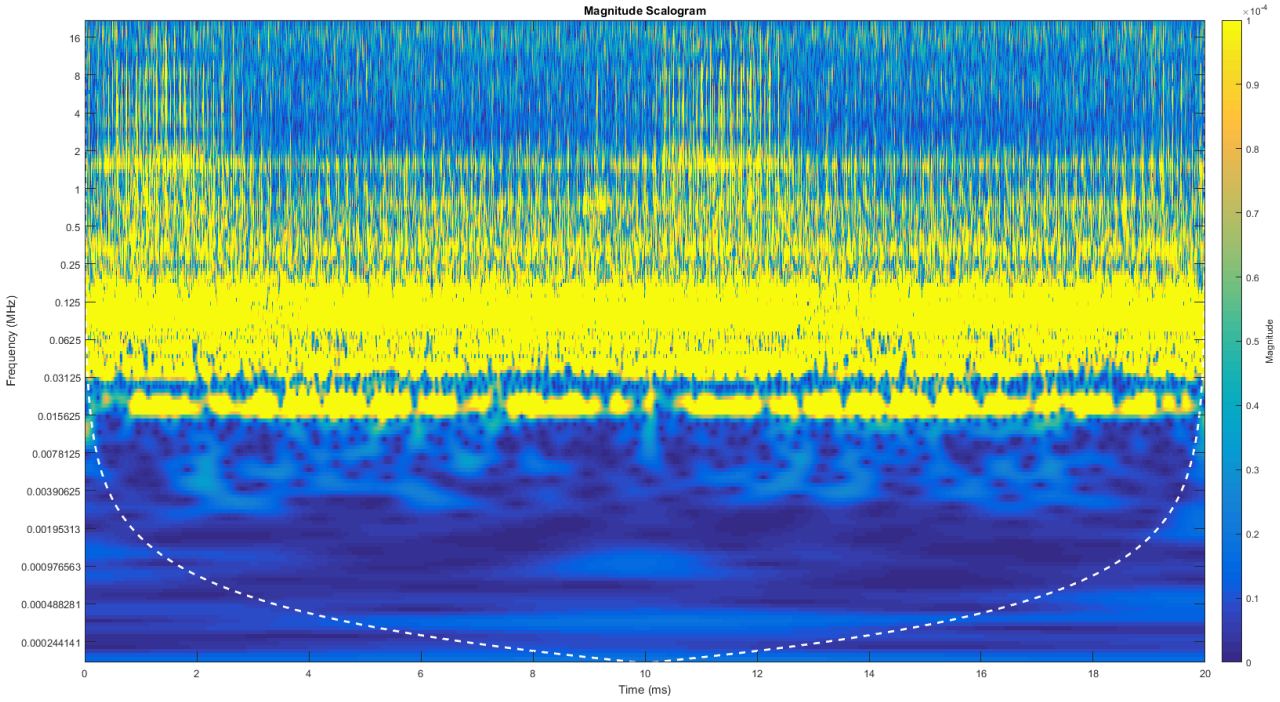


*Figure 5.32a. . Scalogram of humidifier obtained using CWT.*

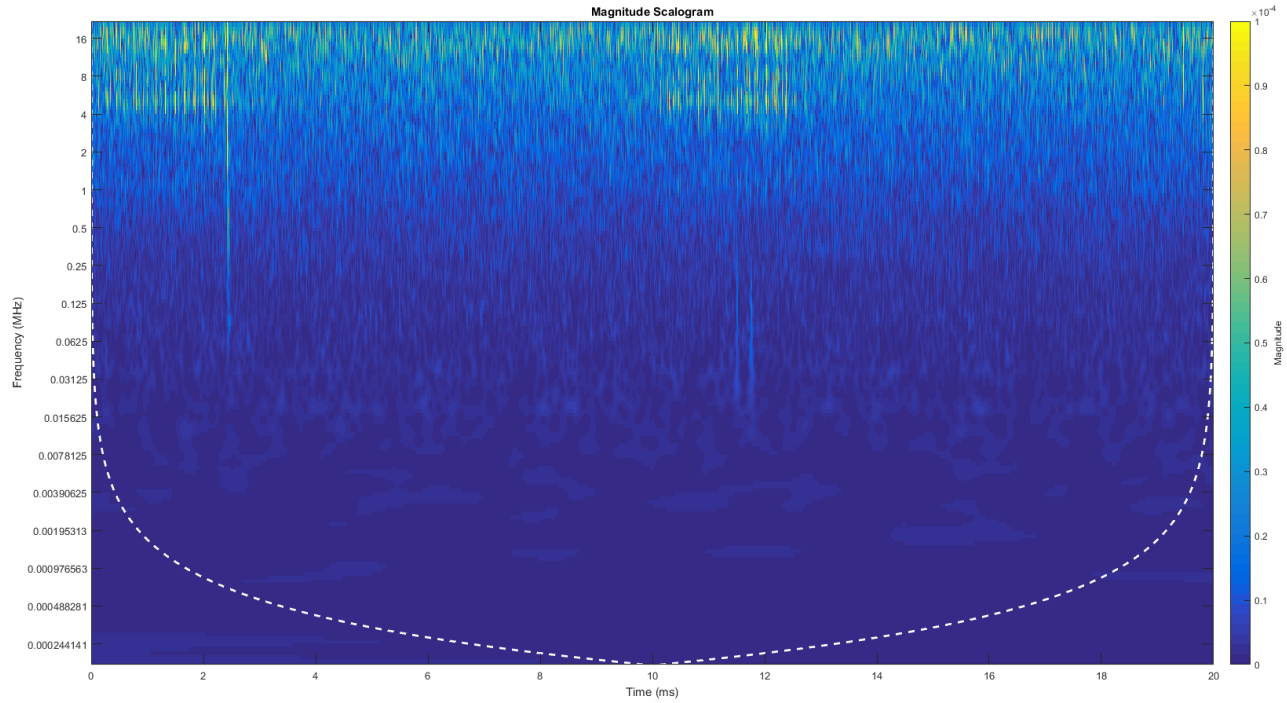


*Figure 5.32b. Scalogram of the humidifier with series arc obtained using CWT.*

## 5.6. SMPS

### 5.6.1. Power Drill

An 1100W power drill was used in the test. Two tests were conducted with this load, the first one was to capture the load signal. The second test captures the load in series with the arc. The two cases, with and without arcing, were compared in the time domain and in the time-frequency domain, using STFT and CWT.

#### *5.6.1.1. Time Domain*

The arc current and voltage, when a power drill is connected in series with an arc, is difficult to interpret in the time domain, as the current waveforms look very similar.

Figure 5.33 shows the waveforms of the power drill without arcing (a) and with arcing (b). The second waveform in both the figures is that of the current. The two current waveforms have different magnitudes and do not have any other observable differences in the time domain. This

In the case with the arc, the shoulders at and near to the zero crossings are not distinguishable from the case without the arc. This very crucial characteristic of the arc is suppressed by the UM. As is evident from the current waveforms, in the time domain there is barely any noticeable variation in the current with series arcing and without.

The arc voltage waveform is not that similar to the characteristic arc voltage. The voltage evidently exists when the arc current is not zero. The periodicity and interruption of the arc are only visible in the arc voltage waveform. The arc voltage waveform in figure 5.33a shows the noise level.

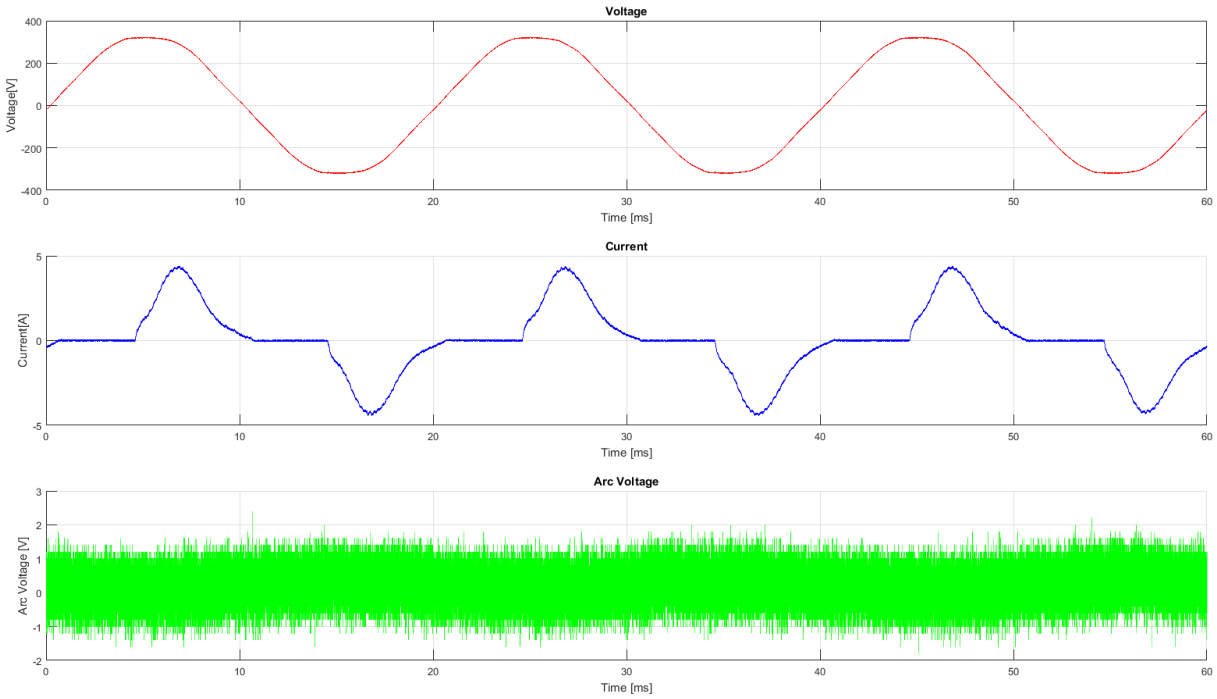


*Figure 5.33a. Time domain representation of the power drill.*

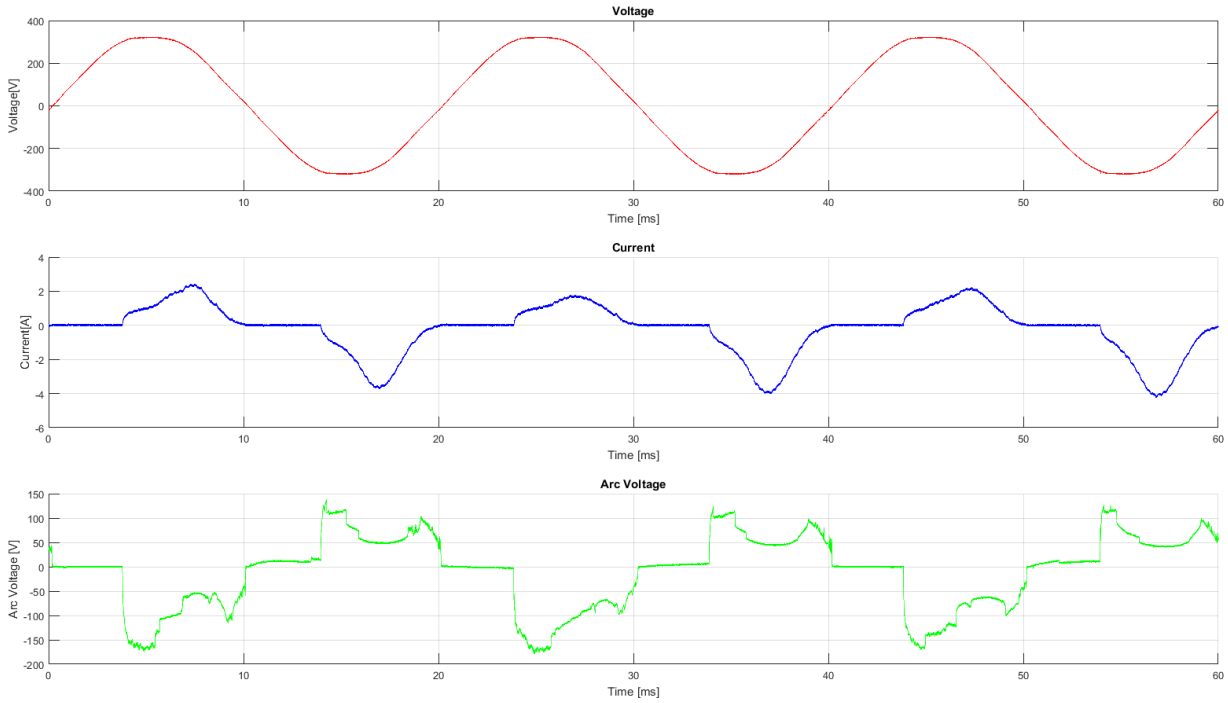


*Figure 5.33b. Time domain representation of the power drill with series arc.*

### *5.6.1.2. Short Time Fourier Transform*

The second waveforms in figure 5.34a and 5.34b show the high-frequency component of the current passing through a power drill, and through a power drill in series with an arc respectively. The STFTs of these signals are also given.

In the time domain, the appearance of the current waveform of a power drill does not show much difference, except for the difference in magnitude.

However, when the high-frequency components of the current with and without arcing is compared, we notice that the difference is in the higher frequency bands. In the case where arcing is present, there appear to be frequency components of higher magnitudes during the time where arcing is present. That is, we see high-frequency components appear after the zero crossing region had been passed. In other words, the high-frequency components are not present in the regions with lower voltage where the arc is not able to sustain itself and extinguishes. However, these high-frequency components are also visible in the waveform of the load itself, making it difficult to differentiate between the two situations.

The STFT also shows the broadband noise that is characteristic of arcing. The STFT for a power drill without arcing shows the presence of high-frequency components and the zero crossings. Even though the STFT for a power drill with series arcing clearly shows the presence of higher frequencies and marks the points near and at the zero crossings very significantly, this criterion is not sufficient as it also appears when the power drill is operated on its own.

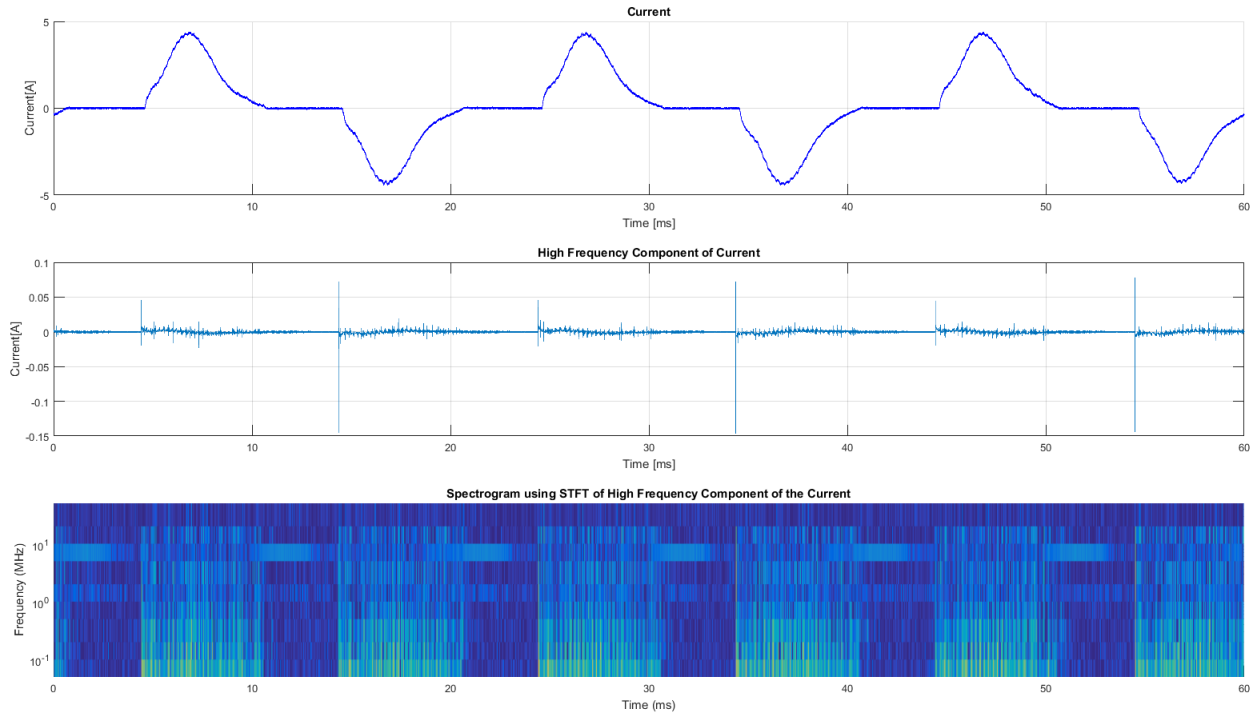


*Figure 5.34a. High-frequency component and STFT of a power drill.*

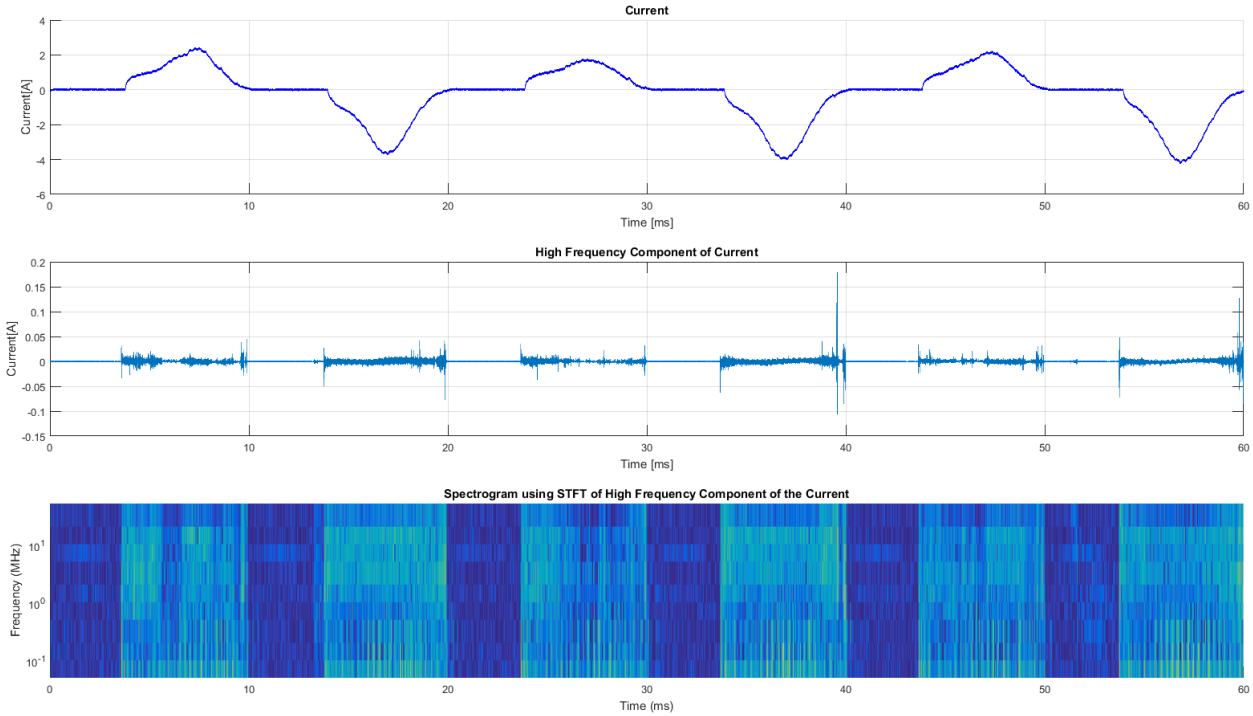


*Figure 5.34b. . High-frequency component and STFT of power drill with the series arc.*

### *5.6.1.3. Continuous Wavelet Transform*

The scalograms in figure 5.35 are obtained using the CWT and applying it to the high-frequency component of the current passing through a power drill (a) and a power drill with series arcing (b).

The scalogram was obtained by applying CWT to the time period from 20ms to 40ms of the high-frequency component of the current.

The power drill exhibits high-frequency patterns similar to arcing with the silence periods near zero crossing. The main difference is in the frequency band, which is more intensive below 1MHz when only the power drill is connected. Arcing shows a more intensity above 1MHz. In the case of the drill, frequency band would be a key factor in distinguishing normal operation from an arc fault.

Although the broadband noise is clearly visible, it is not significant enough. The intensity of the signal at these higher frequencies during the arcing event is highlighted much more when arc is present. The zero crossings are clearly visible. Hence, periodicity and interruption are clearly marked.

CWT highlights the broadband noise much better than STFT. However, in the case of the power drill, one must be careful in order to distinguish series arc from the load.

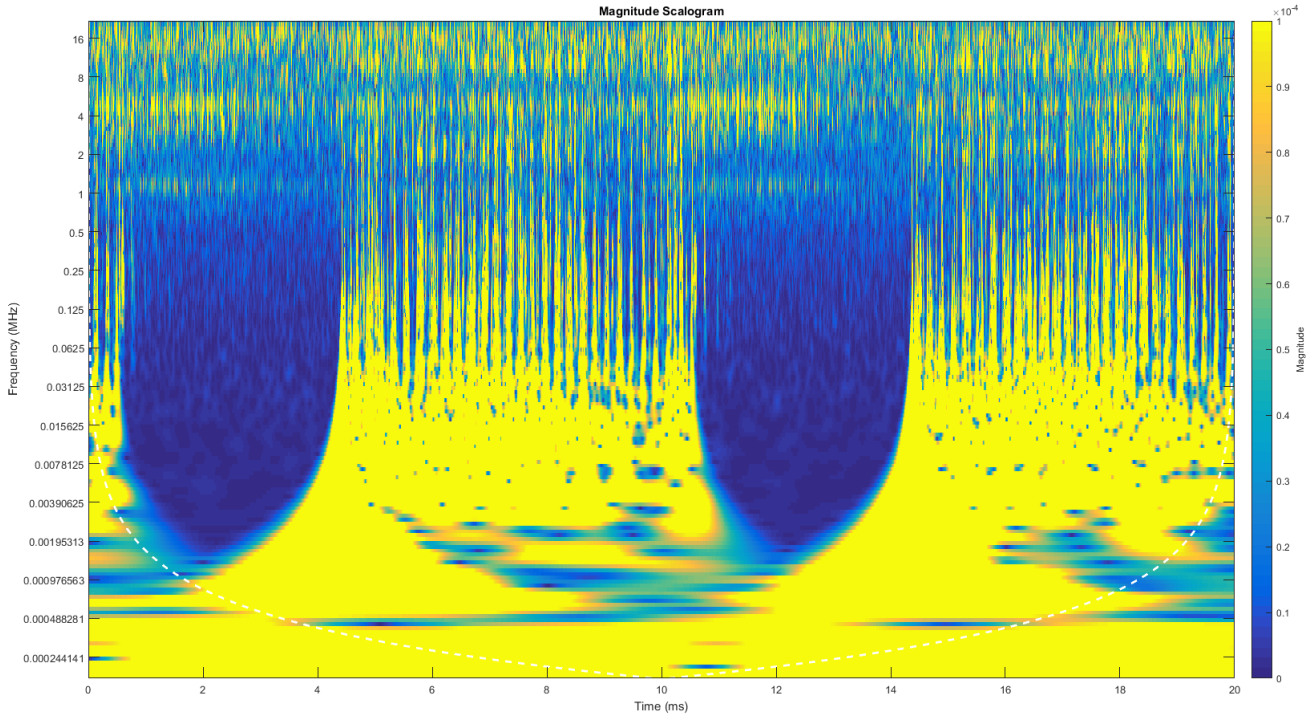


*Figure 5.35a. Scalogram of power drill obtained using CWT.*

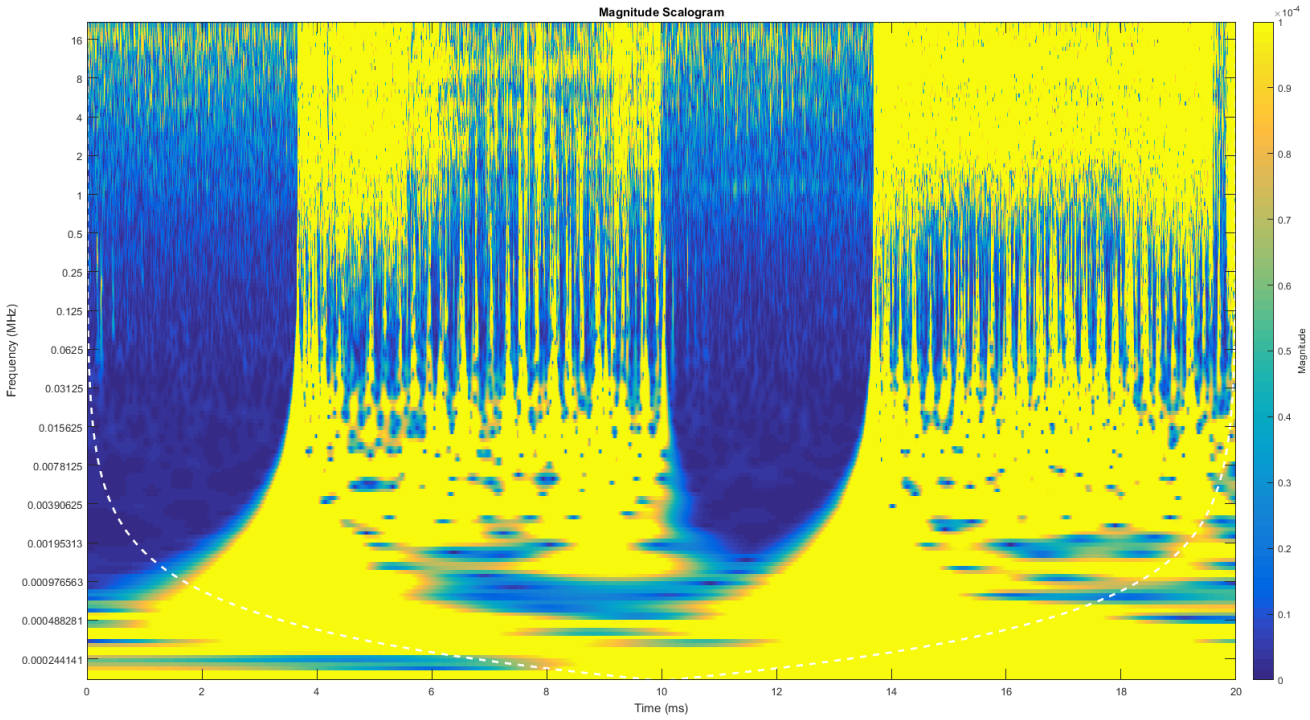


*Figure 5.35b. Scalogram of power drill with series arc obtained using CWT.*

### 5.6.2. Power Supply with Passive Power Factor Correction

A power supply with p-pfc was used in the test. Two tests were conducted with this load, the first one was to capture the load signal. The second test captures the load in series with the arc. The two cases, with and without arcing, were compared in the time domain and in the time-frequency domain, using STFT and CWT.

#### *5.6.2.1. Time Domain*

The arc current and voltage, when a power supply with passive power factor correction is connected in series with an arc, is significantly different to that when there is no series arcing.

Figure 5.36 shows the waveforms of the SMPS load without arcing (a) and with arcing (b).

The second waveform in both the figures is that of the current. In the case with the arc in series with the power supply with passive power factor correction, the current waveform changes drastically. It seems to lose the positive part of the current. It must be noted here that there were some disturbances present in the mains voltage. However, it is evident that although the changes in the current in the time domain are drastic, they do not assist greatly in defining the case with the arc. The periodicity and interruption of the arc are not at all visible. In fact looking at the current waveform in the figure 5.36b one can not even tell whether an arc is present or not.

The arc voltage waveform is very different from the characteristic arc voltage. It seems to be very sporadic. The arc voltage waveform in figure 5.36a shows the noise level.

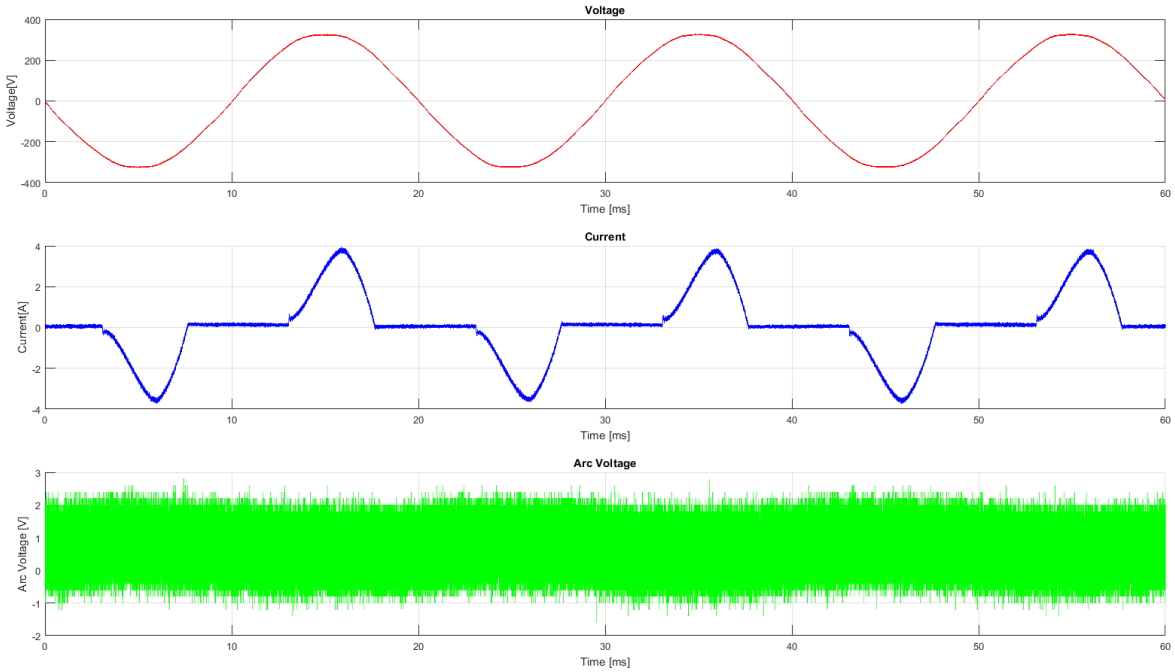


*Figure 5.36a. Time domain representation of the power supply with p-pfc.*

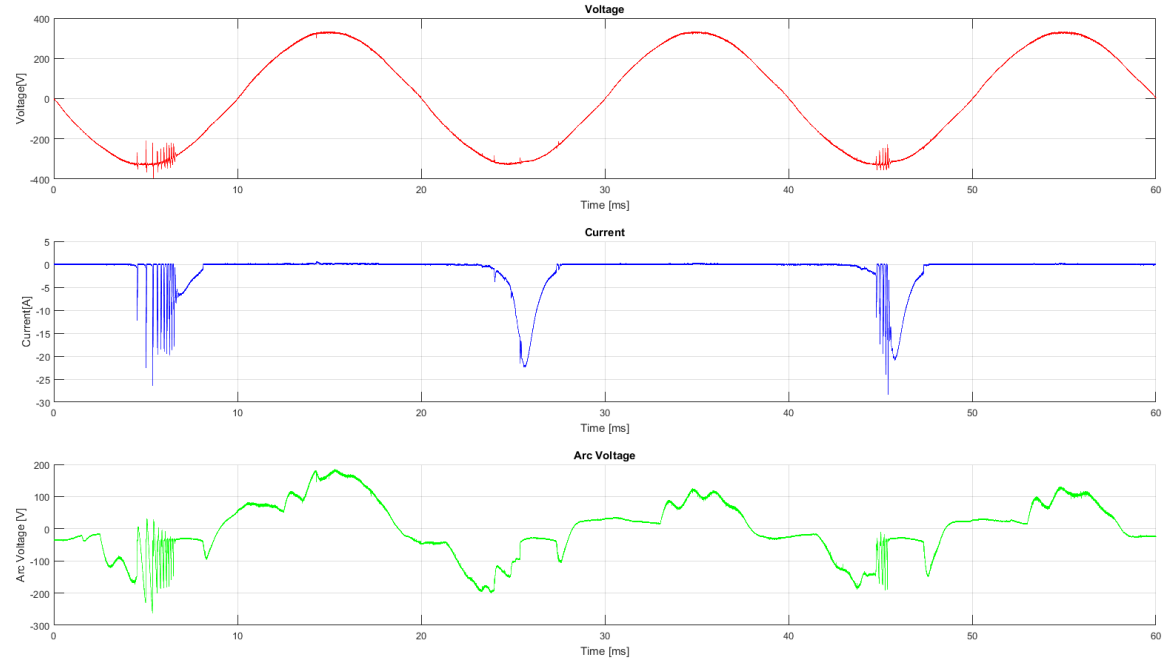


*Figure 5.36b. Time domain representation of the power supply with p-pfc and series arc*

### *5.6.2.2. Short Time Fourier Transform*

The second waveforms in figure 5.37a and 5.37b show the high-frequency component of the current passing through a power supply with passive power factor correction, and through the power supply with passive power factor correction in series with an arc respectively. The STFTs of these signals are also given.

When the high-frequency components of the current with and without arcing is compared, we notice a significant difference. In the case where arcing is present, there appear to be frequency components of higher magnitudes during the time where the arc is present. That is, we see high-frequency components appear after the zero crossing region has been passed. In other words, the high-frequency components are not present in the regions with lower voltage where the arc is not able to sustain itself and extinguishes.

In the case of the desk fan without a series arc, the high-frequency component shows a periodicity at what seem to be the maximas and minimas of the current.

The STFT in figure 5.37b also show the broadband noise that is characteristic of arcing. The STFT for a power supply with passive power factor correction with series arcing clearly shows the presence of broadband noise. In the case of the load, the high frequencies present without arcing are of lower values.

We observe that the interruption of the arc, periodically, at the zero crossings is highly visible in the spectrogram given in figure 5.37b. Furthermore, the broadband noise due to arcing is present.

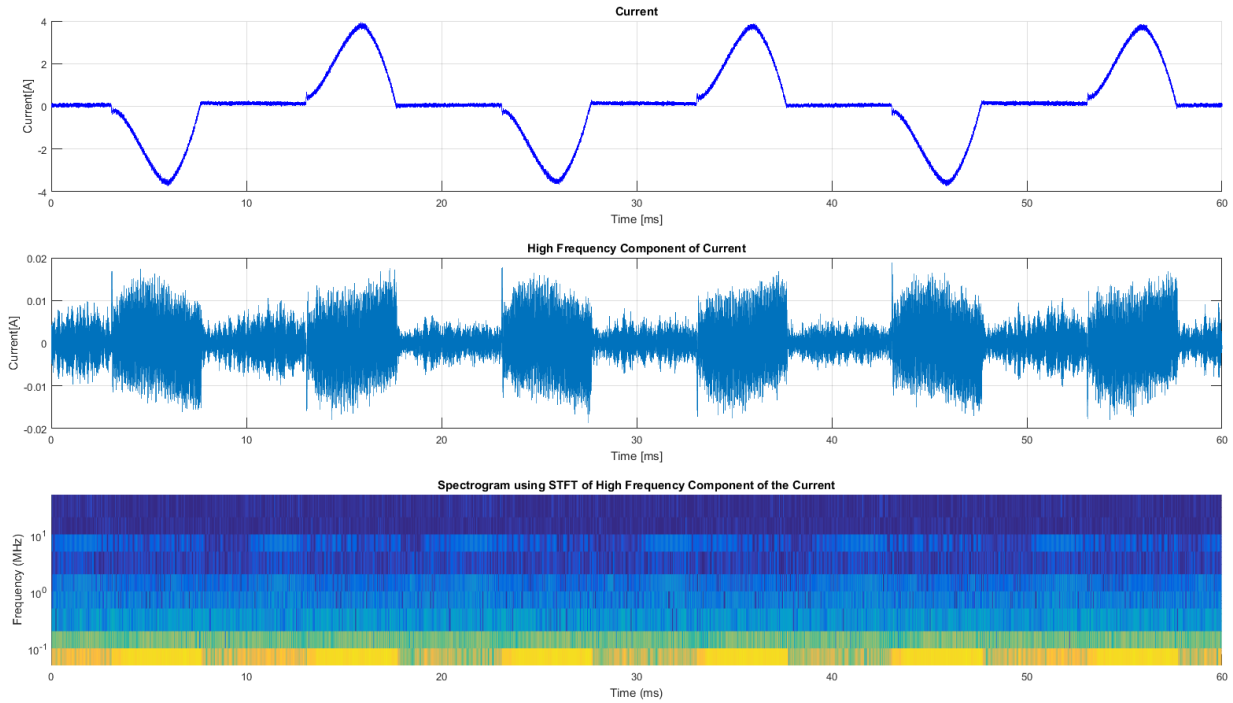


*Figure 5.37a. High-frequency component and STFT of the power supply with p-pfc.*

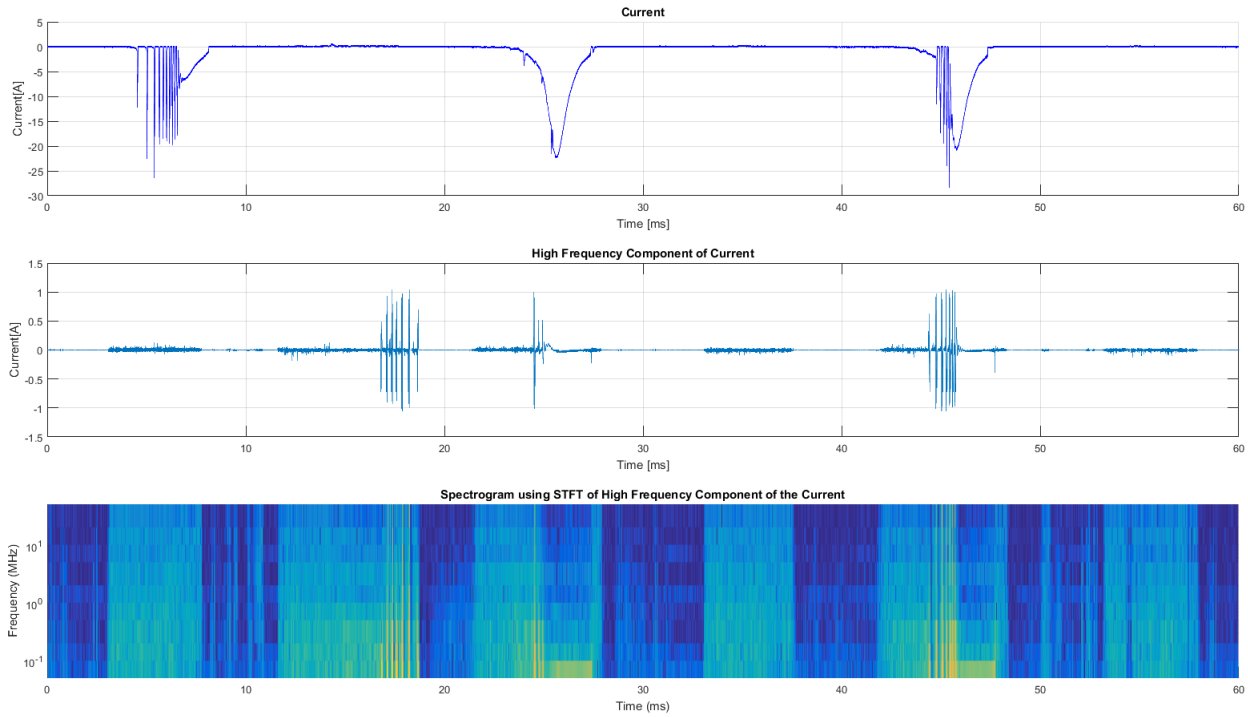


*Figure 5.37b. High-frequency component and STFT of the power supply with p-pfc and series arc.*

### *5.6.2.3. Continuous Wavelet Transform*

The scalograms in figure 5.38 are obtained using the CWT and applying it to the high-frequency component of the current passing through a power supply with passive power factor correction (a) and a power supply with passive power factor correction with series arcing (b). The scalogram was obtained by applying CWT to the time period from 20ms to 40ms of the high-frequency component of the current.

The broadband noise is clearly visible as the frequency band propagating from around 0.25kHz all the way to up to 16Mhz in the case of this load. The intensity of the signal at these higher frequencies during the arcing event is highlighted. Furthermore, the zero crossings are clearly visible. Hence, periodicity and interruption are clearly marked. Furthermore, CWT highlights the broadband noise much better than STFT.

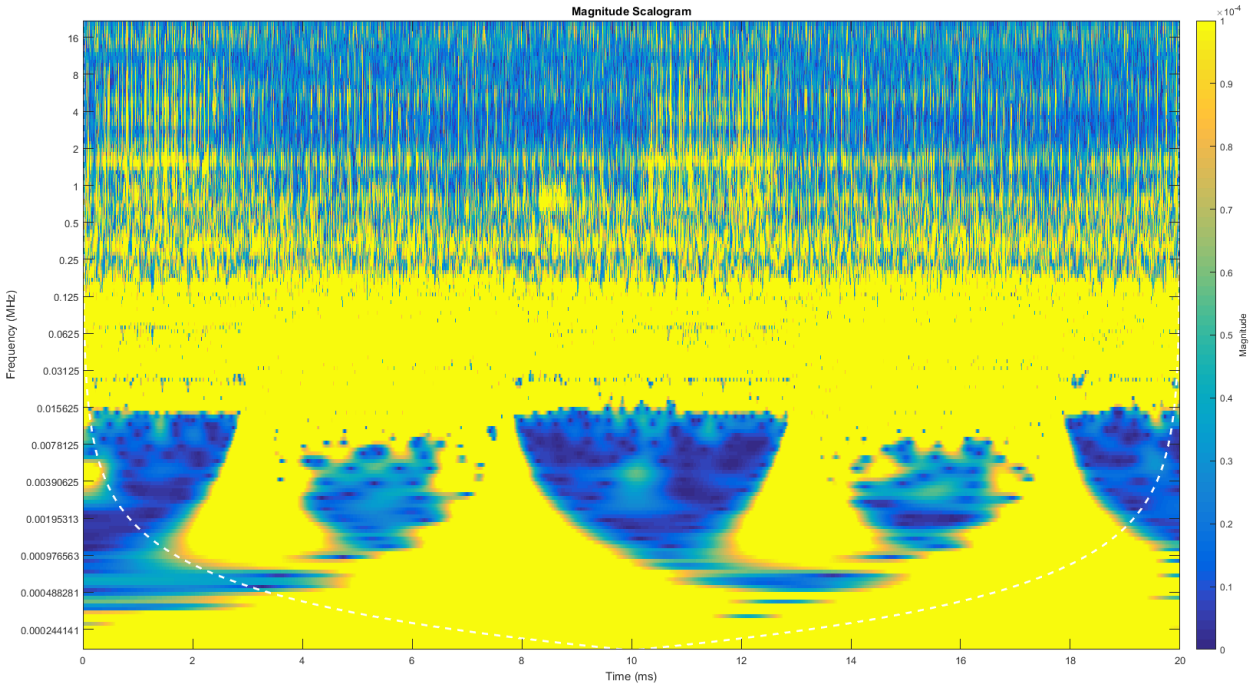


*Figure 5.38a. Scalogram of the power supply with p-pfc obtained using CWT.*

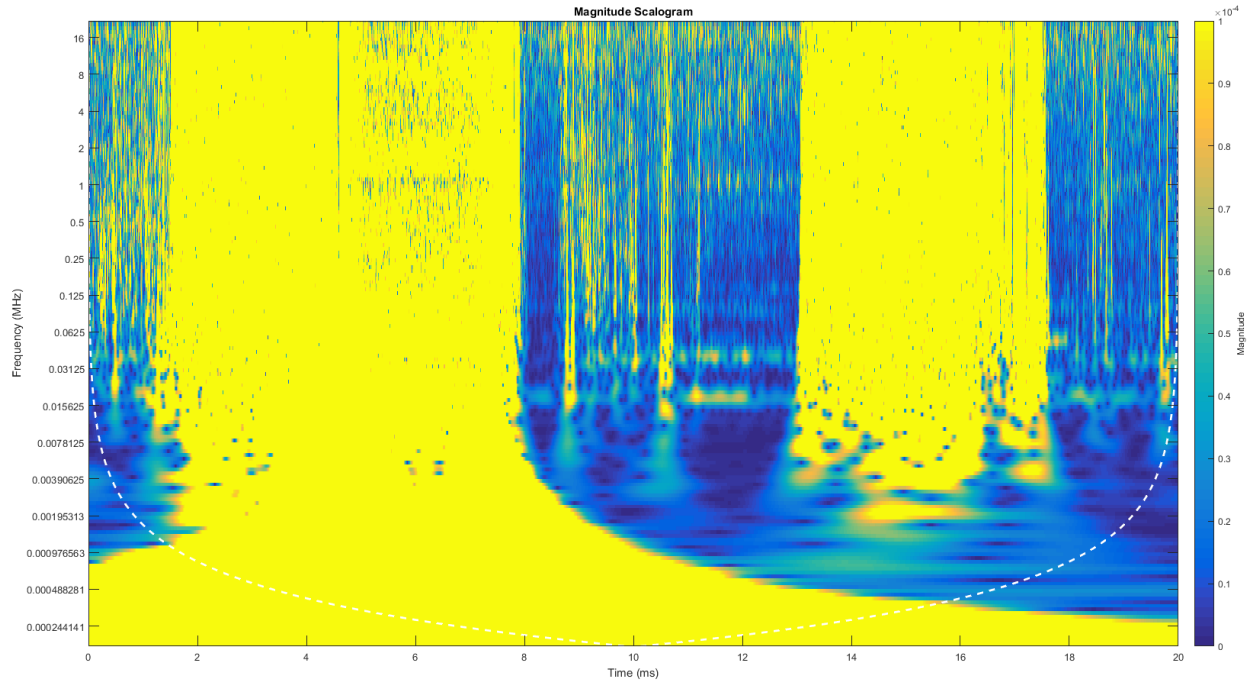


*Figure 5.38b. Scalogram of the power supply with p-pfc and series arc obtained using CWT.*

### 5.6.3. Power Supply with Active Power Factor Correction

A 350W power supply with a-pfc was used in the test. Two tests were conducted with this load, the first one was to capture the load signal. The second test captures the load in series with the arc. The two cases, with and without arcing, were compared in the time domain and in the time-frequency domain, using STFT and CWT.

*5.6.3.1. Time Domain*

The arc current and voltage, when a power supply with active power factor correction is connected in series with an arc, is significantly different to that when there is no series arcing.

Figure 5.39 shows the waveforms of the SMPS load without arcing (a) and with arcing (b).

The second waveform in both the figures is that of the current. In the case with the arc in series with the power supply with active power factor correction, the current waveform does not change drastically. It seems to develop shoulders around the zero crossings. However, it is evident that although the changes in the current in the time domain are drastic, they do not assist greatly in defining the case with the arc. The periodicity and interruption of the arc are more visible compared to the case with passive power factor correction.

The arc voltage waveform is very similar to characteristic arc voltage. The arc voltage waveform in the figure 5.39a shows the noise level.

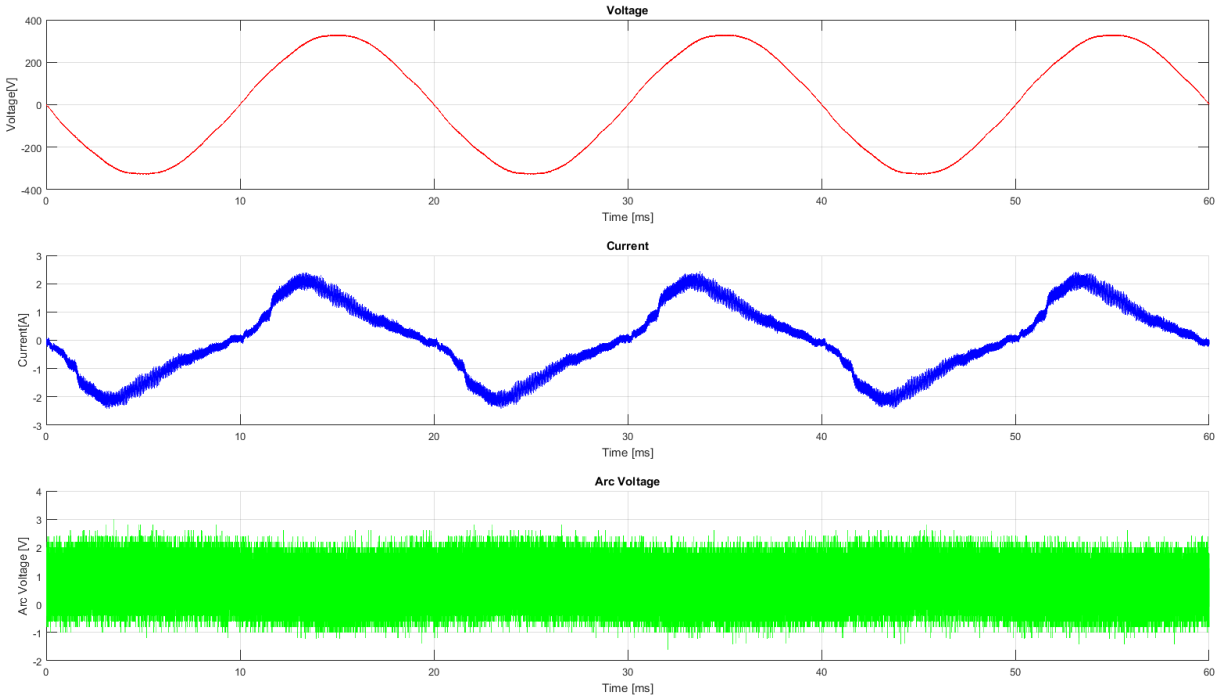


*Figure 5.39a. Time domain representation of the power supply with a-pfc.*

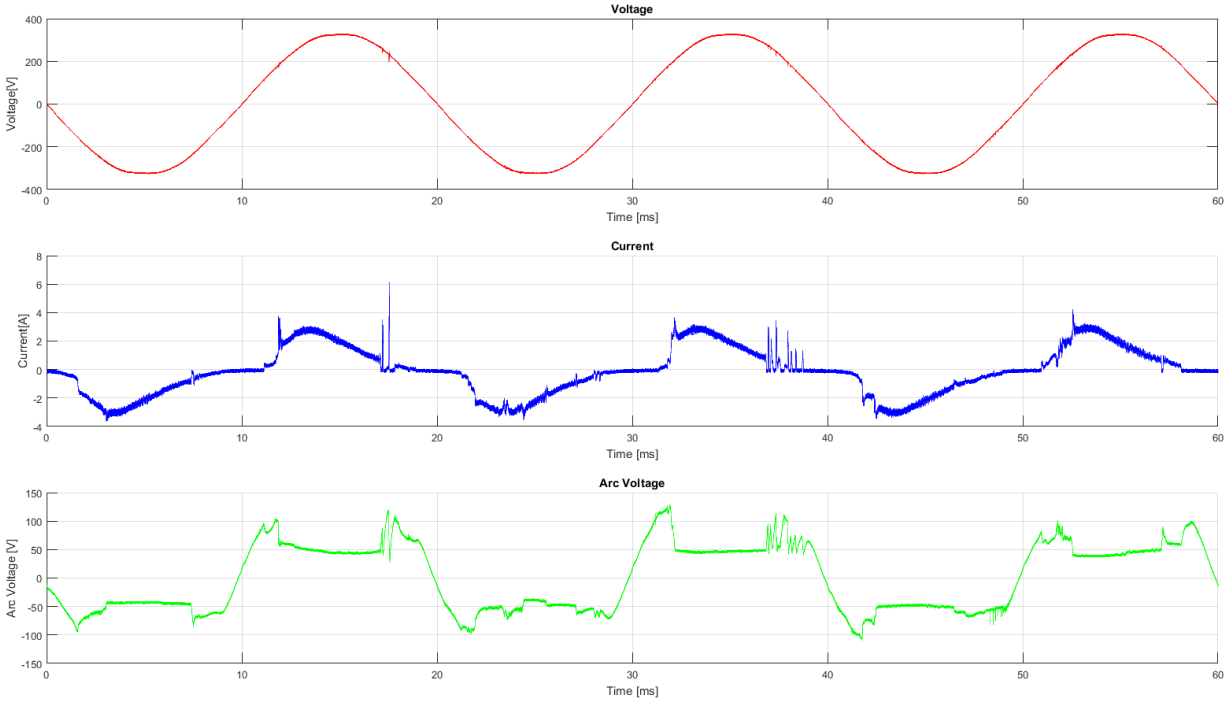


*Figure 5.39b. Time domain representation of the power supply with a-pfc and series arc.*

### *5.6.3.2. Short Time Fourier Transform*

The second waveforms in figure 5.40a and 5.40b show the high-frequency component of the current passing through a power supply with active power factor correction, and through the power supply with active power factor correction in series with an arc respectively. The STFTs of these signals are also given.

When the high-frequency components of the current with and without arcing is compared, we notice a significant difference. In the case where arcing is present, there appear to be frequency components of higher magnitudes during the time where the arc is present. That is, we see high-frequency components appear after the zero crossing region has been passed. In other words, the high-frequency components are not present in the regions with lower voltage where the arc is not able to sustain itself and extinguishes.

In the case of the power supply with active power factor correction without a series arc, the high-frequency component shows periodicity.

The STFT in the case of the load shows frequency components at and around 1MHz.

The STFT in figure 5.40b also shows the broadband noise that is characteristic of arcing. The STFT for a power supply with active power factor correction with series arcing clearly shows the presence of broadband noise. The zero crossings are distinctively marked.

We observe that the interruption of the arc, periodically, at the zero crossings is highly visible in the spectrogram given in figure 5.40b. Furthermore, the broadband noise due to arcing is present.

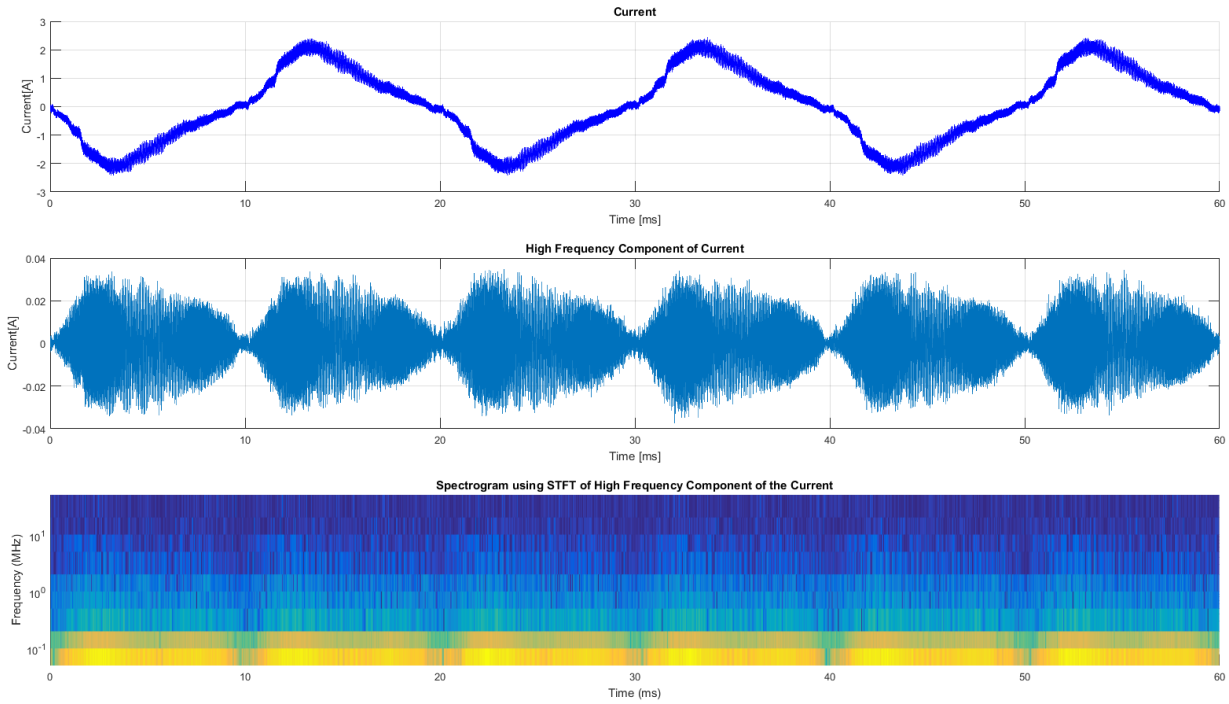


*Figure 5.40a. High-frequency component and STFT of the power supply with a-pfc.*

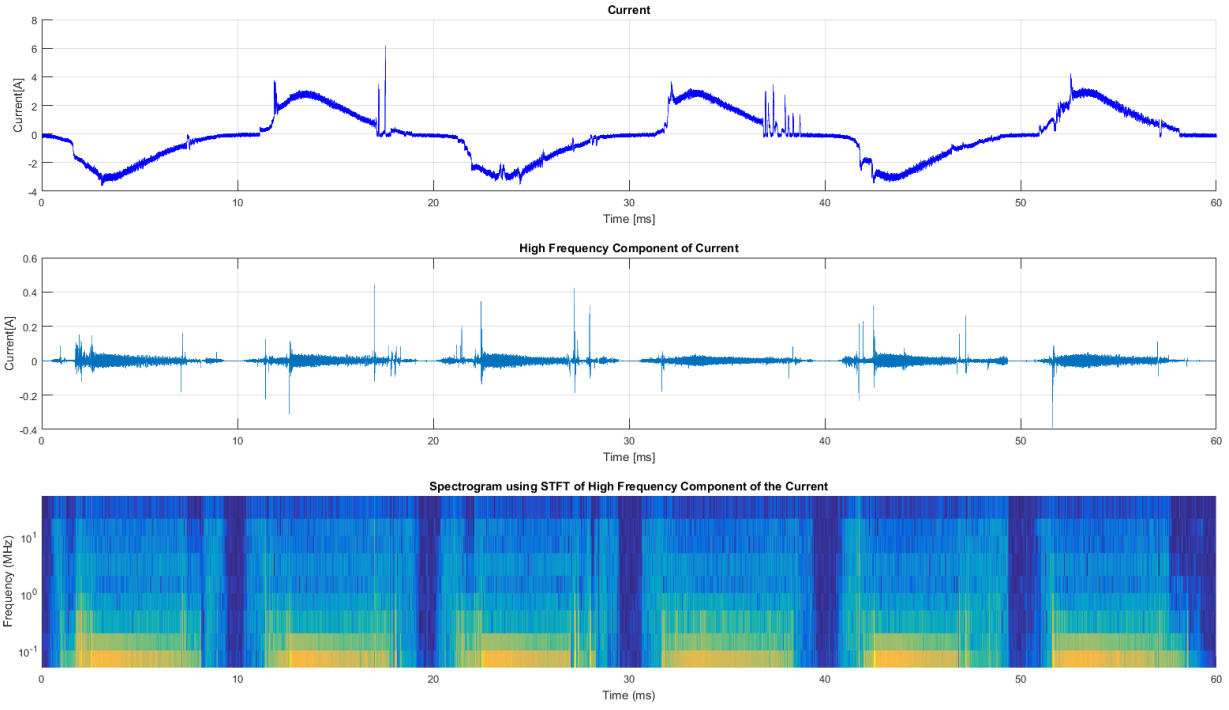


*Figure 5.40b. High-frequency component and STFT of the power supply with a-pfc and series arc.*

### *5.6.3.3. Continuous Wavelet Transform*

The scalograms in figure 5.41 are obtained using the CWT and applying it to the high-frequency component of the current passing through a power supply with active power factor correction (a) and a power supply with active power factor correction with series arcing (b). The scalogram was

obtained by applying CWT to the time period from 20ms to 40ms of the high-frequency component of the current.

The broadband noise is clearly visible as the frequency band propagating from around 0.25kHz all the way to up to 16Mhz in the case of this load. The intensity of the signal at these higher frequencies during the arcing event is highlighted. Furthermore, the zero crossings are clearly visible. Hence, periodicity and interruption are clearly marked. Furthermore, CWT highlights the broadband noise much better than STFT.

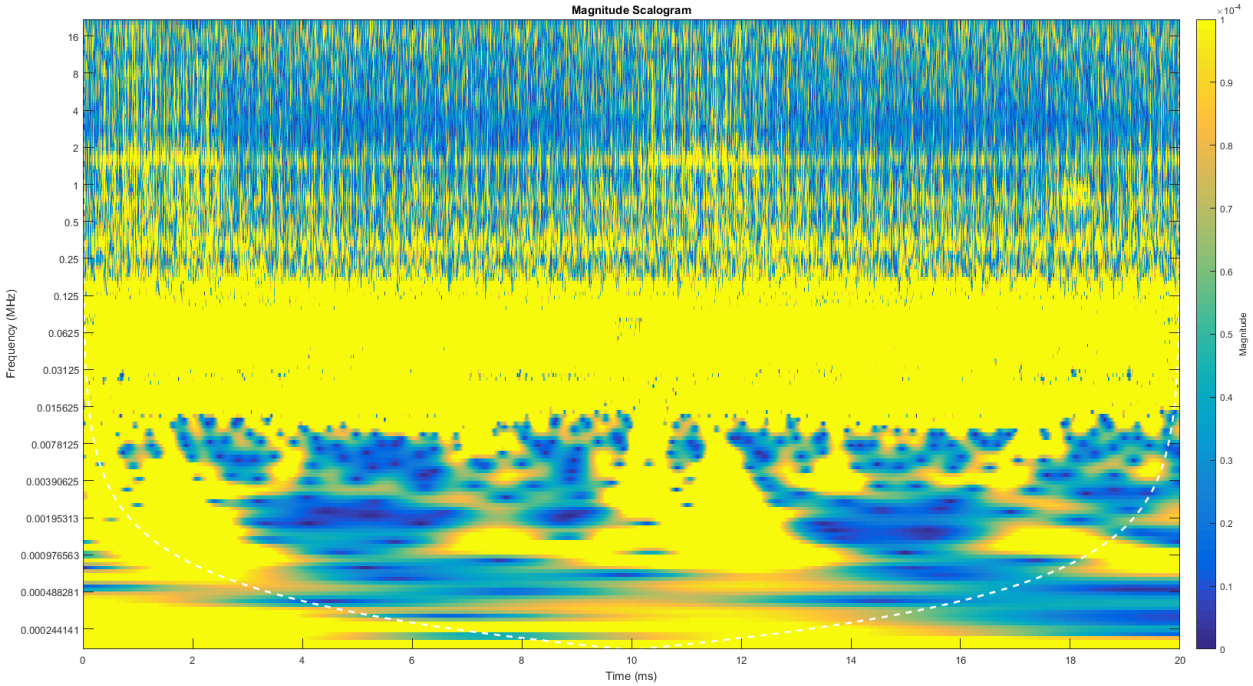


*Figure 5.41a. Scalogram of the power supply with a-pfc obtained using CWT.*

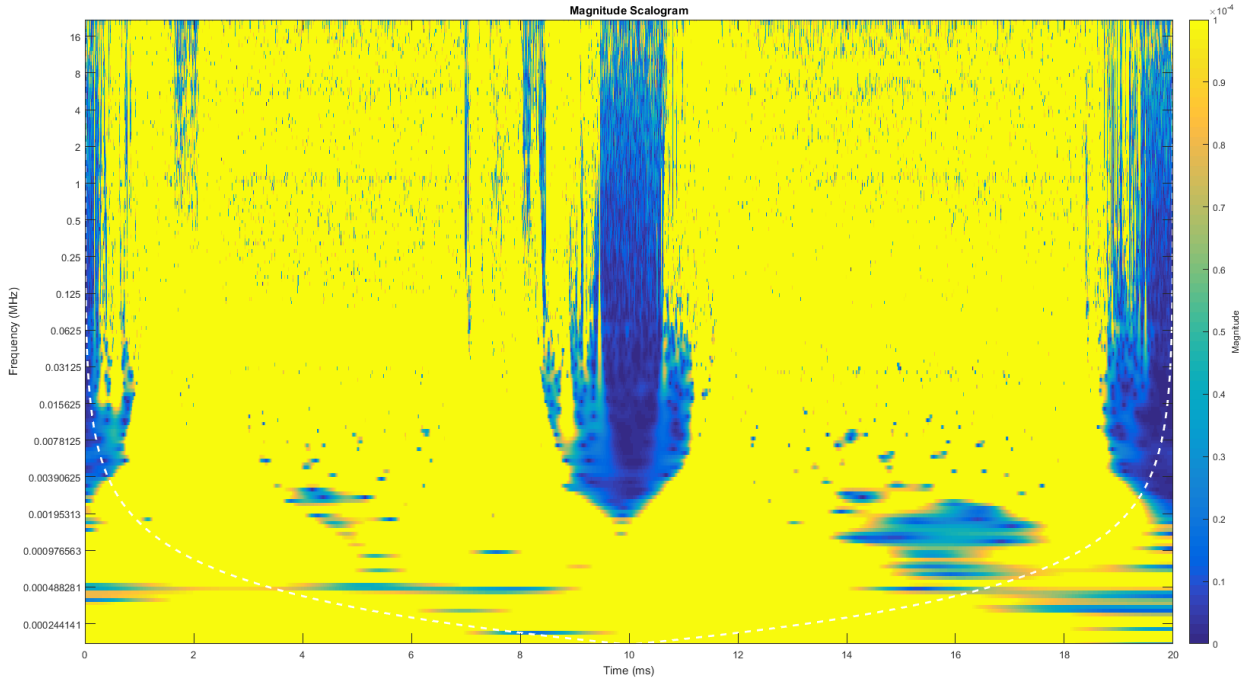


*Figure 5.41b. Scalogram of the power supply with a-pfc and series arc obtained using CWT.*

# 6. Conclusions

The ability of some electrical appliances, used in households, to interfere with or mask arc faults is a major concern to those dealing with arc fault detection. The possibility of an arc fault causing a fire in a home when the owner is not present or asleep has motivated much research in the field of arc fault detection.

In order to prevent fire hazards, it is vital to investigate and analyze the characteristics of arc faults and to study household electrical loads that may interact or interfere with the functioning of this device.

The main characteristic of a series arc, according to [6] is that it generates broadband noise, which could propagate from tens of hertz to 1GHz. Frequency is inversely proportional to energy, hence as frequency increases the energy of the noise decreases. If the behavior of the arc is very consistent, this noise tends to appear only during the conduction of the current as the arc is sustained. As soon as the arc is extinguished the broadband noise disappears. [7].

Another important discriminator of the arc fault is its interruption and periodicity. As the AC source approaches the zero-crossings, the broadband noise disappears. The arc re-establishes and re-extinguishes based on the periodicity of the of the AC source [7]. This means that we are able to distinguish noise which is uncorrelated to the 50Hz.

A systematic approach to categorizing household loads was established to be able to successfully assess the effect of these loads on arc fault detection. Due to the high number of available electrical household appliances, it is of crucial importance that a systematic approach, with the valid technical specification, be employed in order to study the effect of loads on series arc faults.

The Google product category list [8], which Google provides to ensure that advertisements of products are shown with the right search results, was used to narrow down about 300 loads.

These loads were further classified in order to simplify analysis. The component-based categorization method utilized is given in Figure 3.1. The load categorization used, adapted and adequately modified from [11], includes five main categories which are resistive, universal motor, energy efficient lighting, single-phase induction motor, and switched mode power supply.

A total of twelve electrical loads were tested. The EEL category was not tested for this thesis. The loads tested and their respective categories are given in Table 4.3.

After the collection of the data, MATLAB was used for processing the data. The Wavelet Toolbox and the Signal Processing Toolbox were utilized for obtaining the STFTs and CWTs.

CWT eliminates one major limitation of STFT. The STFT has a constant window size and this results in the loss of all time resolution over the duration of the window. Wavelet analysis solves this problem by introducing a windowing technique with variable-sized regions. CWT permits the utilization of long time intervals when more detailed low-frequency information is required, and shorter regions when high-frequency information is required. Furthermore, the freedom to choose the mother wavelet depending on the signal features one is trying to detect is a major strength of the Wavelet analysis.

In all the loads tested, whenever a series arc was introduced we noticed intensive high-frequency components and silent periods at the zero crossings.

Resistive loads, being linear, do not interfere with arc fault detection. All main features of a series arc fault are present in the time domain as well as in time-frequency domain obtained using STFT and CWT.

Some loads exhibited high-frequency components even in the absence of an arc. The high-frequency band was mostly below 1MHz. The loads have these high-frequency components are; vacuum cleaners, cultivator, humidifier, power drill, power supply with passive power factor correction and power supply with active power factor correction.

The power drill seems to be one of the most difficult load when it comes to detecting arc faults. This is because not only did it have high-frequency components above 1 MHz, it also had silent periods around zero crossings. Hence the two main features which are utilized to detect arcs were both presents. The main difference was found in the intensity of the frequency band, which was higher below 1MHz for power drills. Hence, frequency band would be a key factor in distinguishing the normal operation of a power drill from an arc fault.

The cultivator presents high-frequency components which are greater than 1MHz. Hence only relying on the high-frequency to detect arcing would be a poor practice in the case of a cultivator. Hence, also checking the zero crossings, in this case, would prove to be beneficial in successfully detecting arc fault.

In all cases, the CWT of the high-frequency component of the current had better characterization capability due to its resolution. Whenever arcing was present the CWT presented a similar scalogram, where the important features of arc were distinguishable.

Furthermore, the results from the different categories of the loads which were tested proved that the loads can be generalized in the frame of the given categories with the exception of a few.

In order to improve the detection of series arc faults, more loads must be tested and analyzed. Furthermore, research must continue to be conducted regarding other possible signal processing techniques that could improve arc fault detection and reduce nuisance tripping.

# References


[1] Health and Safety Executive, "Electrical safety and you: A brief guide," 2012. [Online]. Available: http://www.hse.gov.uk/pubns/indg231.htm. [Accessed 4 April 2017].

[2] IEC62606, "General requirements for arc fault detection devices," 2013.

[3] J. J. Shea, "Conditions of Series Arcing Phenomena in PVC Wiring," *IEEE Transactions on Components and Packaging Technologies,* vol. 30, no. 3, 2007.

[4] Siemens , "5SM6 AFD Units - Technology Primer," Siemens AG , 2016.

[5] C. Restrepo, P. Staley, A. Nayak, V. Mikani, H. Kinsel, S. R. Titus and J. Endozo, "Systems and Methods for Arc Fault Detection". United States of America Patent US 7864492 B2, 4 January 2011.

[6] F. Blades, "Method and apparatus for detecting arcing in AC power systems by monitoring high frequency noise". United States of America Patent US 5729145 A, 17 March 1998.

[7] C. E. Restrepo, "Arc Fault Detection and Discrimination Methods," in *Electrical contacts - 2007, the 53rd ieee holm conference on Electrical Contacts*, Pittsburgh, 2007.

[8] Google Inc., "Google Product Category," 2016. [Online]. Available: https://support.google.com/merchants/answer/6324436?hl=en. [Accessed 2016].

[9] Amazon.com, Inc., "Amazon full shop directory," Amazon.com, Inc., [Online]. Available: https://www.amazon.de/gp/site-directory/ref=nav_shopall_fullstore. [Accessed 2016].

[10] Walmart, "Walmart All Departments," Walmart, [Online]. Available: https://www.walmart.com/all-departments. [Accessed 2016].

[11] A. Collin, J. Acosta, B. Hayes and S. Djokic, "Component-based Aggregate Load Models for Combined Power Flow and Harmonic Analysis," in *7th Mediterranean Conference and Exhibition on Power Generation, Transmission, Distribution and Energy Conversion*, Agia Napa, 2010.

[12] P. Waide and S. Tanishima, Light's labour's lost - policies for energy efficient lighting., International Energy Agency, 2006.

[13] L. P. Singh and G. Katal, "A Comparative Study on Design and Operation of Fluorescent Lamps, Cfls and Leds," *International Journal of Engineering Research and Applications,* vol. 3, no. 5, pp. 401-407, 2013.

[14] ON Semiconductor, "Power Factor Correction (PFC) Handbook," ON Semiconductor , 2014.

[15] S. G. Sheng, A. Sai and S. Tugio, "Advanced and Economica lHousehold Inverter Air-Conditioner

Controller Solution," in *International IC '99* , Shanghai, 1999.

[16] S. L. Herman, Delmar's Standard Textbook of Electricity, 3 ed., Clifton Park, NY: Delmar Learning, 2004, pp. 998 - 1001.

[17] MathWorks, "Continuous Wavelet Transform and Scale-Based Analysis," The MathWorks, Inc., 2017. [Online]. Available: https://nl.mathworks.com/help/wavelet/gs/continuous-wavelet-transform-and-scale-based-analysis.html. [Accessed 4 April 2017].